

The Role of Claudin Gene Variants in Calcium-Based Kidney Stone Formation

Shane Feinstein

Department of Human Genetics

Faculty of Medicine and Health Sciences

McGill University, Montreal, Quebec, Canada

A thesis submitted to the Faculty of Graduate and Postdoctoral Studies in partial fulfillment of
the requirements of the degree of Master of Science

© Shane Feinstein, 2023

Abstract

Kidney stones contain calcium crystals that precipitate out of the urine and then aggregate to form stones. This causes severe discomfort to the patient and can damage the kidneys, especially if stones are recurring. Hypercalciuria is a major risk factor for kidney stone formation and can be caused by either increased calcium excretion or decreased calcium reabsorption in the nephrons of the kidneys. Claudins are a large family of transmembrane proteins that are found in the tight junctions of epithelial cells. Claudins interact with each other to form various kinds of ion-specific pores and barriers that together regulate the paracellular exchange of calcium and other ions between epithelial cells such as in the nephrons of the kidneys. Certain claudin variants such as those in *CLDN16* have been well documented as a monogenic cause of kidney stones while other claudin variants such as those in *CLDN14* have been associated with kidney stones in genome-wide association studies.

The Gupta laboratory recruited a cohort of children and adults with recurrent kidney stones to determine if they had DNA sequence variants in claudin genes. We identified 13 rare or novel variants in claudin genes in the cohort. I did functional studies on these variants by stably transfecting Madin-Darby Canine Kidney (MDCK) cells with plasmids carrying the claudin sequence variants and then using confocal imaging to determine the localization of the claudins. Dextran assays were used to determine the paracellular permeability of the cell layers to small molecules and trans-epithelial electrical resistance (TEER) assays were used to determine ionic conductance.

One of the *CLDN8* variants (*CLDN8* A94V) showed disrupted localization to the tight junctions that resulted in a cell layer that was more permeable to both ions and small molecules compared to the protein encoded by the wildtype allele. Another variant (*CLDN8* M97T) localized similarly to the protein encoded by the wildtype allele but still resulted in a cell layer that was more permeable to small molecules compared to the wildtype. By contrast, the *CLDN4* variants (*CLDN4* A82T & *CLDN4* A113T) both showed no difference in localization or permeability compared to the wildtype protein. These functional studies will allow us to model rare, genetic causes of kidney stones in the future and help predict the likelihood of kidney stone recurrence based on genotype, especially in younger patients who lack the typical environmental risk factors.

Résumé

Les calculs rénaux sont formés de cristaux de calcium qui s'agrègent ensemble et précipitent de l'urine. Ces calculs sont en général douloureux pour les patients et peuvent endommager les reins, en particulier s'ils sont récurrents. L'hypercalciurie est un facteur de risque majeur et peut être causé soit par une augmentation de l'excrétion de calcium, ou par une diminution de la réabsorption du calcium dans les néphrons des reins. Les claudines sont une grande famille de protéines transmembranaires qui sont trouvés dans les jonctions serrées des cellules épithéliales. Les claudines interagissent entre elles pour former divers types de pores et de barrières ioniques qui régulent ensemble l'échange paracellulaire de calcium et d'autres ions entre les cellules épithéliales, comme par exemple, dans les néphrons. Des variants de claudines particuliers tels que ceux affectant *CLDN16* ont été bien documentés en tant que cause monogénique de calculs rénaux, tandis que d'autres variants de claudine tels que ceux affectant *CLDN14* ont été associés à des calculs rénaux dans des études d'association pangénomique.

Le laboratoire Gupta a recruté une cohorte d'enfants et d'adultes souffrant de calculs rénaux récurrents pour déterminer s'ils avaient des variants de séquence d'ADN dans les gènes des claudines. Nous avons identifié treize variants rares ou nouveaux dans la cohorte. J'ai fait des études fonctionnelles sur ces variants en transfectant de manière stable des cellules Madin-Darby Canine Kidney (MDCK) avec des plasmides portant les variants de de la séquence des claudines, puis en utilisant l'imagerie confocale pour déterminer si ces variants affectent la localisation des claudines. L'analyse de dextrane a été utilisée pour déterminer la perméabilité paracellulaire des couches cellulaires aux petites molécules et le test de résistance électrique transépithéliale (TEER) a été utilisé pour déterminer la conductance ionique.

L'un des variants de *CLDN8* (*CLDN8 A94V*) a montré une localisation perturbée aux jonctions serrées, ce qui a entraîné une couche cellulaire plus perméable aux ions et aux petites molécules par rapport à la protéine encodée par l'allèle de type sauvage. Un autre variant, (*CLDN8 M97T*) était localisé de manière similaire à la protéine encodée par l'allèle de type sauvage, mais a tout de même abouti à une couche cellulaire qui était plus perméables aux petites molécules par rapport à la protéine encodée par l'allèle de type sauvage. Par contre, les variants *CLDN4* (*CLDN4 A82T* et *CLDN4 A113T*) n'ont montré aucune différence de localisation ou de perméabilité par rapport à la protéine de type sauvage. Ces études fonctionnelles nous permettront à l'avenir de modéliser les causes génétiques rares des calculs rénaux et d'aider à

prédire la probabilité de récurrence des calculs rénaux en fonction du génotype, en particulier chez les patients plus jeunes qui ne présentent pas les facteurs de risque environnementaux typiques.

Table of Contents

<i>Abstract</i>	2
<i>Résumé</i>	3
<i>List of Abbreviations</i>	7
<i>List of Figures</i>	10
<i>List of Tables</i>	10
<i>Acknowledgements</i>	11
<i>Format of the thesis</i>	11
<i>Contribution of the authors</i>	11
<i>Chapter 1: Introduction</i>	12
Epidemiology and Overview of Kidney Stones	12
Evidence of Genetic Contribution to Kidney Stone Risk	13
Kidney Anatomy and Physiology	14
Calcium and Magnesium Reabsorption Along the Nephron	15
Hormonal Factors in Ion Homeostasis and Kidney Stones	16
Genes Known to Influence Kidney Stone Formation	17
The Role of Tight Junctions in Epithelial Cells.....	19
Claudin Expression and Function.....	19
Claudin Variants Associated with Kidney Stones in Animal Models.....	21
Claudin Variants Associated with Kidney Stones in Humans	22
The Gupta Lab Kidney Stone Cohort and Sequenced Claudin Variants	24
Hypothesis and Aims.....	26
<i>Chapter 2: Materials and Methods</i>	27
pEGFP plasmid	27
Madin-Darby Canine Kidney Cells (MDCK).....	27
Stable Transfection of Plasmids into MDCK Cells	27
Immunofluorescence Staining	28
Colocalization Analysis	28
Western Blot Analysis	30
Transepithelial Electrical Resistance (TEER).....	30
Dextran Assays.....	31
Statistical Analysis	31

Chapter 3: Results	32
CLDN4 A82T	34
CLDN4 A113T	38
CLDN6 P211T.....	41
CLDN8 A94V	43
CLDN8 M97T	52
CLDN11 S157F	57
CLDN17 A94V	59
Testing of Claudin-8 Antibodies.....	62
Chapter 4: Discussion	64
Overview of the Variants	64
CLDN4	64
CLDN6	66
CLDN8	67
CLDN11	70
CLDN17	71
Limitations of the Eukaryotic Expression Vector and the Transfection Method	72
Limitations of Bioinformatic Tools	72
Other Limitations of This Project.....	73
Chapter 5: Conclusion & Future Directions	75
Remaining <i>CLDN</i> Variants	75
Identifying Additional <i>CLDN</i> Variants Using the UK Biobank.....	75
Further Sequencing of Patients.....	75
Other Methods to Determine Calcium Permeability	76
The Role of Hormones in <i>CLDN</i> Expression and Localization.....	76
Conclusion.....	76
References	78
Appendix	86

List of Abbreviations

µg: Microgram

µl: Microlitre

µm: Micrometre

ACMG: American College of Medical Genetics and Genomics

ANOVA: Analysis of variance

Ca²⁺: Calcium ion

CaSR: Calcium-sensing receptor

CD: Collecting duct

CKD: Chronic kidney disease

CMV: Cytomegalovirus

Cl⁻: Chloride ion

CLDN: Claudin

C-CPE: C-terminal end of *Clostridium perfringens* enterotoxin

CPE: *Clostridium perfringens* enterotoxin

DMEM: Dulbecco's Modified Eagle Medium

DNA: Deoxyribonucleic acid

DT: Distal tubule

ECL: Extracellular loop

EGFP: Enhanced green fluorescent protein

ENaC: Epithelial sodium channel

ER: Endoplasmic Reticulum

FBS: Fetal bovine serum

FHHNC: Familial hypomagnesemia and hypercalciuria with nephrocalcinosis

FITC: Fluorescein isothiocyanate

G418: Geneticin

GFP: Green fluorescent protein

GHS: Genetic Hypercalciuric Stone-forming

gnomAD: Genome Aggregation Database

GWAS: Genome-wide association study

HEK293: Human embryonic kidney 293

HIV: Human immunodeficiency virus
IF: Immunofluorescence
K⁺: Potassium ion
kDa: KiloDalton
KO: Knockout
LLC-PK1: Lilly Laboratories Cell-Porcine Kidney 1
LOH: Loop of Henle
MDCK II: Madin-Darby canine kidney II
Mg²⁺: Magnesium ion
MGP: Matrix Gla Protein
mIMCD: Mouse Inner Medullary Collecting Duct
ml: Millilitre
mm: Millimetre
mM: Millimolar
mRNA: Messenger ribonucleic acid
MUHC: McGill University Health Center
Na⁺: Sodium ion
NGS: Normal goat serum
NKCC2: Apical Na⁺-K⁺-2Cl⁻ cotransporter
PBS: Phosphate buffered saline
PCR: Polymerase chain reaction
PDZ: Post-synaptic density 95 *Drosophila* disc large zonula occludens-1
PFA: Paraformaldehyde
PT: Proximal tubule
PTH: Parathyroid hormone
RAAS: Renin-angiotensin-aldosterone system
RNA: Ribonucleic acid
SLC3A1: Solute carrier family 3 member 1
SLC34A1: Solute carrier family 34 member 1
SLC4A1: Solute carrier family 4 member 1
SLC7A9: Solute carrier family 7 member 9

SNP: Single Nucleotide Polymorphisms

SV40: Simian vacuolating virus 40

TAL: Thick ascending limb of loop of Henle

TEER: Transepithelial electrical resistance

TM: Transmembrane domain

VDR: Vitamin D receptor

WT: Wild-type

ZO-1: Zonula Occludens 1

List of Figures

Figure 1: Calcium and Magnesium Reabsorption in the Human Nephron	16
Figure 2: Expression of Claudins in the Human Nephron.....	21
Figure 3: MDCK Cells Showing Endogenous CLDN4 & CLDN8 Expression.....	33
Figure 4: MDCK Cells Stably Transfected with CLDN4WT or CLDN4A82T.....	34
Figure 5: Pearson's Correlation Coefficient of CLDN4WT & Variants	35
Figure 6: TEER of CLDN4WT vs CLDN4A82T	36
Figure 7: TEER at 72 hours for CLDN4WT & Variants	37
Figure 8: Permeability of CLDN4WT & CLDN4A82T to 4kD Neutral Dextran.....	38
Figure 9: MDCK Cells Stably Transfected with CLDN4WT or CLDN4A113T.....	39
Figure 10: TEER of CLDN4WT vs CLDN4A113T	40
Figure 11: Permeability of CLDN4WT & CLDN4A113T to 4kD Neutral Dextran.....	41
Figure 12: MDCK Cells Stably Transfected with CLDN6WT or CLDN6P211T	42
Figure 13: Pearson's Correlation Coefficient for CLDN6WT & CLDN6P211T	43
Figure 14: MDCK Cells Stably Transfected with CLDN8WT or CLDN8A94V	45
Figure 15: Mander's M1 for CLDN8WT & Variants	46
Figure 16: Mander's M2 for CLDN8WT & Variants	47
Figure 17: Pearson's Correlation Coefficient for CLDN8WT & Variants	48
Figure 18: CLDN8WT & CLDN8A94V with Calnexin Antibody	49
Figure 19: TEER of CLDN8WT vs CLDN8A94V	50
Figure 20: TEER Readin at 72 hours for CLDN8WT & Variants	51
Figure 21: Permeability of CLDN8WT & CLDN8A94V to 4kD Neutral Dextran	52
Figure 22: MDCK Cells Stably Transfected with CLDN8WT or CLDN8M97T	53
Figure 23: TEER of CLDN8WT vs CLDN8M97T	54
Figure 24: Permeability of CLDN8WT & CLDN8M97T to 4kD Neutral Dextran	55
Figure 25: Western Blot of CLDN8WT & Variants	56
Figure 26: Western Blot Control Showing GAPDH	56
Figure 27: Western Blot Quantification	57
Figure 28: MDCK Cells Stably Transfected with CLDN11WT or CLDN11S157F	58
Figure 29: CLDN11WT with CLDN11 Antibody	59
Figure 30: MDCK Cells Stably Transfected with CLDN17WT or CLDN17A94V	60
Figure 31: Pearson's Correlation Coefficient for CLDN17WT & CLDN17A94V	61
Figure 32: Permeability of CLDN17WT & CLDN17A94V to 4kD Neutral Dextran	62
Figure 33: Structure of CLDN8 Protein	70

List of Tables

Table 1: Variants and Predicted Effects	25
Table 2: Variant Localization and Permeability.....	32
Table 3: Primers Used for Resequencing Plasmids.....	33
Table 4: CLDN8 Antibody Reactivity.....	63

Acknowledgements

I would like to give a big thank you to my supervisory committee members Dr. Thomas Kitzler and Dr. Tomoko Takano for their generous contribution of advice on the direction of my project. I would like to thank Dr. Aimee Ryan who was a steady contributor of feedback at lab meetings. I would like to thank Yuan Zhuang for training me on cell culture and other techniques for this project and all the prior work she contributed to advance this project prior to me taking it over. I would like to thank my lab-mates Vasikar Murugapoopathy and Dr. Carlos Agustin Isidro Alonso for all their advice on my project and support throughout all my studies. I would like to thank Jean-Francois Boisclair Lachance for his help finding lab supplies and in setting up and maintaining crucial lab equipment. I would like to thank Elizabeth Ann Legere for showing me methods for data analysis. I would like to thank Dr. Sero Andonian for letting our lab recruit patients from his urology clinic. I owe a great debt to Rimi Joshi for recommending the lab of Dr. Indra Gupta. Most importantly, I would like to thank Dr. Indra Gupta for being the best supervisor I could have possibly hoped for and for making this project possible.

Format of the thesis

This thesis was written according to the format and guidelines of the office of Graduate and Postdoctoral Studies of McGill University. All human studies have REB approval from the Research Institute of the McGill University Health Center (RI-MUHC).

Contribution of the authors

The candidate conducted all experiments presented in this paper. Jasmine El Andaloussi recruited the cohort of kidney stone patients and controls from urology clinics at the MUHC. The site-directed mutagenesis of the claudin variants as well as the cloning of both WT and variant claudins was performed by prior Master student Yuan Zhuang except for the CLDN17 WT and CLDN17 A94V where the cloning was performed by Dr. Carlos Agustin Isidro Alonso. Dr. Indra Gupta along with the candidate was involved in experimental design and analysis of data with support and advice from Dr. Aimee Ryan.

Chapter 1: Introduction

Epidemiology and Overview of Kidney Stones

Kidney stones affect around 10% of the population in North America and there is evidence that the prevalence has been increasing in recent decades^{1, 2}. It is already much higher in some parts of the world such as the Middle East where it is estimated to affect as much as 25% of the population³. Men are affected more often than women with the lifetime risk of kidney stones estimated to be around 19% for men in the United States⁴. Kidney stones can cause severe discomfort to the patient and can damage the kidneys, especially if they are recurring. Patients with kidney stones have twice the risk of impaired renal function compared to the general population and are at an increased risk of developing chronic kidney disease (CKD)^{5, 6}. This increased risk positively correlates with the number of stone recurring events⁷. Unfortunately, about half of all kidney stone patients have a recurrence within five years of the initial stone⁸.

Kidney stones form when the urine becomes supersaturated with a particular mineral. The mineral crystallizes out of solution and aggregates to form a stone that is retained in the kidney. It is not clear if the stones originate in the tubular lumen of the nephron or originate in the interstitium where they then grow and rupture into the tubular lumen. In either case, once a stone is large enough it can block the flow of urine either at the point where it originated or by breaking free and becoming lodged further down the urinary tract.

Most stones contain calcium crystals and are composed of calcium-oxalate, calcium-phosphate or a mix of the two⁸. Stones can also be composed of struvite, cystine or uric acid. Struvite stones are caused by bacterial infection. Cystine stones are caused by cystinuria, a recessive genetic disorder that is caused by a mutation in a cystine transporter. Uric acid stones form from supersaturated levels of uric acid in the urine which can either be a genetic condition or can be caused by a diet high in meat and seafood⁹. Uric acid in humans is formed through purine degradation and these foods have higher purine content compared to other protein sources.

Certain drugs such as protease inhibitors and long-term use of proton-pump inhibitors are known to promote stone formation¹⁰. Many environmental and lifestyle factors play a role in the risk of stone formation. For instance, obesity, diabetes, and hypertension are all positively associated with kidney stones. Exposure to high temperatures, chronic dehydration, and a diet high in sodium and/or oxalate also contribute to the risk of calcium-based stone formation.

Elevated levels of calcium in the urine, known as hypercalciuria is a major risk factor for calcium-based stones. Hypercalciuria can be caused by either increased calcium excretion or decreased calcium reabsorption in the kidneys. There is some evidence that vitamin D supplementation can lead to hypercalciuria at high doses¹¹. Counterintuitively, high dietary calcium intake does not increase kidney stone risk. A low-calcium diet may even increase the intestinal absorption of oxalate, thereby increasing kidney stone risk.

Treatment options include surgery to remove larger or obstructive stones and anti-lithogenic drugs to decrease the risk of recurrence. The current standard of care includes pain management in the short term and lifestyle interventions such as increasing water intake and dietary changes in the long term to prevent future stone formation¹². In the case of recurrent stone formers, the most commonly prescribed drugs are thiazide diuretics, citrate, and allopurinol¹². Thiazide diuretics work by inhibiting sodium and chloride reabsorption in the distal tubule of the nephron which has the effect of decreasing calcium excretion¹³. Allopurinol is used to reduce uric acid levels in the blood and is an effective treatment for uric acid based stones⁹.

Citrate may directly inhibit the crystallization and aggregation of both calcium-oxalate and calcium-phosphate-based stones or it may work by binding to calcium in the intestines which reduces the urinary calcium load³. Although, the human body has endogenous citrate, levels can be increased by supplementation. Oral supplementation with citrate also decreases the acidity of the urine because the liver metabolizes it to bicarbonate which increases alkalinity³. This is important because many kinds of kidney stones including calcium-based stones precipitate more readily at lower pH levels, although calcium-phosphate stones can also precipitate at abnormally high pH levels as well, so this leaves a narrow window of optimal urine pH to prevent stone formation.

Evidence of Genetic Contribution to Kidney Stone Risk

Although, there are many environmental factors that can instigate or contribute stone formation, there are also genetic risk factors. A large study on the concordance of kidney stones in monozygotic versus dizygotic twins found a 56% heritability of kidney stone risk¹⁴. Another twin study found that electrolyte balance was highly heritable with 52% heritability for 24 hour urinary calcium levels and 43% heritability for 24 hour urinary sodium levels¹⁵. Hypercalciuria

which is one of the biggest risk factors for kidney stones is estimated to have a greater than 50% heritability¹⁶. Around 15% of kidney stone patients seen at clinics have a known monogenic cause¹⁶. For pediatric patients that number increases to around 30%¹⁷. This percent will probably increase as more genes are discovered. Like other common diseases, there are probably also a large number of polygenic risk factors for kidney stones that in combination with other genes and environmental factors have an effect.

Kidney Anatomy and Physiology

The kidneys have a key role in electrolyte and fluid homeostasis in the human body. They filter around 180 liters of blood per day in the average adult¹⁸. The kidneys also maintain the acid/base balance of the body and play a role in blood pressure regulation. Blood enters the kidney and is filtered so that proteins and other large molecules are typically excluded from the urine. Water and ions are reabsorbed by tubular epithelium until a concentrated urine composed of ammonia, uric acid, water, and ions remains. The urine filtrate is then stored in the bladder and excreted from the body. The filtering units of the kidney that are responsible for urine processing are called nephrons.

The nephron begins with the renal corpuscle that includes the Bowman's capsule along with capillaries. The Bowman's capsule feeds into the proximal tubule which reabsorbs around 65% of the filtered solutes that pass through the nephron including 80% of the bicarbonate¹⁸. This segment of the nephron is considered to be leaky as it exhibits a low trans-epithelial electrical resistance (TEER) compared to the rest of the nephron¹⁹. One lab found an average TEER of about $18 \Omega \cdot \text{cm}^2$, although reported TEER values for the proximal tubule vary somewhat and higher values have also been reported²⁰.

After the proximal tubule is the loop of Henle (LOH) which is composed of the thin descending limb followed by the thin ascending limb and the thick ascending limb (TAL) and ending with a small region called the macula densa. The TAL is particularly important as most magnesium is reabsorbed in this section of the nephron²¹. The TAL has a positive voltage maintained by apical K^+ channels which drives the reabsorption of Ca^{2+} and other cations paracellularly. It is also known to have a very low trans-epithelial electrical resistance similar to the proximal tubule¹⁹. Following the LOH is the distal tubule (DT) that typically has a higher

trans-epithelial electrical resistance but is still responsible for some ion reabsorption. The nephron ends with the collecting duct which empties into the ureter which feeds into the bladder.

Calcium and Magnesium Reabsorption Along the Nephron

Although 99% of all calcium in the human body is stored in bone, the 1% that is circulating needs to be tightly regulated so that the amount absorbed in the diet is balanced by the amount that is excreted in the feces and urine²². The concentration of Ca^{2+} in plasma is maintained at 2.1-2.6 mmol/L in the human body²³. While some of this is bound to proteins or interacting with various anions, about half is circulating in its ionized form²⁴. The excretion of this ionized form of Ca^{2+} is regulated by the kidneys and most adults excrete around 200 mg/day in their urine²⁴.

Hypercalciuria can result when the calcium load in the filtrate exceeds the capacity of the nephron to reabsorb it. Most of the calcium reabsorbed by the kidneys (60-70%) is reabsorbed in the proximal tubule of the nephron. This is modulated by the CaSR²⁵. The loop of Henle absorbs 20% of the calcium load and most of that is in the thick ascending limb (TAL). The CaSR also plays a role in regulating calcium absorption in the TAL by modulating the expression of claudins. The calcium reabsorption in both aforementioned segments is for the most part a passive process coupled to sodium reabsorption and occurs paracellularly, but the CaSR also influences active calcium transport in the distal tubule²⁶.

Approximately 15% of the filtered calcium load remains by the time it enters the distal tubule which absorbs about 10% leaving 5% to be absorbed by the collecting duct^{22, 27}. Permeability is low in the distal tubule and collecting duct of the nephron, so calcium reabsorption here takes place predominantly transcellularly through active transport. The first segment of the nephron where there is experimental evidence that calcium-phosphate crystals can precipitate is in the Loop of Henle with calcium-oxalate crystallization occurring downstream in the distal tubule²⁸. Crystals that first appear in these segments then aggregate in the collecting duct and ureter to form a true stone²⁹.

The plasma Ca^{2+} concentration is regulated predominantly by three organs: the intestines (dietary absorption), kidneys (renal reabsorption) and bones (bone turnover) with the help of various hormones such as parathyroid hormone (PTH)³⁰. Magnesium (Mg^{2+}) is a divalent cation that is second only to Ca^{2+} in abundance in the human body and is regulated by the same three

organs³¹. It is re-absorbed by the same paracellular pathways in the nephron that reabsorb Ca^{2+} but in a slightly different distribution. While most of the Ca^{2+} is reabsorbed in the proximal tubule, most of the Mg^{2+} (50-70%) is reabsorbed in the TAL³². About 25% of Mg^{2+} is reabsorbed in the proximal tubule and there appears to be a transcellular pathway for reabsorption in the distal tubule which reabsorbs about 10%^{19, 32}.

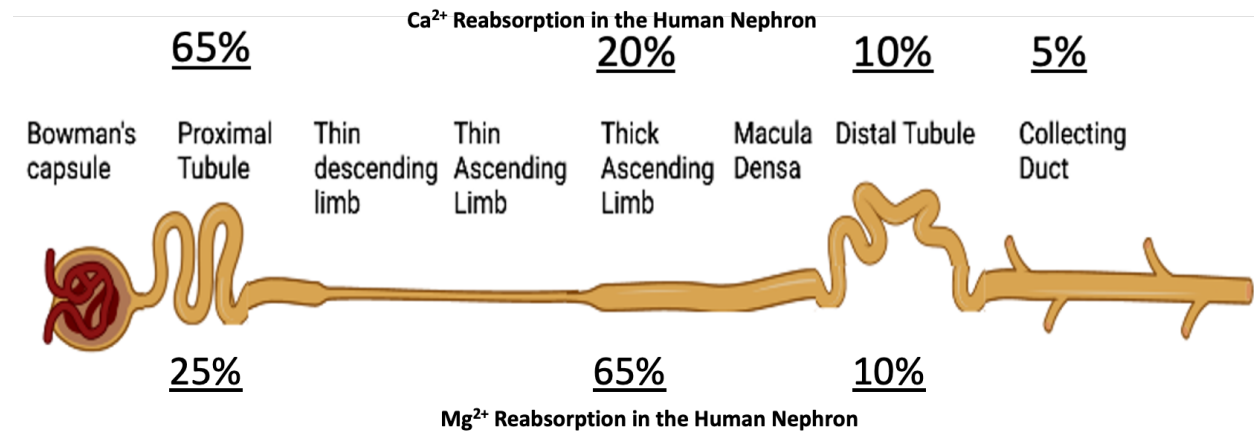


Figure 1: Calcium and Magnesium Reabsorption in the Human Nephron

Hormonal Factors in Ion Homeostasis and Kidney Stones

Aldosterone is crucial in the regulation of sodium (Na^+) and potassium (K^+) homeostasis in the body. When Na^+ levels are low, aldosterone triggers increased reabsorption of Na^+ in the nephron and increased excretion of K^+ by acting on mineralocorticoid receptors³³. These receptors then increase the expression of epithelial sodium channels (ENaC) and $\text{Na}^+-\text{K}^+-\text{ATPase}$ units in the principal cells within the collecting duct^{33, 34}. Aldosterone also influences the composition of the tight junctions in the distal tubule and collecting duct of the nephron by increasing the expression and localization of CLDN8³⁴. This connection between salt intake, aldosterone and CLDN8 has been verified in a mouse model. Mice showed an increase in aldosterone and CLDN8 protein abundance in the kidneys when fed a low salt diet and a decrease in both when fed a high salt diet³⁴. However, when aldosterone is activated inappropriately during periods of high sodium levels it can lead to both heart and renal disease as part of the renin-angiotensin-aldosterone system (RAAS)³³. There is an increased risk of hypertension among kidney stone formers and problems with ion homeostasis may be the causal link³⁵.

Rat models were used to study the effects of testosterone exposure in the womb on later in life hypertension risk. This early testosterone exposure appears to dysregulate the RAAS in adulthood causing increased blood pressure but also appears to selectively target the rate limiting enzyme involved in aldosterone biosynthesis (aldosterone synthase) leading to a significant decrease in circulating plasma levels of aldosterone despite activation of the RAAS³⁶.

Multiple studies have found an association between higher testosterone levels and a higher risk of calcium-oxalate based kidney stones in rat models along with a protective effect of estrogen³⁷. Male mice have lower renal reabsorption of Ca²⁺ and higher urinary Ca²⁺ levels than female mice³⁸. Testosterone and estrogen both appear to influence the transcription of Ca²⁺ transport proteins in the nephron including TRPV5 and calbindin-D28K, with testosterone downregulating and estrogen upregulating these important transporters³⁸.

Although the evidence in humans is less clear-cut, one large-scale study conducted in Taiwan shows that both naturally occurring, and surgically induced menopause increases the risk of developing kidney stones in women³⁹. Another study conducted in China showed that higher estrogen levels in post-menopausal women had a protective effect against calcium-oxalate based kidney stones³⁷. Meanwhile, a large-scale study in Switzerland found a correlation between higher overall androgen levels with higher 24-hour urinary calcium excretion in a cohort of kidney stone formers suggesting an increased kidney stone risk associated with high androgen levels⁴⁰. However, they also found that higher levels of the specific androgen, dehydroepiandrosterone (DHEA) were associated with lower urinary oxalate excretion suggesting a protective effect.

Genes Known to Influence Kidney Stone Formation

There are many monogenic causes of kidney stone formation. Between 30-40 genes with Mendelian inheritance have been identified so far^{17, 41, 42}. These include recessive, dominant, and X-linked mutations. Many studies have also found an association between certain allele variants and kidney stones that may contribute to an overall polygenic risk for kidney stone development.

Mutations in genes that code for amino acid transport proteins can cause kidney stones, such as *SLC3A1* & *SLC7A9* which affect the proximal tubule and cause the disease cystinuria type 1. Mutations in *SLC4A1* which is expressed in the collecting duct of the nephron causes distal renal tubular acidosis along with hypercalciuria and kidney stones. GWAS studies have

found variants in *SLC34A1*, which encodes for a phosphate transporter to also be associated with kidney stones^{43, 44}.

A range of genetic mutations that affect glyoxalate metabolism causes the disease primary hyperoxaluria (PH) which leads to kidney stones and renal dysfunction due to the accumulation of oxalate⁴⁵. Patients with Bartter syndrome have mutations in genes that are involved in sodium transport in the nephron, specifically in the thick ascending limb⁴⁶. This in turn causes hypercalciuria and kidney stone formation. Patients with Dent disease, otherwise known as X-linked nephrolithiasis, typically have a mutation in the chloride channel, *CLCN5* which is expressed in the proximal tubule leading to both hypercalciuria and kidney stones. Notably, there are mutations in multiple members of the *CLDN* gene family that are causal for kidney stones. Claudin proteins are expressed in the tight junctions of epithelial cells throughout the nephron and will be discussed in more detail in subsequent sections.

SNPs in the *MGP* gene that codes for a calcium binding protein, have been associated with a risk of both arterial calcification and kidney stone formation⁴⁷. The protein has a high affinity for hydroxyapatite (otherwise known as calcium phosphate), phosphate ions, and calcium and functions as a calcification inhibitor. Kidney stones can be composed of calcium phosphate making this gene very important for preventing stone formation.

Hypomorphic variants in the *CaSR* have been associated with an increased risk of kidney stones^{48, 49}. Other variants in *CaSR* have been associated with hypercalcemia, hyperparathyroidism, and hypercalciuria along with an increased risk of kidney stones⁵⁰. The calcium sensing receptor (CaSR) blocks calcium absorption in the TAL by stimulating expression of *CLDN14*^{48, 49}. Another way in which the CaSR regulates calcium homeostasis is by decreasing parathyroid hormone (PTH) secretion⁵⁰. CaSR also has a role in fluid reabsorption and acid secretion in the proximal tubule²⁵.

Vitamin D receptor (*VDR*) variants are associated with increased risk and earlier onset for kidney stones^{51, 52}. Vitamin D is necessary to absorb calcium from the diet, therefore gain of function mutations in *VDR* may increase the amount of absorbed calcium while loss of function mutations may decrease the amount of absorbed calcium. Variants in *VDR* have been associated with low bone density and an increased risk of fracture⁵³.

Another mechanism for this may involve citrate which is known to be an inhibitor of calcium-based stone formation. Patients with *VDR* variants have lower urinary citrate levels than

controls and knockdown of the gene in rats causes an increase in calcium excretion in the urine⁵⁴. Another study has paradoxically found that excessive VDR activity causes hypercalciuria in Genetic Hypercalciuric Stone-forming (GHS) rats⁵⁵.

Most likely, there are still monogenic causes that have not been identified and many polygenic risk factors that are not yet known.

The Role of Tight Junctions in Epithelial Cells

Cells in the nephron, like other epithelial tissues, are connected to adjacent cells by complexes of junctional proteins. One such complex is the tight junction which is found in the apical part of lateral cell membranes. Tight junctions indirectly link the actin cytoskeleton of adjacent cells. Tight junctions serve to form an impermeable barrier between epithelial cells, but some are “leakier” than others and allow the passage of select ions between the cells in a process known as paracellular transport.

Notably, the gastrointestinal tract tends to have very leaky tight junctions and therefore exhibits low trans-epithelial electric resistance (TEER)⁵⁶. There are 40 known proteins that can form part of the tight junctions, but ion selectivity and overall leakiness is attributed to a single protein family: the claudins.

Claudin Expression and Function

Claudins are a large family of transmembrane proteins that are important members of the tight junctions of epithelial cells throughout the body, including the nephron. They also play a role in the maintenance of cell polarity⁵⁷. Claudin genes are often dysregulated in cancer and *CLDN6* may act as a tumor suppressor gene⁵⁷. Rare claudin variants have even been implicated in neural tube defects⁵⁸. Claudins range in size from 21-28 kDa⁵⁹. All claudin proteins have two extra-cellular loops and four transmembrane domains. The first extracellular loop is responsible for ion selectivity while the second extracellular loop is responsible for interacting with other claudins to form dimers⁶⁰. The first extra-cellular loop contains a conserved disulfide bond which may help stabilize the protein. The second extra-cellular loop of certain claudins contains a *Clostridium perfringens* enterotoxin (CpE) binding site. The C-terminal end of this enterotoxin (C-CPE) can remove certain claudins from the tight junctions⁶¹. Many viruses target specific claudin proteins to facilitate entry into the cell or to disseminate viral particles including Hepatitis C virus, Dengue virus, West Nile virus and HIV⁶².

Both palmitoylation and phosphorylation can alter the localization of the claudin to the tight junction⁶⁰. Palmitoylation helps the claudin to associate with the membrane by increasing the hydrophobicity through the attachment of fatty acids. In vitro studies using MDCK II cells found that non-palmitoylated CLDN14 could still localize to the tight junctions but not as efficiently as palmitoylated CLDN14⁶³. There are two known palmitoylation sites. Both are in intracellular domains, one following the second transmembrane domain and one following the fourth transmembrane domain.

Phosphorylation allows a claudin to be successfully integrated into the tight junction. There is some evidence that it is the phosphorylation of claudins that regulates the formation of the tight junctions by increasing the colocalization of the claudins with ZO-1^{64, 65}. The region near the C-terminus of the claudin has a phosphorylation site followed by a PDZ binding domain in most, but not all claudins. The PDZ binding domain serves as an interaction site for tight junction-associated cytoplasmic proteins such as ZO-1. This ZO-1 interaction links the claudin to the cytoskeleton of the cell as ZO-1 interacts with actin filaments⁶⁶. Removing this PDZ binding domain, which includes the last four amino acids of the protein can disrupt the function of claudins by interfering with the ZO-1 interaction⁶⁷.

Claudins form both heterodimers and homodimers that create various kinds of ion-specific pores and barriers that together regulate the paracellular exchange of calcium and other ions between epithelial cells⁶⁸. For example, CLDN16 and CLDN19 form a heterodimer that functions as a pore for Ca^{2+} and Mg^{2+} but when CLDN16 binds to CLDN14 instead, this pore function is lost⁶⁹. The first claudins were identified in 1998 and since that time at least twenty-four different claudins have been identified in mammals⁷⁰. Humans only have 23 of these, as CLDN13 is not present⁶⁰. Interestingly, claudins are found even in invertebrates that lack tight junctions such as *C. elegans*⁷¹.

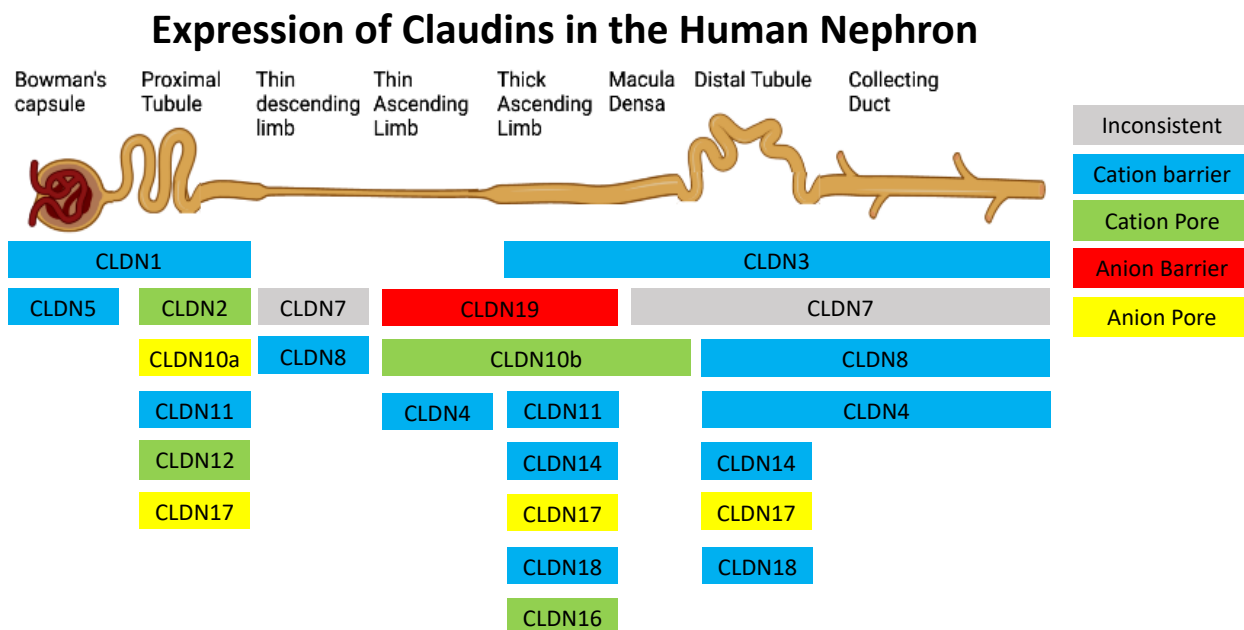


Figure 2: Expression of Claudins in the Human Nephron

Claudin expression in the adult human nephron based on a mixture of protein and RNA expression data from both literature review and Protein expression and RNA expression databases. Only expression where multiple, independent sources agree is shown^{69, 72-78}.

Claudin Variants Associated with Kidney Stones in Animal Models

CLDN2 is expressed in the proximal tubule of the nephron where it forms a homodimer and acts as a cation pore^{68, 79}. It is also expressed in many other tissues including the intestines. Mutations in *CLDN2* have been significantly associated with kidney stone formation in humans and *Cldn2* null mice exhibit hypercalciuria⁴. There is evidence that the hypercalciuria is caused not only by decreased absorption in the proximal tubule but also by decreased intestinal calcium secretion leading to an overall increase in net calcium absorption in the intestines⁴.

Cldn2/Cldn12 double KO mice exhibit a more severe phenotype than either single KO, including reduced bone mineral density, hypocalcemia, and severe hypercalciuria⁸⁰. This is evidence that these two claudins perform a similar but independent function in mice and one can compensate for a reduction in the other.

In mice, CLDN12 is expressed in the proximal tubule of the nephron where it is hypothesized to form a cation pore⁸¹. *Cldn12* knock-out models have reduced calcium permeability in the proximal tubule. However, the knock-out mice appear to compensate for this

by a reduction in the expression of claudins that form cation barriers in other parts of the nephron, so they do not develop hypercalciuria⁸¹. Both CLDN2 and CLDN12 expression in the intestinal tract of mice responds to signaling from vitamin D⁷⁵. *Vdr* knockout mice show decreased expression of both claudins⁷⁵.

CLDN10 is expressed in the TAL of the nephron in both humans and mice. Its function may vary based on the isoform (CLDN10a vs CLDN10b). Mouse knock-out models of *Cldn10* show an increased reabsorption of divalent cations in the TAL of the nephron along with a decrease in sodium reabsorption⁸². These mice also exhibit hypermagnesemia and nephrocalcinosis.

Claudin Variants Associated with Kidney Stones in Humans

Variants in intronic regions of *CLDN2* in humans that cause decreased *CLDN2* expression in the pancreas are associated with an increased risk of nephrolithiasis while noncoding variants that result in increased *CLDN2* expression in the pancreas are associated with an increased risk of pancreatitis and a decreased risk for nephrolithiasis⁴. A rare, gain of function, missense variant in *CLDN2* (G161R) was found to cause both hypercalciuria and kidney stones as well as obstructive azoospermia in a Middle Eastern family^{4, 83}. *CLDN2* is found on the X-chromosome and this variant appears to only cause kidney stones in men, however female carriers do appear to have slightly elevated urine calcium levels⁴.

Synonymous *CLDN14* mutations have been associated with hypercalciuria⁸⁴ and an increased risk for kidney stone formation⁸⁵. A large-scale GWAS study identified two common, synonymous SNPs that strongly correlate with both kidney stones and reduced bone density in an Icelandic cohort: rs219779[C] (R81R) and rs219780[C] (T229T)⁸⁶. These variants result in an increase in transcription of CLDN14. The mechanism responsible for the increase is not known but could be related to mRNA stability or availability of appropriate tRNAs for the codon which could affect the rate of transcription. It is also possible that these synonymous variants are in linkage disequilibrium with an exonic variant that is driving the phenotype.

However, a case-control study out of India identified the minor *CLDN14* variant rs219780[A] as conferring a greater risk for kidney stones than the common variant and a case-control study out of Egypt identified the minor variant rs219780[T] as the risk variant^{87, 88}. It could be that the variant carrying the greatest risk depends on the ethnicity of the patient cohort.

These three synonymous variants all code for the amino acid threonine. There are three different tRNA anticodons (TGA, TGT, TGC) that recognize four different codons for threonine (ACT, ACA, ACG, ACC). These tRNAs are not necessarily present in equal proportions in the human body and it is possible that transcript levels for each different tRNA could vary due to variants in the tRNA genes found in different ethnic populations. This might account for the discrepancy among the various *CLDN14* synonymous variant studies.

Further studies have identified other synonymous, non-coding and intronic variants in *CLDN14* that associate with kidney stones including one (rs78250838:C>T) found in a pediatric cohort that was predicted by in silico analysis to introduce a binding site for the transcription factor, novel insulinoma-associated 1 (INSM1)⁸⁹. Studies in vitro confirmed that INSM1 could bind to the site which was found upstream of *CLDN14* and that this results in increased transcription of *CLDN14* in cultured cells⁸⁹. It was then confirmed in mice that INSM1 is endogenously expressed in the TAL of the nephron, the same location as *CLDN14*⁸⁹.

Meanwhile, non-synonymous, homozygous mutations in *CLDN14* cause a recessive form of non-syndromic deafness that is not associated with kidney stones⁹⁰. The *CLDN14* variants linked to kidney stones all appear to upregulate transcription, resulting in a hypermorphic phenotype, while the variants linked to deafness appear to cause instability in the protein resulting in a hypomorphic phenotype⁸⁵.

In the kidney *CLDN14* is expressed in the distal tubule and the TAL of the nephron where it functions as a cation barrier and helps regulate the exchange of calcium and magnesium^{69, 73, 74}. Expression of *CLDN14* is increased by the CaSR, which is activated by high Ca^{2+} levels. *CLDN14* knockout in animal models causes hypocalciuria and hypomagnesiuria^{91, 92}. There is evidence that *CLDN14* competes with *CLDN19* as an interaction partner for *CLDN16* (also known as Paracellin-1) and disrupts the ability of *CLDN16* to create a cation pore⁹².

Rare mutations in *CLDN16* or *CLDN19* cause the genetic disorder familial hypomagnesemia with hypercalciuria and nephrocalcinosis (FHHNC)⁹³. *CLDN16* & *CLDN19* are expressed in the TAL of the nephron where they form a heterodimer that functions as a cation pore⁹⁴. Patients with FHHNC develop calcium phosphate-based kidney stones and chronic kidney disease due to the disruption of paracellular ion transport in the thick ascending limb of the nephron⁹³. This causes high levels of Ca^{2+} and Mg^{2+} in the urine and progressive deterioration of kidney function. In about half of cases, patients will need renal replacement

therapy by their twenties⁹⁵. Other symptoms include weakness, seizures and in the case of *CLDN19* mutation, loss of vision⁹⁶.

Most of the *CLDN16* mutations that cause FHHNC have an amino acid change in the extracellular loops or one of the transmembrane domains of the protein and result in accumulation of the protein in the endoplasmic reticulum and lysosomes of the cell⁹⁵. However, one *CLDN16* mutation that causes a less severe form of FHHNC causes an amino acid change in the PDZ binding domain of the protein (T233R) which disrupts its ability to interact with ZO-1 and affects its ability to localize to the tight junctions⁹⁷. Although, most of *CLDN16* protein with this mutation accumulates in the lysosomes, a small percent of it is found in the tight junctions which suggests that it can still localize there but might disassociate more readily without ZO-1 anchoring it in place⁹⁷. It is possible that the phenotype of the T233R variant is less severe (in comparison to other *CLDN16* mutations) because this causes a hypomorphic mutation rather than a complete loss of function, resulting in kidney stones but not progressive loss of renal function.

Unfortunately, FHHNC patients see very limited benefit from thiazide diuretics (the current standard of care for kidney stones) and most progress to renal failure with a need for dialysis. One proposed treatment that seems to alleviate calcium wasting in a mouse model of FHHNC is the diuretic furosemide, which is thought to increase the reabsorption of calcium in the distal nephron through TRPV5 stimulation⁹⁸.

The Gupta Lab Kidney Stone Cohort and Sequenced Claudin Variants

The Gupta laboratory recruited a cohort of 114 patients with recurrent, calcium-based kidney stones including both children and adults to determine if any of them had DNA sequence variants in claudin genes. Most of the patients (65%) developed their first stone before the age of 40 and 15% developed their first stone before the age of 20, suggesting they might be genetically predisposed. The majority of the cohort (73%) were Canadians of European descent including French Canadian, but other ancestries were represented as well including Asian, Hispanic, and Middle Eastern. The sex of the cohort was evenly split (50% male, 50% female) and 32% indicated a family history of kidney stones.

Thirteen rare (<1% frequency in gnomAD database) or novel (not found in gnomAD database) sequence variants were identified using next generation sequencing and then

confirmed by Sanger sequencing. However, the reported frequency of some of the variants has changed since the time they were sequenced for this project. One formerly novel mutation (CLDN18 H212D) is now considered rare, and three variants previously considered rare (CLDN8 A94V, CLDN8 M97T, CLDN24 V97I) are no longer considered rare (frequency is now >1% in the gnomAD database). Furthermore, one variant CLDN16 K29E was discovered to be a base-pair change to a non-coding region using the updated human genome reference hg38 (compared to the earlier hg19). This reduced the non-synonymous variants to twelve. Each mutation was found in only one patient. Although, one patient had two distinct non-synonymous, *CLDN4* mutations, the rest were heterozygous for the given mutation. It's not yet clear whether the *CLDN4* mutations were in a cis or trans configuration in the patient.

It is also relevant to note that the cohort was enriched for the common, synonymous *CLDN14* variant rs219780[C] which is associated with an increased risk of kidney stones in European populations⁸⁶. Whereas in the general European population 62% of people are homozygous for [C] at this location; in our cohort 77.6% were homozygous⁸⁶. Only *CLDN* genes were sequenced so it is unknown if any of the patients also harbored other genetic variants associated with kidney stones.

Gene	Chromosome	Base Change	Amino Acid Change	rs#	Frequency	ACMG Prediction	ClinVar Prediction	Varsome Prediction
CLDN4	chr7	c.244G>A	p.A82T	rs782448196	rare	uncertain significance	none	pathogenic
CLDN4	chr7	c.337G>A	p.A113T	rs199567908	rare	likely benign	none	benign
CLDN6	chr16	c.613C>A	p.P211T	N/A	novel	likely benign	none	benign
CLDN7	chr17	c.163G>A	p.V55I	rs1298150934	rare	uncertain significance	none	uncertain
CLDN8	chr21	c.281C>T	p.A94V	rs61743791	0.0135	benign	benign	uncertain
CLDN8	chr21	c.290T>C	p.M97T	rs55884670	0.0168	benign	benign	benign
CLDN11	chr3	c.470C>T	p.S157F	N/A	novel	uncertain significance	none	pathogenic
CLDN12	chr7	c.292A>G	p.M98V	rs76988307	rare	benign	none	benign
CLDN17	chr21	c.281C>T	p.A94V	N/A	novel	uncertain significance	none	uncertain
CLDN18	chr3	c.634C>G	p.H212D	rs1271367873	rare	likely benign	none	benign
CLDN23	chr8	c.268G>A	p.A90T	rs201513699	rare	benign	none	benign
CLDN24	chr4	c.289G>A	p.V97I	rs141964006	0.0216	benign	none	benign

Table 1: Variants and Predicted Effects

Table showing variants and the effects predicted on the website Varsome. Rare is classified as an allele frequency of less than 1% in the general population. Novel is classified as not found in the Varsome database. ACMG is an *in silico* prediction based on allele frequency and conservation of the protein across species. ClinVar is an assessment based on functional data submitted by labs and clinical testing facilities. The Varsome prediction is a combination of the individual pathogenicity scores of several *in silico* prediction tools.

Hypothesis and Aims

Hypothesis:

I hypothesize that the proteins encoded by the claudin sequence variants will affect the permeability and/or paracellular transport of calcium through kidney cell monolayers.

To test this hypothesis, I am performing functional studies on these variants by stably transfecting kidney epithelial cell lines with plasmids carrying the claudin sequence variants identified in the patients. I will test this hypothesis through the following aims:

Aim 1: Determine the localization of WT and variant claudin proteins in kidney epithelial cells.

Aim 2: Measure the permeability of cell layers stably expressing WT and variant claudin proteins.

Chapter 2: Materials and Methods

pEGFP plasmid

The plasmid, pEGFP was used as the vector for expressing both the wildtype and variant claudin proteins. This plasmid uses a CMV promoter to constitutively express the claudin protein with a green fluorescent protein (EGFP) tag fused to the N-terminus. It also uses a SV40 promoter to express a G418 resistance gene which allows for selection of cells using media containing the antibiotic G418 sulfate.

Madin-Darby Canine Kidney Cells (MDCK)

MDCK cells are a cell line that was originally derived from the kidney of a healthy, adult cocker spaniel in 1953 and serve as a model for kidney epithelial cells. Several strains have been developed from the original heterogeneous cell line. MDCK II cells originate from a high passage parental strain. They tend to have “leakier” tight junctions than other MDCK strains (TEER around 100 Ω cm²) and are the most commonly used strain^{99, 100}. MDCK II cells express the following claudins endogenously: CLDN1, CLDN2, CLDN3, CLDN4, & CLDN7¹. Cells were grown in Dulbecco’s Modified Eagle Medium (DMEM) along with 10% fetal bovine serum (FBS) and 1% penicillin/streptomycin from Wisent BioProducts, Quebec, Canada. Cells were incubated at 37 degrees Celsius and 5% CO₂.

Stable Transfection of Plasmids into MDCK Cells

The cells were transfected with the pEGFP plasmid using Polyjet, a lipofectamine based transfection reagent. G418 sulfate from Wisent Biobar (Cat# 400-130-IG) in a concentration of 1.6 mg/mL, replaced the penicillin/streptomycin blend in the media following successful transfection to help select for transfected cells. The cells were then sorted as single cells into a 96 well plate using Fluorescence-activated cell sorting (FACS). Three individual clones expressing the variant and three individual clones expressing the wildtype claudin were grown up from those single cells. Each clone was assigned a unique number (e.g., C1, C2, C3) and in cases where an individual clone was lost, became contaminated or lost GFP expression, the transfection process was repeated to ensure at least 3 stable clones for each WT and variant CLDN.

All plasmids used for transfections were previously sequenced by the former students who did the cloning of the WT and variant claudins in this project. For variants that looked out of the ordinary when imaged, I sent additional samples for sequencing to Genome Quebec. This was done for verification purposes using new primers that I designed.

Immunofluorescence Staining

The GFP tag fused to the N-terminal domain of the claudin protein was used to visualize the location of the claudin in the cells using confocal imaging. For all variants and WT cells, Invitrogen primary antibody mouse ZO-1 was used to mark the location of the tight junctions in the cell with M555 secondary antibody. Glass coverslips were seeded with cells and grown until confluency. The cells were rinsed with phosphate buffer saline (PBS) and fixed with 4% PFA for 20 minutes at room temperature. Cells were blocked for 1 hour at room temperature using 10% normal goat serum (NGS), 0.3% triton-100, in PBS and then incubated with primary antibody overnight at 4 degrees Celsius with primary antibody ZO-1 in concentration: 1/100 from Invitrogen (Ref# 33-9100), 0.3% triton-100 and 5% NGS in PBS. The cells were incubated with Alexa Fluor-conjugated secondary antibody M555 in concentration: 1/500 from Invitrogen (Ref# A21127), 0.3% triton-100, in PBS for 1 hour at room temperature. The cells were incubated in DAPI from Invitrogen at a concentration of 1/1000 in PBS for 15 minutes at room temp. The coverslips were then affixed to glass slides using SlowFade Gold.

To assess colocalization of CLDN8 A94V with the endoplasmic reticulum of the cell a primary antibody to Calnexin was used in concentration of 1/100 from Invitrogen (Ref# PA5-77839), with Alexa Fluor-conjugated secondary antibody R555 in concentration of 1/500 from Invitrogen (Ref# A32732). Endogenous expression of claudins in MDCK cells was assessed using rabbit CLDN8 from Invitrogen (Ref# 40-07002) and rabbit CLDN4 from Invitrogen (Ref# 364800) both in concentration of 1/100 along with Alexa-Fluor conjugated secondary antibody R488 in concentration of 1/500 from Invitrogen (Ref# A11034).

Colocalization Analysis

Slides were imaged using a Zeiss LSM780 laser scanning confocal microscope. Z-stacks were taken, and maximum intensity projections were created using each stack and these were then used to create the images of each variant and WT clone. Colocalization analysis was

performed using Zeiss software to assess the Mander's coefficients (M1 & M2) and the Pearson's correlation coefficient (PCC) of claudin signal localizing with ZO-1 signal^{101, 102}. Most images taken were in Z-stacks so to calculate the Mander's coefficients and PCC scores for colocalization a single image was chosen from each stack based on the brightest ZO-1 signal. At least three images of each clone were chosen based on the best representation of the phenotype.

I kept the settings for M1 and M2 consistent so that M1 always shows the percent of green pixels (CLDN) that colocalize with red pixels (ZO-1) and M2 always shows the percent of red pixels (ZO-1) that colocalize with green pixels (CLDN). This is an important distinction because the CLDN protein in this case is overexpressed while the ZO-1 is endogenous to the cells. So, although I used an amount of antibody that shows the ZO-1 as bright or in some cases brighter than the CLDN there is always more CLDN protein expressed in the cells than there is ZO-1 and this affects these numbers.

The M1 signal denotes the amount of the CLDN that ends up at the tight junctions compared to the total amount of CLDN that is expressed. This means that clones that are expressing more CLDN protein ubiquitously will have a lower M1 score than clones expressing less CLDN protein even if the affinity for the tight junctions is the same because the tight junctions can only hold so much of the CLDN protein and the rest will accumulate in the cytosol leading to a lower percent of the total amount of protein being found in the tight junctions.

The M2 score denotes the overall amount of tight junctions (represented by ZO-1) that have a CLDN localized to them compared to all the ZO-1 that is expressed in the cell. In most cases, ZO-1 is found in the cell junctions (both adherens junctions and tight junctions) and not in the cytoplasm of the cell. CLDNs tend to have a strong affinity for ZO-1 so subsequently the M2 score is consistently very high for most of my clones and is more representative of the research question of this project which is concerned with the amount of CLDN found in the tight junctions.

The Pearson's Correlation Coefficient (PCC) is perhaps the best measure of overall colocalization because it looks at both the colocalization of red with green and the colocalization of green with red and creates an average score taking into account both measures compared to protein abundance. It is still important to evaluate all three because each one gives you different information about the localization of the CLDN.

Western Blot Analysis

RIPA buffer was used for cell lysates. Formula for RIPA buffer: 150 mM NaCl, 5mM EDTA (pH 8), 50mM Tris (pH 8), 1% NP-40 (IGEPAL CA-630), 0.5% sodium deoxycholate, 0.1% sodium dodecyl sulfate (SDS), dH₂O. Lysates were agitated for 30 minutes in RIPA buffer at 4 °C. Protein concentration of lysates was calculated by Bradford assay. Protein samples of approximately 20µg were loaded and run on a 10% SDS-PAGE gel.

The following primary antibodies were used on western blots: rabbit CLDN8 in concentration of 1/500 from Invitrogen (Ref# 40-07002), mouse GAPDH in concentration of 1/10,000 from Cell Signaling Technology (Ref# 2118L). Primary antibodies were left to shake overnight at 4 degrees Celsius. Secondary HRP-linked antibodies both anti-rabbit (Cell Signaling Technology, Ref# 70745) and anti-mouse (Cell Signaling Technology, Ref# 7076S) were used in concentration of 1/5,000.

Transepithelial Electrical Resistance (TEER)

CellZscope[®] system (NanoAnalytics, Münster, Germany) was used to determine the resistance of cell layers through continuous, non-invasive monitoring of cell layers with stable tight junctions (4 days after seeding). Cells were seeded (0.1×10^6 cells) on Falcon Corning inserts with membranes containing size 0.4 µm pores. These were placed in the CellZscope[®] system and incubated at 37 degrees Celsius and 5% CO₂ with 1.5mL of media in basal compartment (below insert) and 0.8mL in the apical compartment (above insert). Media used was DMEM from Wisent Biobar with 10% FBS and 1% penicillin/streptomycin added for both stably transfected cells and untransfected control cells. TEER measurements were started four days after seeding.

Measurements were taken every hour for a period of three days and recorded in $\Omega \cdot \text{cm}^2$. The readings from three wells containing the same clone were then averaged together to create a graphical image of the change in resistance over time but each well was plotted separately for the final 72-hour time point where statistical analysis was done. Three different clones were assessed for each variant.

Dextran Assays

A FITC 4kD neutral dextran was used to assess paracellular permeability. Inserts with cell monolayers were removed from the TEER machine and allowed to recover in fresh DMEM media containing 10% FBS and 1% penicillin/streptomycin for 24 hours before beginning dextran experiment. 1.5mL was added to basal compartment (below insert) and 500uL was added to apical compartment (above insert). A stock solution of 20mg/mL was diluted to a concentration of 100ug/mL by adding 2.5uL to the 500uL in the apical compartment. Cells were then incubated at 37 Celsius for three hours. Three samples of 100uL were taken from the basal compartment and placed in 96 well plate which was analyzed using a Perkin Elmer 1420 multilabel counter plate reader (501 Rowntree Dairy Rd unit 6, Woodbridge, ON 14L 8H1) to determine the fluorescence of each sample, using setting: Fluorescein 485/535nm 1.0s. The fluorescence of the media without dextran (read at the same time as experiment) was subtracted from the fluorescence reading to remove background contributed by the media.

Statistical Analysis

Good Calculators (free online calculator) was used to calculate the Anova one-way analysis of variance for dextran experiments, including degrees of freedom. Two-tailed p-values comparing WT to variant were calculated using GraphPad online calculator unpaired, T-test. In keeping with current convention standards for medical research, p-values were considered significant if less than 0.05. If p-values were greater than 0.01 they were reported to two decimal places, if between 0.01 and 0.001 they were reported to three decimal places, and if less than 0.001 they were reported as $<0.001^{103}$.

Chapter 3: Results

Stable cell lines were created using MDCK II to express the variant and the wildtype sequences for each claudin that was assessed. Three clones of each were assessed to determine if they were able to localize to the tight junction and any difference in permeability to 4kD dextran or transepithelial electrical resistance as shown in Table 2. CLDN antibodies were used to verify that MDCK II cells express endogenous CLDN4 but not CLDN8 (Figure 3).

Gene	Variant	Localization Based on IF	Change in Permeability to Dextran	Change in TEER Resistance
CLDN4	A82T	localizes to tight junctions	no change	no change
CLDN4	A113T	localizes to tight junctions	no change	no change
CLDN6	P211T	localizes to tight junctions	N/A	N/A
CLDN7	V55I	N/A	N/A	N/A
CLDN8	A94V	localizes to the E.R.	increased	decreased
CLDN8	M97T	localizes to tight junctions	increased	no change
CLDN11	S157F	N/A	N/A	N/A
CLDN12	M98V	N/A	N/A	N/A
CLDN17	A94V	localizes to tight junctions	no change	N/A
CLDN18	H212D	N/A	N/A	N/A
CLDN23	A90T	N/A	N/A	N/A
CLDN24	V97I	N/A	N/A	N/A

Table 2: Variant Localization and Permeability

Table showing results of localization and permeability assays. Change in claudin variant transfected cell line is compared to WT transfected cell line. N/A means the variant has not yet been assessed. ER=endoplasmic reticulum.

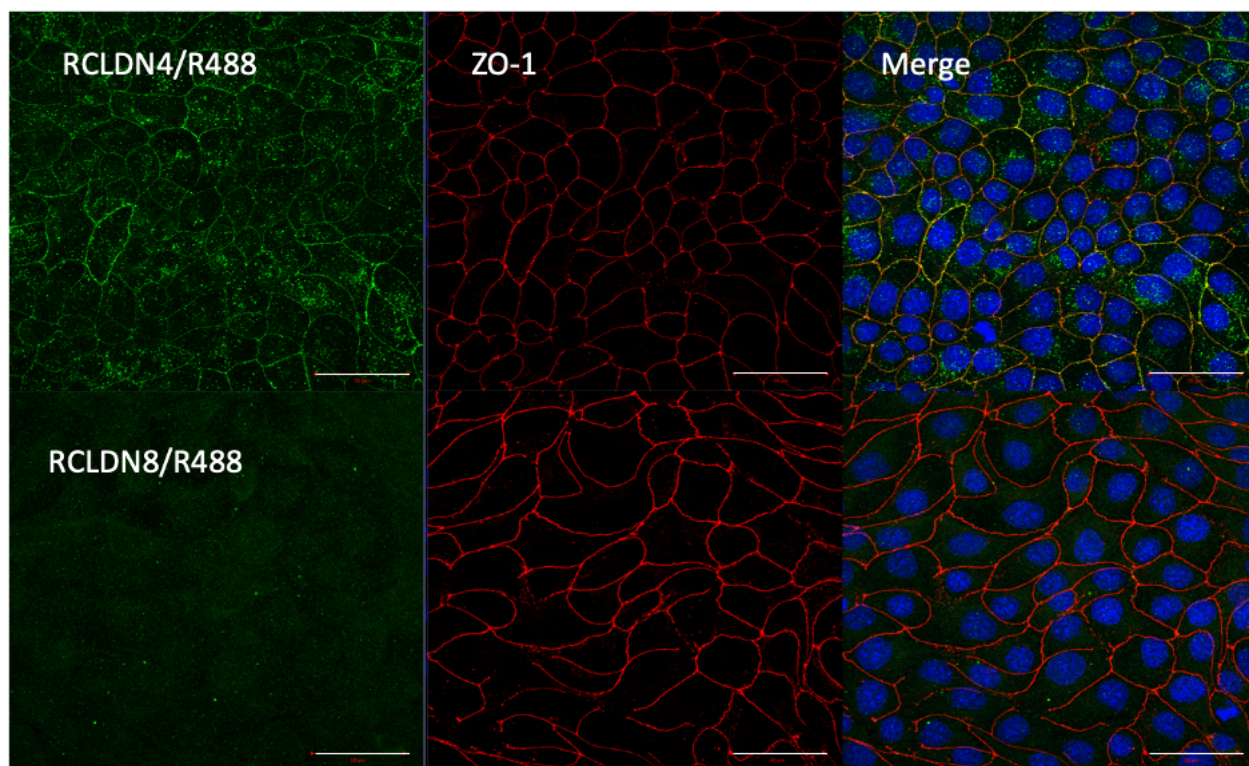


Figure 3: MDCK Cells Showing Endogenous CLDN4 & CLDN8 Expression

Rabbit CLDN4 primary antibody (top) and rabbit CLDN8 primary antibody (bottom) with R488 secondary antibody (green), location of tight junctions marked by ZO-1 (red) and merge showing colocalization of claudin with ZO-1 in yellow, and cell nuclei stained blue with DAPI. This suggests that MDCK II cells express Claudin-4 protein but no to little Claudin-8 protein. Scale bar (shown in white) denotes 50 μm .

primer name	primer sequence 5'-3'
CLDN8A94V fwd	GTTTAGTGAACCGTCAGATCC
CLDN8A94V rev	CAGAATGTGAGCCTTCACC
CLDN8 fwd	ATGGACGAGCTGTACAAGTC
CLDN8 rev	GATCAGTTATCTAGATCCGGTGG
EGFP/CLDN11 fwd	ACGGGACTTTCCAAAATGTCG
EGFP/CLDN11 rev	ACCTCTACAAATGTGGTATGGC
CLDN11/EGFP fwd	GTACAAGTACTCAGATCTCGAGC
CLDN11/EGFP rev	TTATACGTGGGCACTCTTCG

Table 3: Primers Used for Resequencing Plasmids

Table shows primers used to re-sequence the following plasmids: CLDN8 WT, CLDN8 A94V, CLDN11 WT, and CLDN11 S157F

CLDN4 A82T

Confocal imaging with IF showed that this variant could localize to the tight junctions similar to CLDN4 WT (Figure 4). However, the Pearson's Correlation Coefficient (PCC) showed a significant decrease in colocalization compared to WT (Figure 5). TEER experiments showed that there is no difference in resistance between cells expressing CLDN4 A82T, cells expressing CLDN4 WT and untransfected MDCK II cells (Figures 6 & 7). Dextran experiments also showed that there is no difference in cell layer permeability to small molecules between cells expressing CLDN4 A82T and CLDN4 WT (Figure 8).

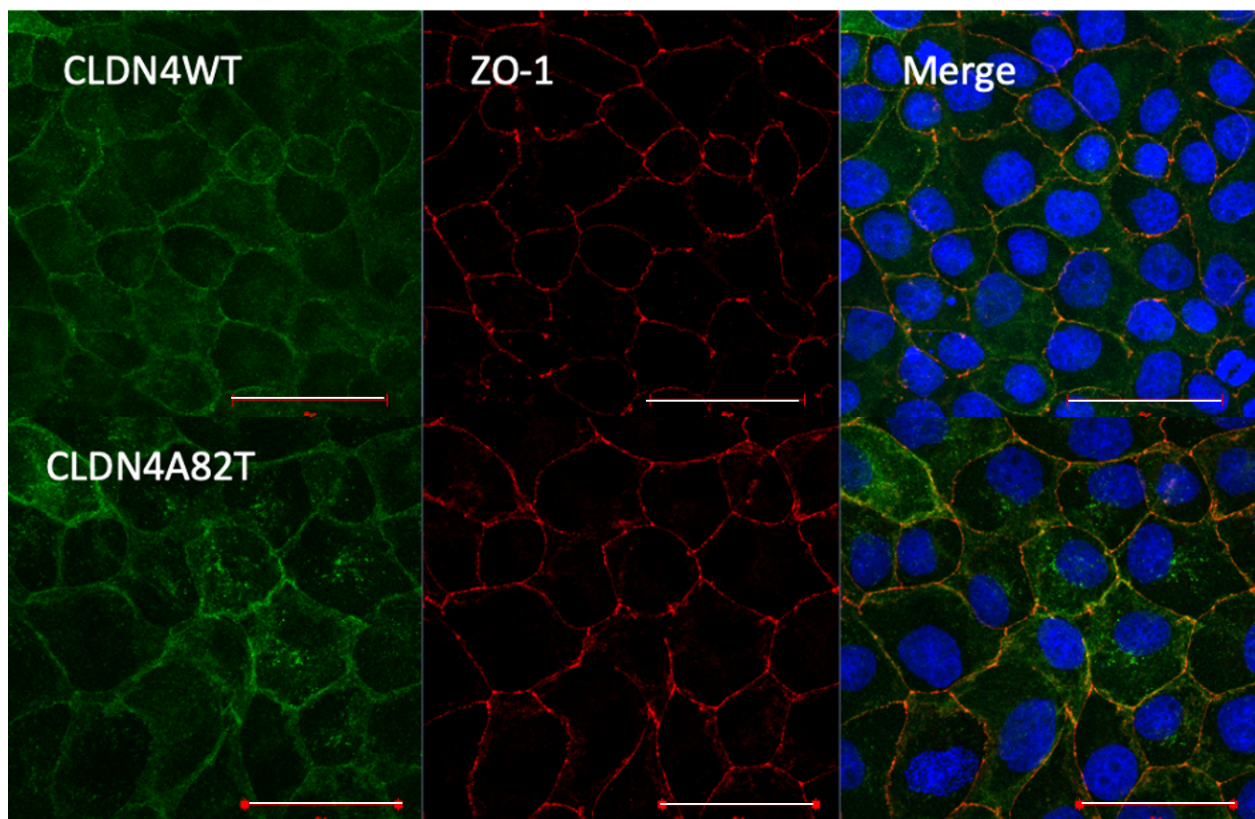


Figure 4: MDCK Cells Stably Transfected with CLDN4WT or CLDN4A82T

Fluorescent images left to right: CLDN4-EGFP fusion protein (green), immunofluorescent detection of tight junction marker zona occludens (ZO-1) (red), and merge with cell nuclei

stained blue with DAPI. CLDN4 WT & CLDN4 A82T co-localize with ZO-1 in the membrane (yellow signal). Scale bar (shown in white) denotes 50 μm .

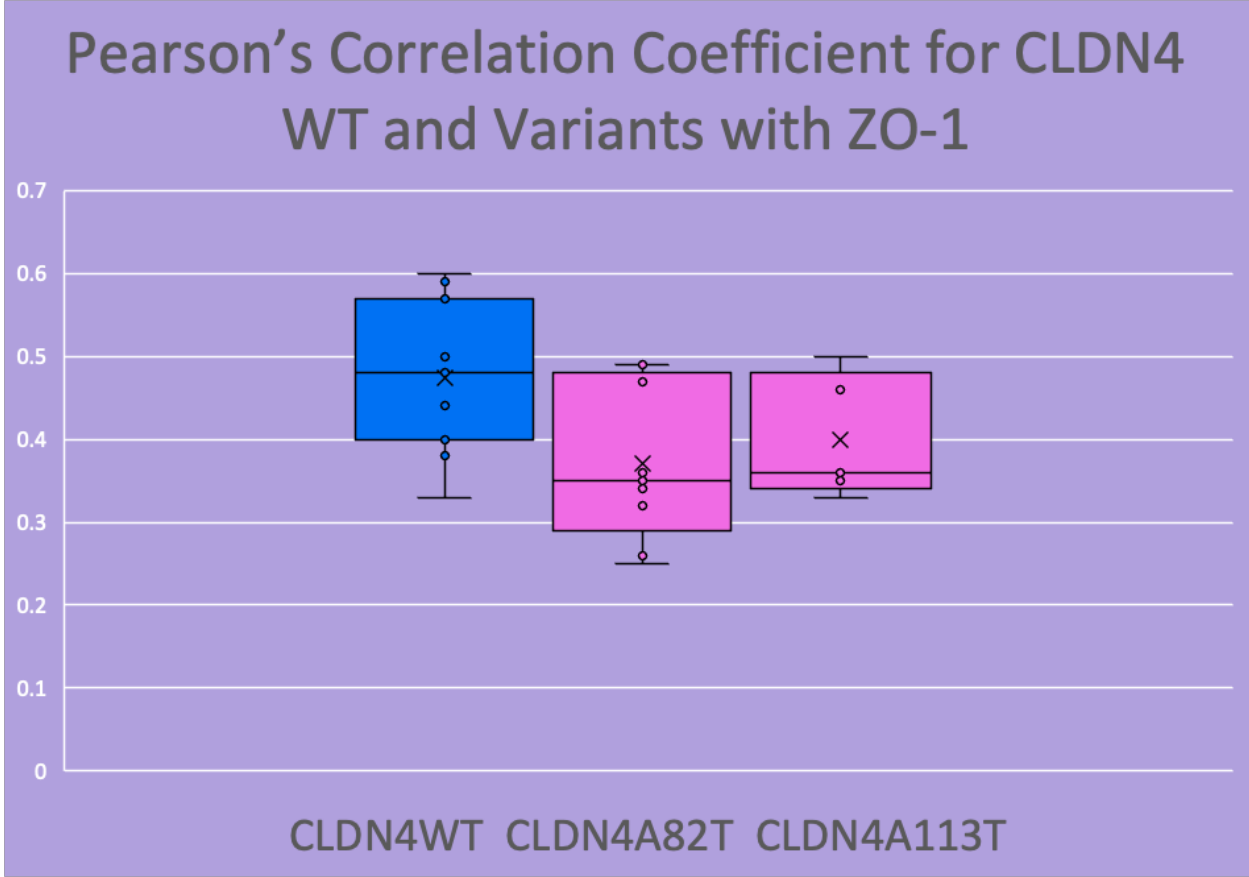


Figure 5: Pearson's Correlation Coefficient of CLDN4WT & Variants

PCC shows that both CLDN4 variants colocalize less well with ZO-1 than CLDN4 WT, however this was only significant for CLDN4A82T. N=3 clones of each variant and WT. CLDN4WT vs CLDN4A82T Student's T-Test p-value=0.02, CLDN4WT vs CLDN4 A113T Student's T-Test p-value=0.13

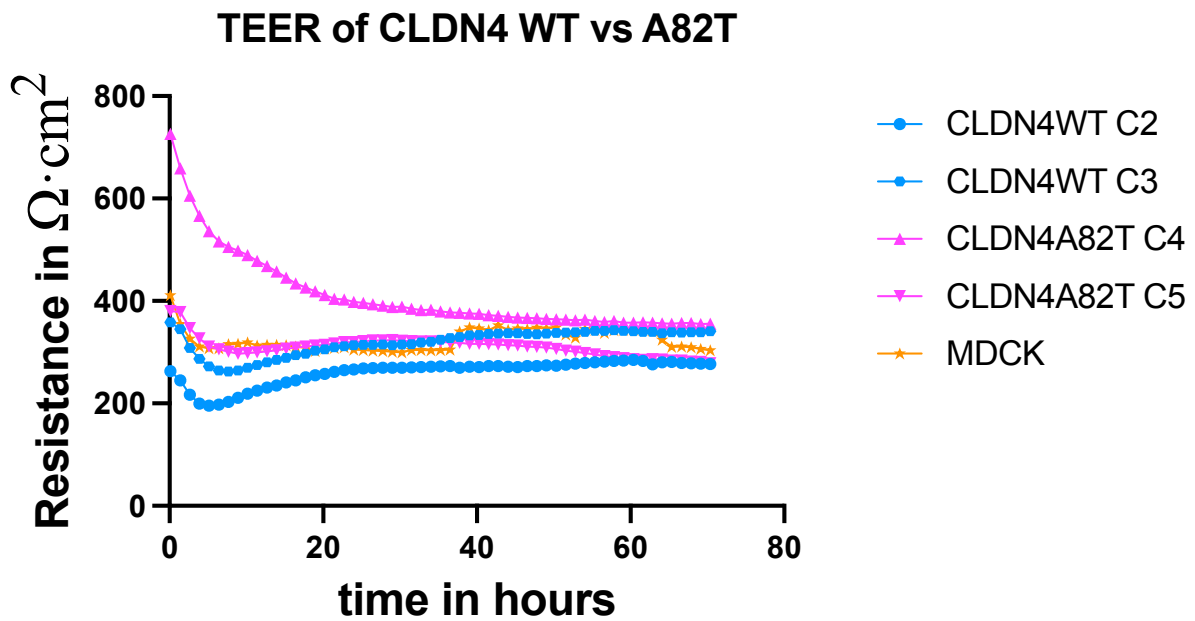


Figure 6: TEER of CLDN4WT vs CLDN4A82T

TEER experiment testing cell monolayers of MDCK II cells transfected with either CLDN4 WT, CLDN4 A82T, or untransfected control MDCK II cells, over the course of 72 hours with time 0 being four days from initial seeding of insert. Each line shown is an average of readings from three wells all containing the same clone. This shows that neither the CLDN4 WT nor CLDN4 A82T clones are different from untransfected MDCK II cells.

TEER at 72 hours for CLDN4 WT and Variants

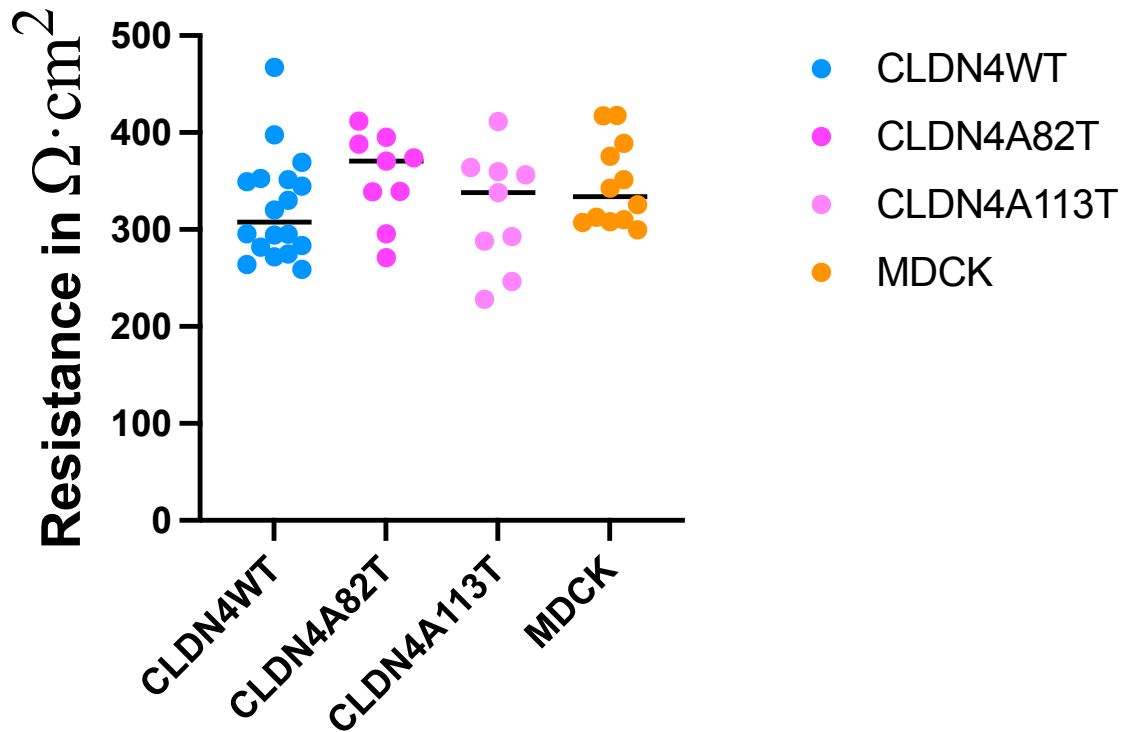


Figure 7: TEER at 72 hours for CLDN4WT & Variants

TEER reading at final 72-hour timepoint (7 days from seeding) for all wells containing MDCK II cells transfected with either CLDN4 WT, CLDN4 A82T, CLDN4 A113T or untransfected control MDCK II cells. This combines three separate TEER experiments. There was no significant change in resistance for CLDN4 A82T clones compared to CLDN4 WT; N=3 clones, Student's T-Test p-value=0.15. There was no significant change in resistance in the CLDN4 A113T clones compared to CLDN4 WT; N=3 clones, Student's T-Test p-value=0.94.

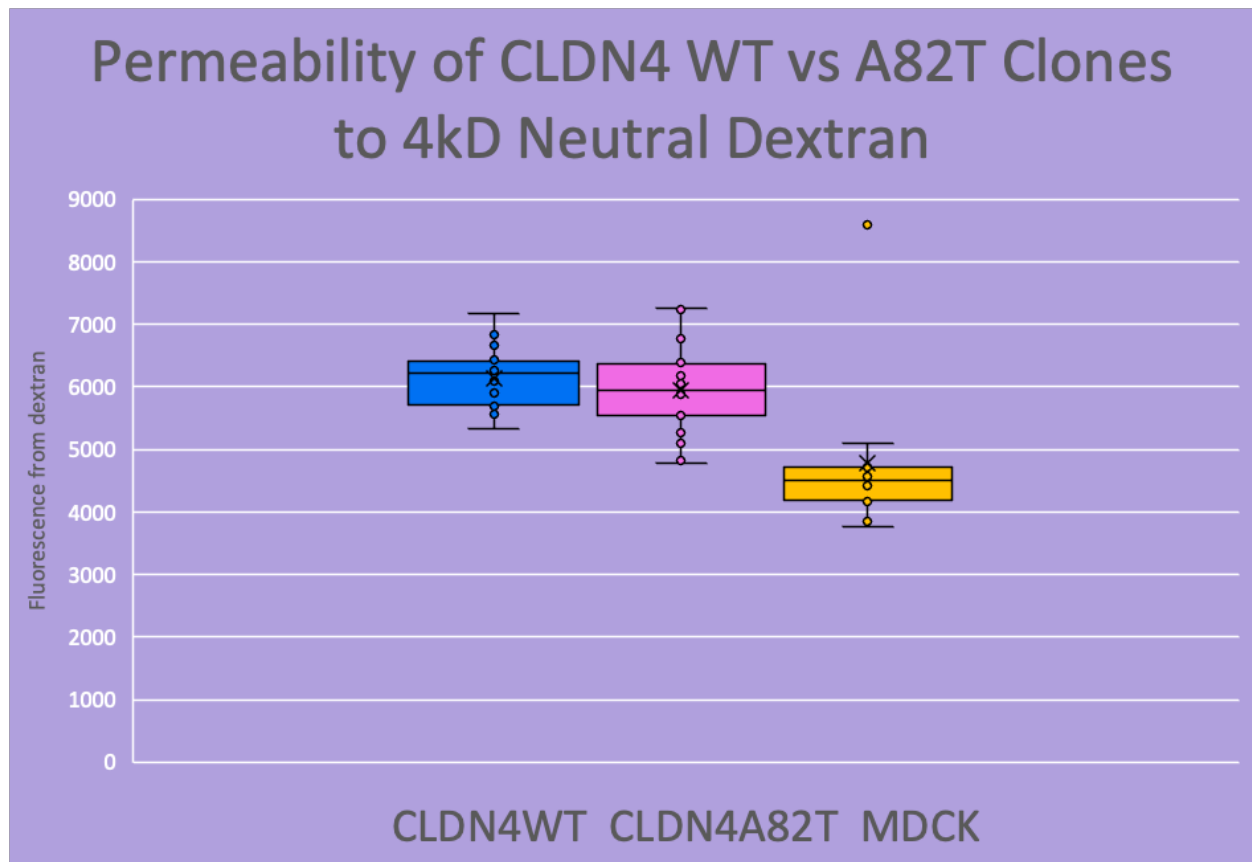


Figure 8: Permeability of CLDN4WT & CLDN4A82T to 4kD Neutral Dextran

Dextran experiment showing the amount of fluorescence due to dextran that made it through a monolayer of MDCK II cells transfected with either CLDN4 WT, CLDN4 A82T, or untransfected control MDCK II cells after 3 hours, (8 days after seeding). This shows that there was no significant difference between CLDN4WT and A82T clones. N=2 clones, Student's T-Test p-value=0.26

CLDN4 A113T

Confocal imaging with IF showed that this variant could localize to the tight junctions similar to CLDN4 WT (Figure 9). The PCC showed a decrease in colocalization compared to WT, but this was not significant (Figure 5). TEER experiments showed that there was no significant difference in resistance between cells expressing CLDN4 A113T, cells expressing CLDN4 WT and untransfected MDCK II cells (Figures 7 & 10). Dextran experiments also showed that there is no difference in cell layer permeability to small molecules between cells expressing CLDN4 A113T and CLDN4 WT (Figure 11).

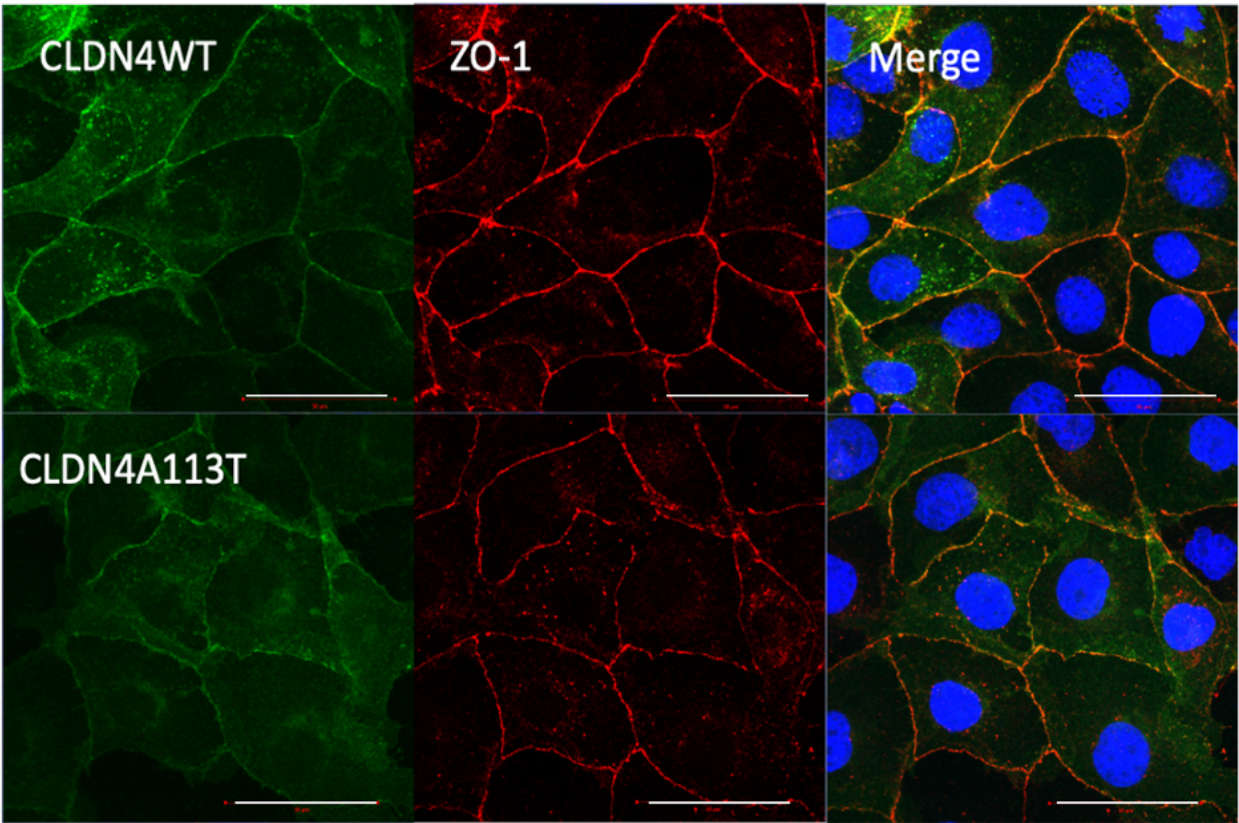


Figure 9: MDCK Cells Stably Transfected with CLDN4WT or CLDN4A113T

Fluorescent images left to right: CLDN4-EGFP fusion protein (green), immunofluorescent detection of tight junction marker zona occludens (ZO-1) (red), and merge with cell nuclei stained blue with DAPI. WT CLDN4 & CLDN4 A82T co-localize with ZO-1 in the membrane (yellow signal). Scale bar (shown in white) denotes 50 μ m.

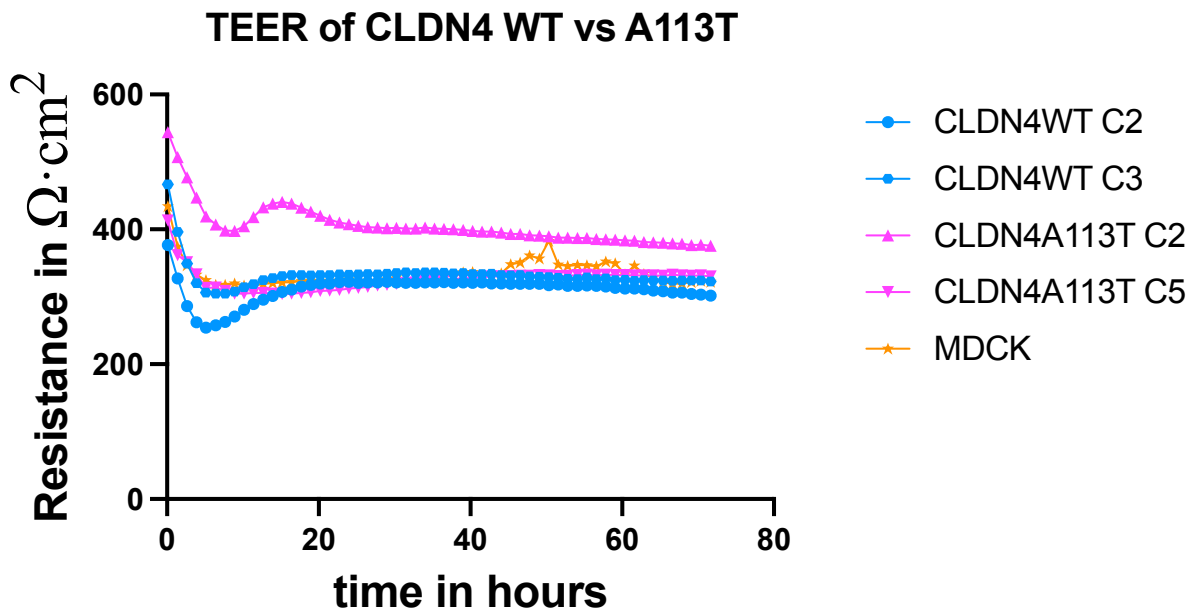


Figure 10: TEER of CLDN4WT vs CLDN4A113T

TEER experiment testing cell monolayers of MDCK II cells transfected with either CLDN4 WT, CLDN4 A113T, or untransfected control MDCK II cells, over the course of 72 hours with time 0 being four days from initial seeding of insert. Each line shown is an average of readings from three wells all containing the same clone. One variant clone does appear to have increased resistance but overall, there is no difference between CLDN4 WT, CLDN4 A113T and untransfected MDCK II cells.

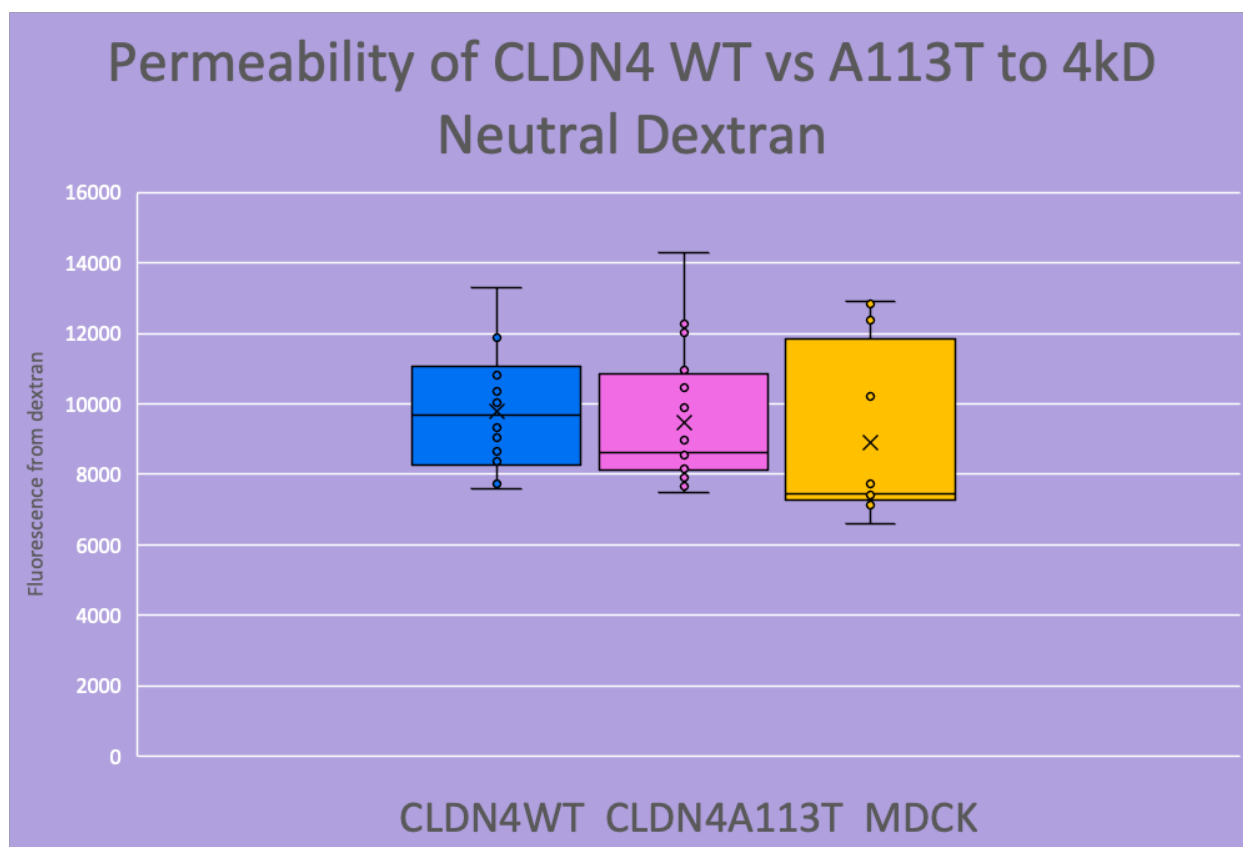


Figure 11: Permeability of CLDN4WT & CLDN4A113T to 4kD Neutral Dextran

Dextran experiment showing the amount of fluorescence due to dextran that made it through a monolayer of MDCK II cells transfected with either CLDN4 WT, CLDN4 A113T, or untransfected control MDCK II cells after 3 hours, (8 days after seeding). This shows there was no significant difference between CLDN4 WT and A113T clones. N=2 clones, Student's T-Test p-value=0.56

CLDN6 P211T

Confocal imaging with IF showed that this variant could localize to the tight junctions similar to CLDN6 WT (Figure 12), however it seemed to cause a significant increase in affinity for the tight junctions compared to CLDN6 WT according to the PCC (Figure 13).

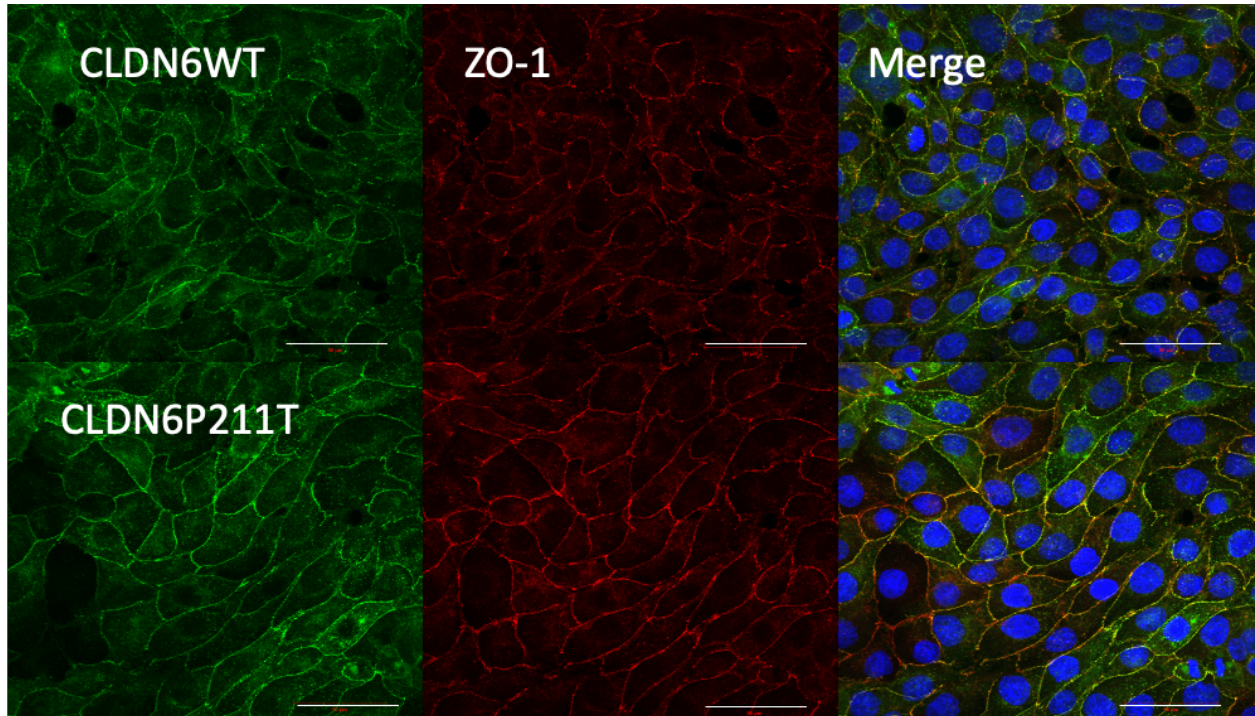


Figure 12: MDCK Cells Stably Transfected with CLDN6WT or CLDN6P211T

Fluorescent images left to right: CLDN6-EGFP fusion protein (green), immunofluorescent detection of tight junction marker zona occludens (ZO-1) (red), and merge with cell nuclei stained blue with DAPI. WT CLDN6 & CLDN6 P211T co-localize with ZO-1 in the membrane (yellow signal). Scale bar (shown in white) denotes 50 μm .

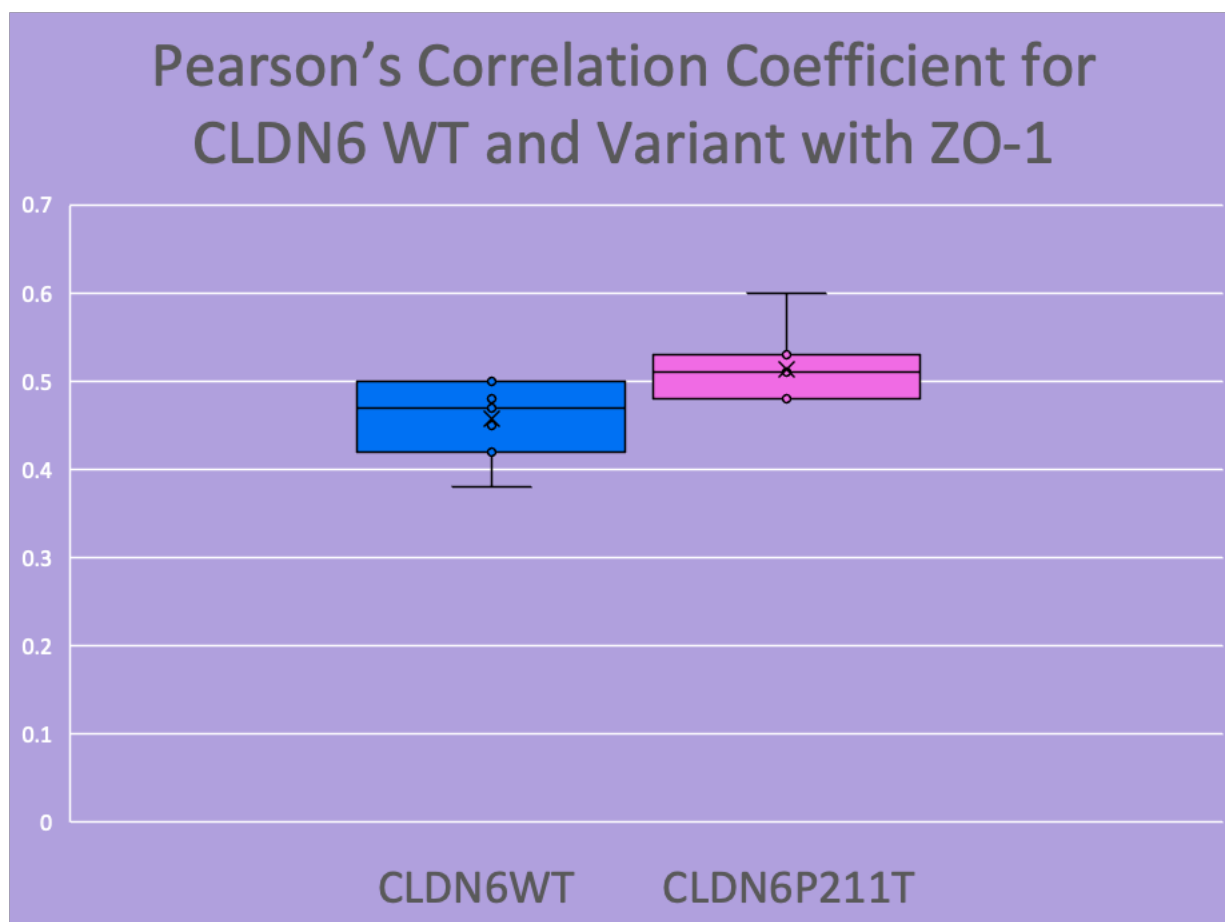


Figure 13: Pearson's Correlation Coefficient for CLDN6WT & CLDN6P211T

PCC shows that CLDN6 P211T colocalizes to the tight junctions better than CLDN6 WT. N=3 clones of both WT and variant, Student's T-Test p-value= 0.03

CLDN8 A94V

CLDN8 A94V failed to localize normally to the tight junctions of MDCK II cells (Figure 14). Most of the protein was detected perinuclearly and in the cytoplasm with only a small amount appearing in the membrane. Even when in the membrane, it did not appear to have significant overlap with ZO-1 which suggested that it was not efficiently localizing to the tight junctions. The Mander's M1 score (Figure 15) which shows the amount of CLDN colocalized with ZO-1, showed that despite the appearance of the protein, there was in fact some CLDN8 A94V protein making it to the tight junctions. However, the Mander's M2 score (Figure 16) which shows the amount of ZO-1 colocalized with CLDN, and Pearson's Correlation Coefficient (PCC) (Figure 17) showed that the variant colocalized much less well than WT.

Calnexin (a chaperone protein) was used as a marker for the endoplasmic reticulum (ER) of the cell. IF imaging showed overlap between the location of calnexin and the location of the variant CLDN8 A94V which suggests that after translation, the protein was trapped within the ER and unable to move into the Golgi apparatus (Figure 18).

I re-sequenced the plasmid that I used to transfect the cells and confirmed that both the WT and variant claudin-EGFP fusion were in frame and that there were no other mutations within the protein. The primers, shown in Table 3, were specifically designed to establish that the eGFP was in frame with CLDN sequence. Further IF experiments showed that while CLDN8 WT colocalized with CLDN4 in the tight junction of MDCK II cells, CLDN8 A94V had little to no colocalization with CLDN4.

TEER experiments showed that cells expressing CLDN8 A94V had reduced resistance compared to cells expressing CLDN8 WT and untransfected MDCK II cells which means that the cell layers should be more permeable to ions like calcium (Figures 19 & 20). Meanwhile, dextran experiments showed that cell layers expressing CLDN8 A94V had increased permeability to neutral small molecules compared to CLDN8 WT (Figure 21). A western blot showed a decrease in CLDN8 protein compared to WT for the A94V variant (Figures 25-27).

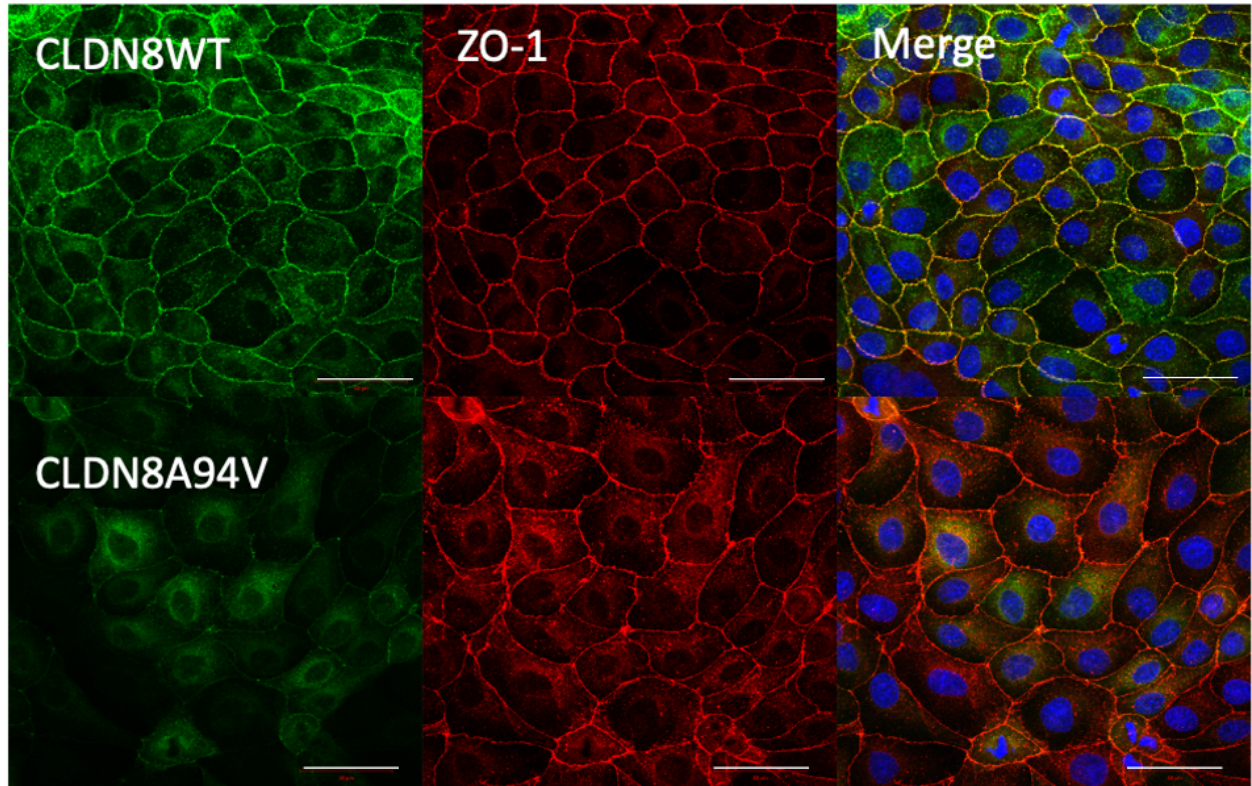


Figure 14: MDCK Cells Stably Transfected with CLDN8WT or CLDN8A94V

Fluorescent images left to right: CLDN8-EGFP fusion protein (green), immunofluorescent detection of tight junction marker zona occludens (ZO-1) (red), and merge with cell nuclei stained blue with DAPI. WT CLDN8 co-localizes with ZO-1 in the membrane (yellow signal). CLDN8A94V localizes around the nucleus of the cell, does not show strong co-localization with ZO-1 and exhibits decreased EGFP signal. Scale bar (shown in white) denotes 50 μ m.

Mander's M1 score for CLDN8 for Colocalization of CLDN8WT and Variants with ZO-1

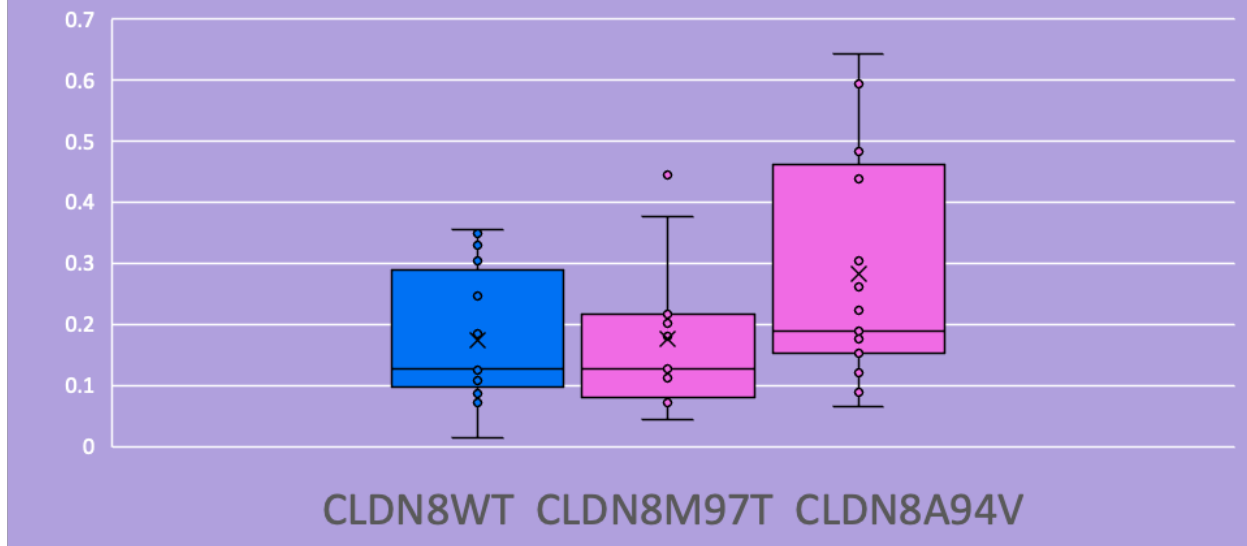


Figure 15: Mander's M1 for CLDN8WT & Variants

M1 shows that a greater percent of the overall CLDN8 A94V variant colocalizes with ZO-1 compared to CLDN8 WT (Student's T-test p-value=0.04), while there is no significant difference between the WT protein and CLDN8 M97T variant (Student's T-test p-value=0.94). This is deceptive however, due to the difference in protein abundance which is not factored into this score. CLDN8 WT has far more protein abundance in the cells based on Western blot and so there is more left-over protein in the cells with no ZO-1 partner to colocalize with. Still, this does suggest that at least some of the CLDN8 A94V protein is making it to the tight junctions.

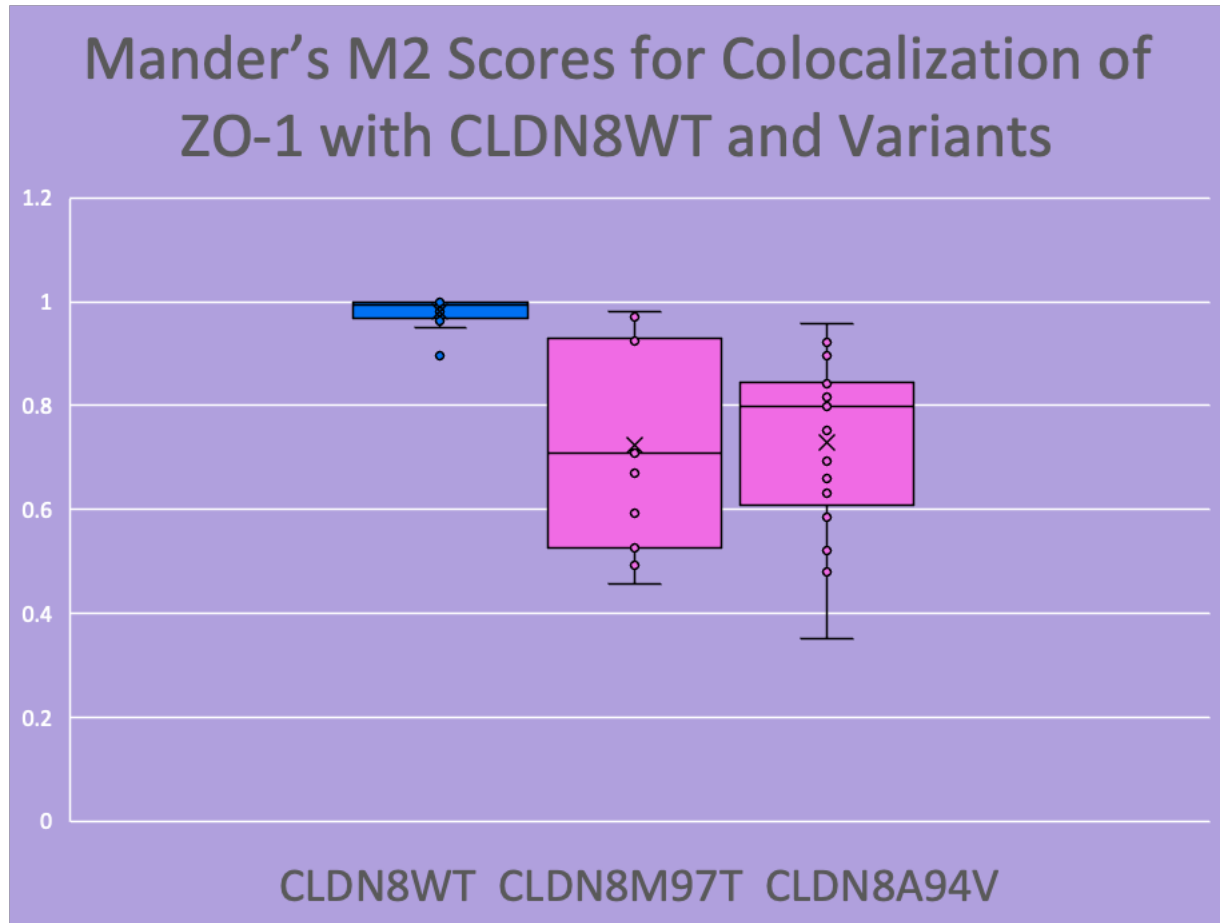


Figure 16: Mander's M2 for CLDN8WT & Variants

M2 shows that ZO-1 colocalizes less with both CLDN8 variants than with CLDN8 WT. N=3 clones of each variant and WT. CLDN8WT vs CLDN8A94V Student's T-Test p-value<0.001, CLDN8WT vs CLDN8 M97T Student's T-Test p-value<0.001

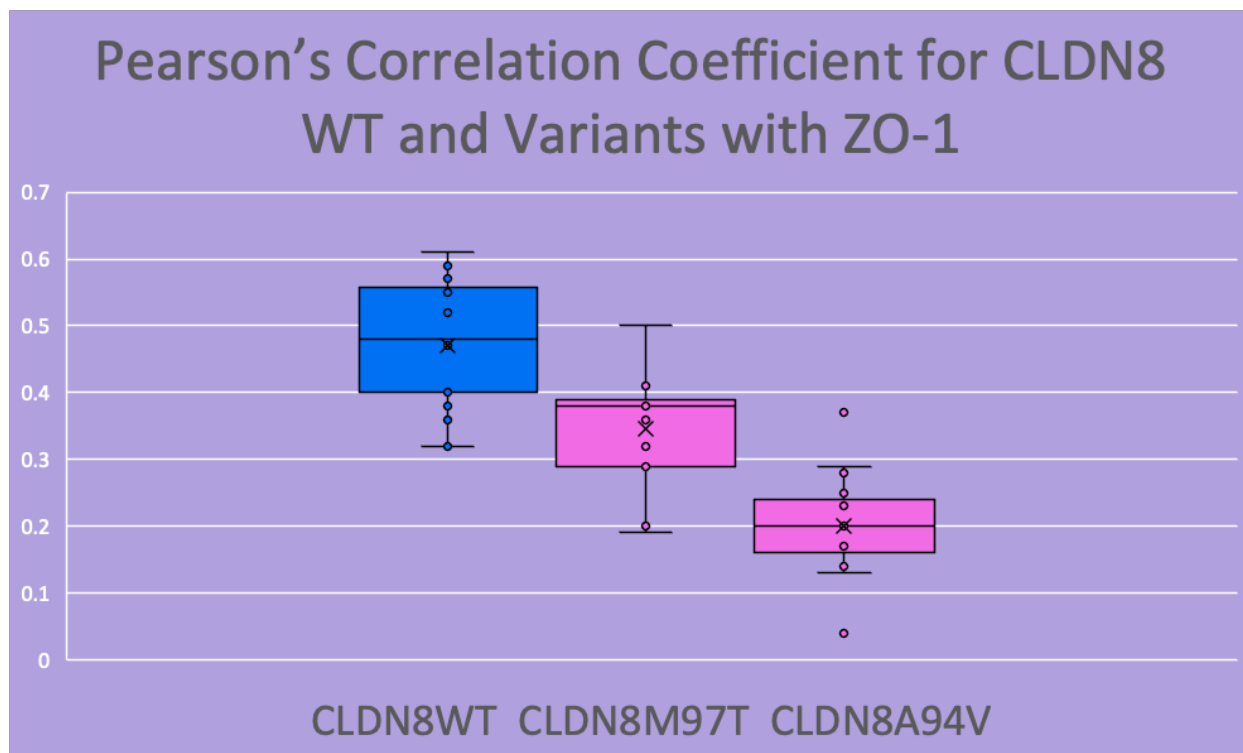


Figure 17: Pearson's Correlation Coefficient for CLDN8WT & Variants

PCC shows that both CLDN8 variants colocalize less well with ZO-1 than CLDN8 WT. N=3 clones of each variant and WT. CLDN8WT vs CLDN8A94V Student's T-Test p-value <0.001, CLDN8WT vs CLDN8 M97T Student's T-Test p-value=0.001

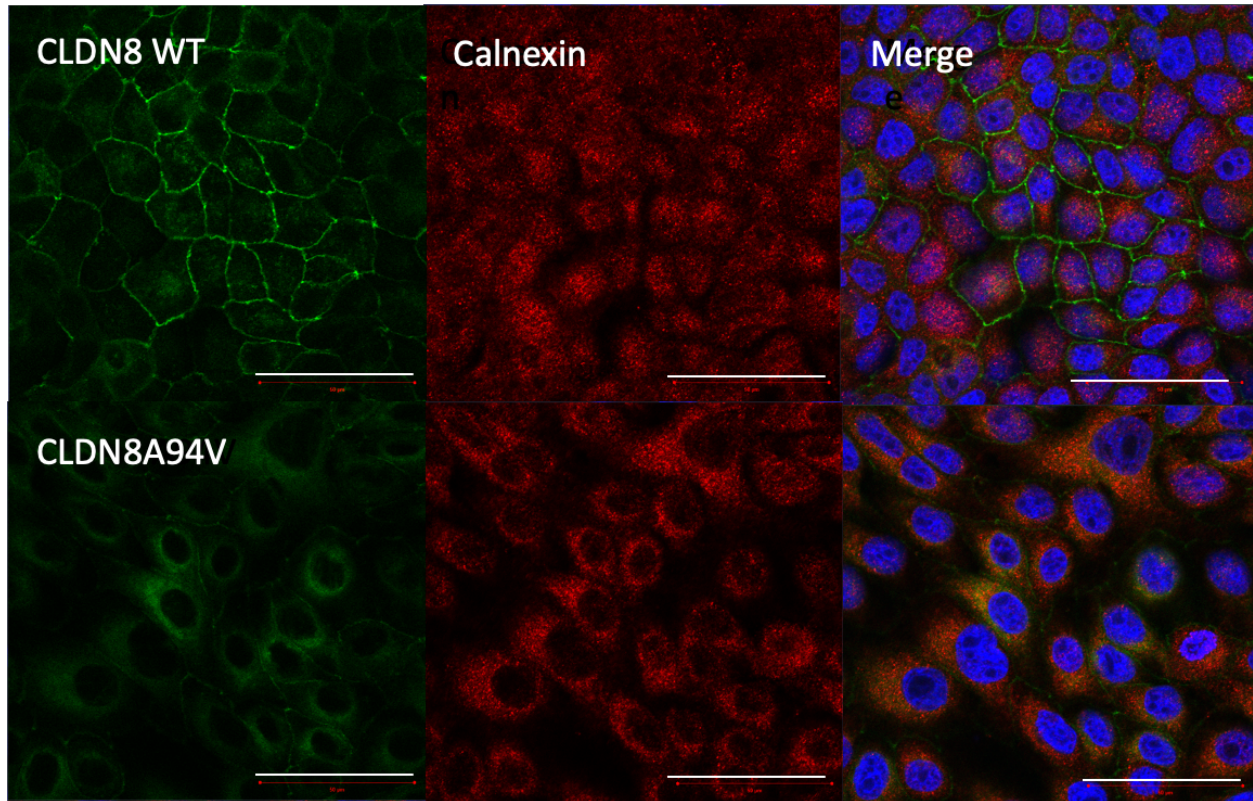


Figure 18: CLDN8WT & CLDN8A94V with Calnexin Antibody

Fluorescent images left to right: CLDN8-EGFP fusion protein (green), immunofluorescent detection of endoplasmic reticulum marker calnexin (red), and merge with cell nuclei stained blue with DAPI. CLDN8 A94V shows localization that overlaps with localization of calnexin. Scale bar (shown in white) denotes 50 μm .

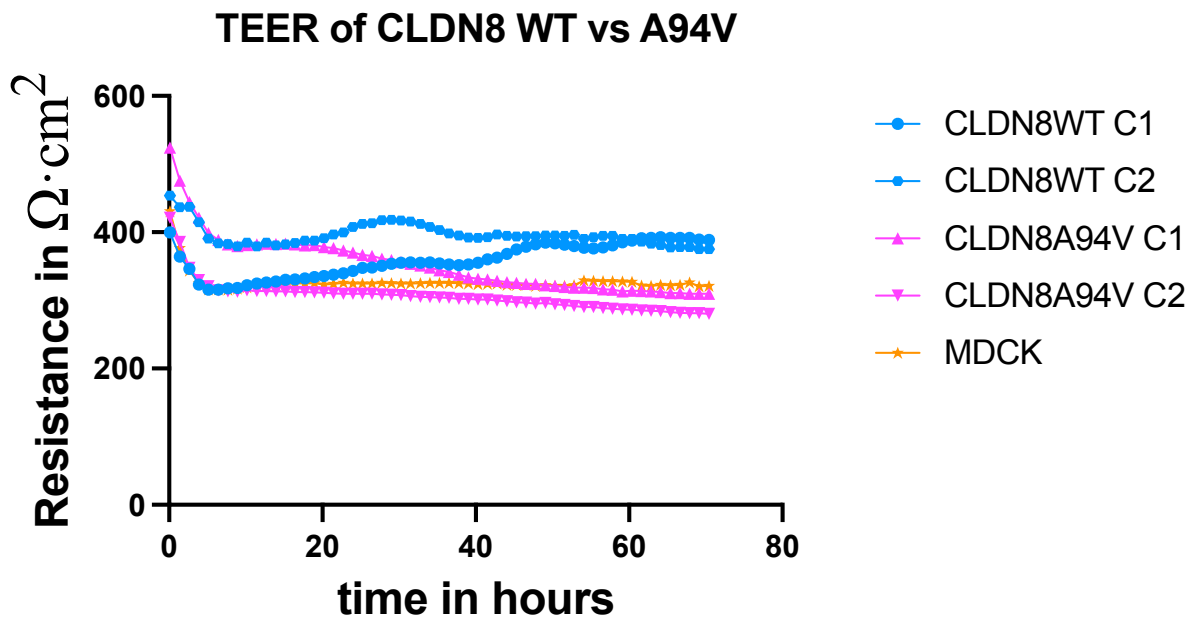


Figure 19: TEER of CLDN8WT vs CLDN8A94V

TEER experiment testing cell monolayers of MDCK II cells transfected with either CLDN8 WT, CLDN8 A94V, or untransfected control MDCK II cells, over the course of 72 hours with time 0 being four days from initial seeding of insert. Each line shown is an average of readings from three wells all containing the same clone. This shows that CLDN8WT transfected cells have an increased resistance compared to both the A94V variant and untransfected MDCK II cells. Meanwhile the variant CLDN8 A94V has lower resistance than even untransfected MDCK II cells.

TEER Reading at 72 hours for CLDN8 WT and Variants

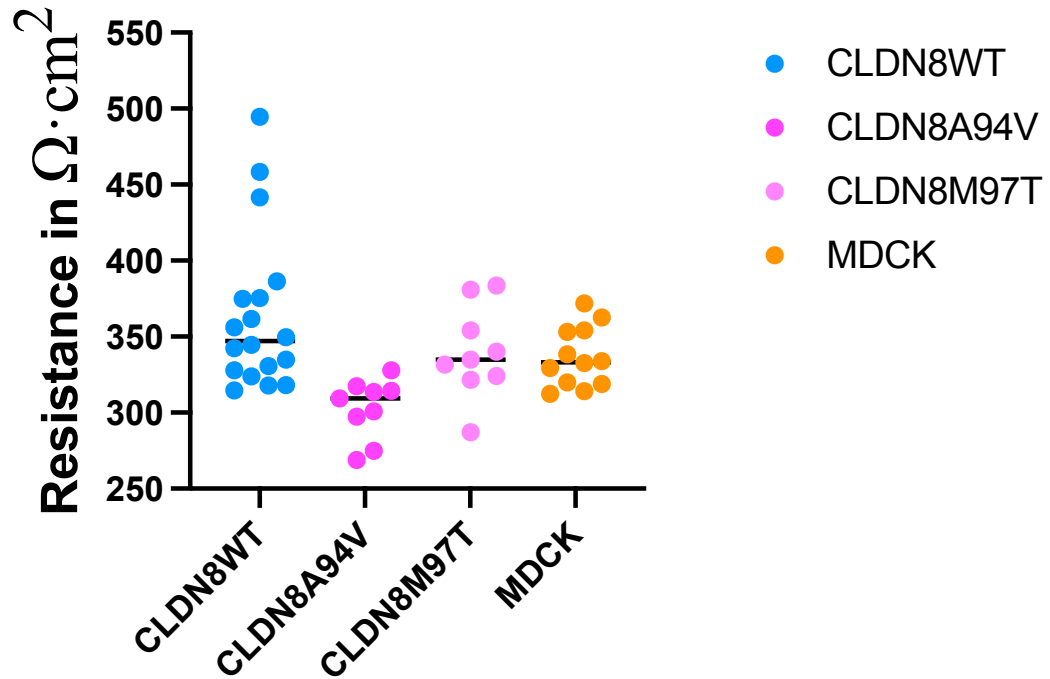


Figure 20: TEER Reading at 72 hours for CLDN8WT & Variants

TEER reading at final 72-hour timepoint (7 days from seeding) for all wells containing MDCK II cells transfected with either CLDN8 WT, CLDN8 A94V, CLDN8 M97T or untransfected control MDCK II cells. This combines three separate TEER experiments. There was a significant decrease in resistance showing an increase in ion permeability in the CLDN8 A94V clones compared to CLDN8 WT; N=3 clones, Student's T-Test p-value=0.005. There was no significant difference in the CLDN8 M97T clones compared to CLDN8 WT; N=3 clones Student's T-Test p-value= 0.54

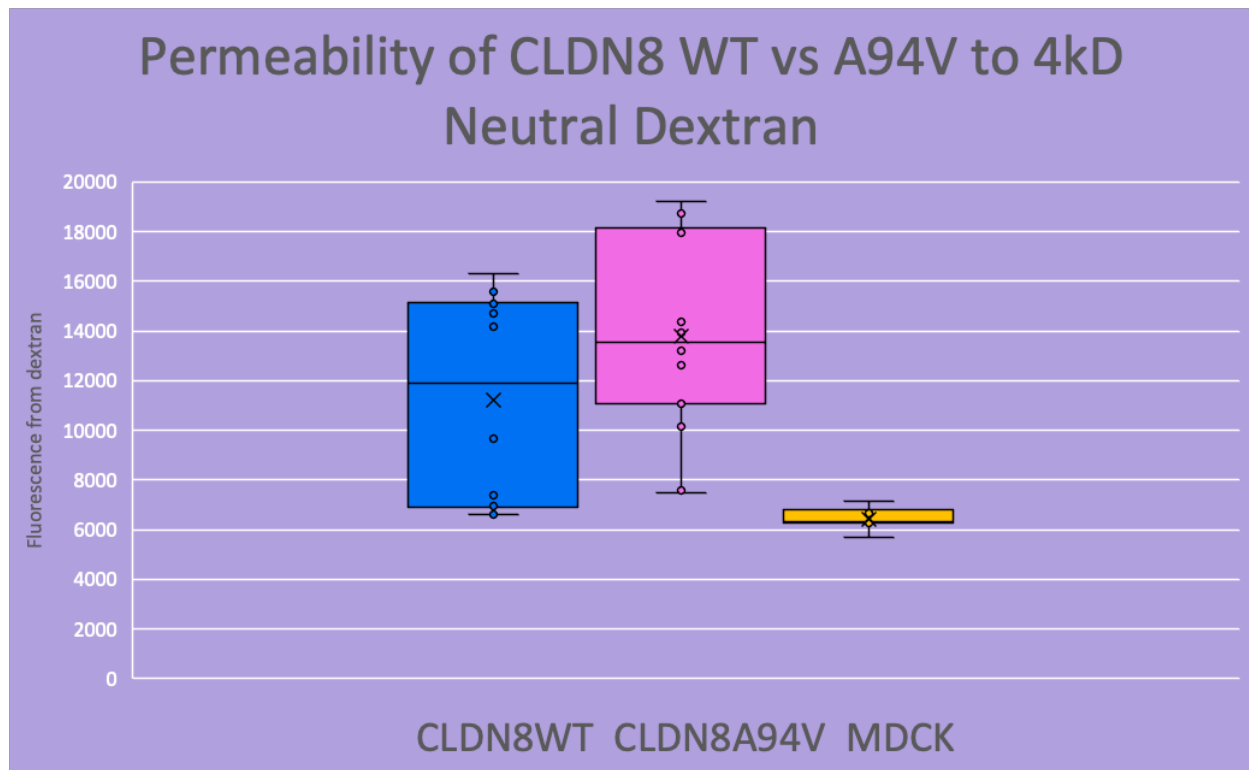


Figure 21: Permeability of CLDN8WT & CLDN8A94V to 4kD Neutral Dextran

Dextran experiment showing the amount of fluorescence due to dextran that made it through a monolayer of MDCK II cells transfected with either CLDN8 WT, CLDN4 A94V, or untransfected control MDCK II cells after 3 hours, (8 days after seeding). This shows a non-significant increase in permeability among the CLDN8 A94V clones compared to WT. N=2 clones, Student's T-Test p-value=0.06

CLDN8 M97T

Confocal imaging showed that this variant could localize to the tight junctions (Figure 22), however based on the M2 (Figure 16) and PCC (Figure 17), it didn't localize as well as CLDN8 WT. TEER experiments showed no significant difference in resistance of the variant compared to WT (Figures 20 & 23) so it is unclear if ion permeability would be affected. Dextran experiments, however, did show an increase in permeability to small molecules (Figure 24). A western blot showed a large decrease in CLDN8 protein expression compared to WT (Figures 25-27).

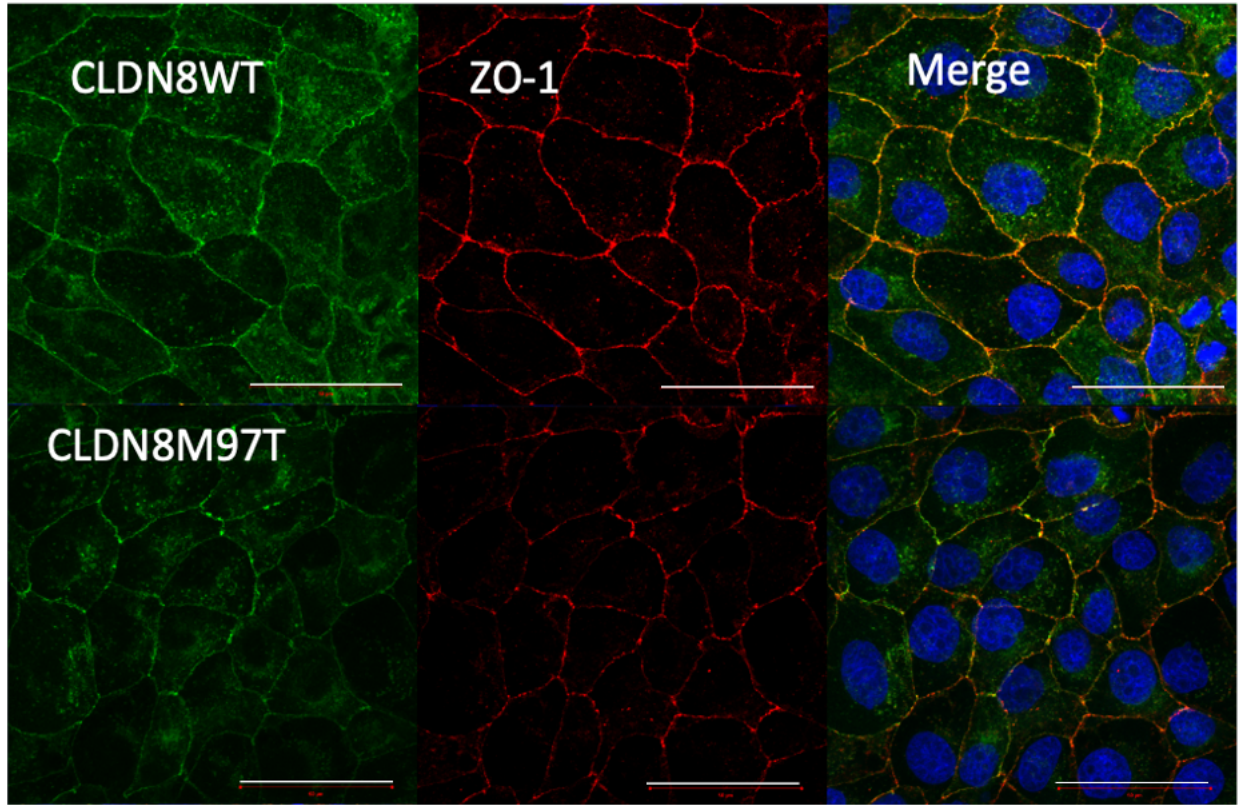


Figure 22: MDCK Cells Stably Transfected with CLDN8WT or CLDN8M97T

Fluorescent images left to right: CLDN8-EGFP fusion protein (green), immunofluorescent detection of tight junction marker zona occludens (ZO-1) (red), and merge with cell nuclei stained blue with DAPI. WT CLDN8 & CLDN8 M97T co-localize with ZO-1 in the membrane (yellow signal). Scale bar (shown in white) denotes 50 μm .

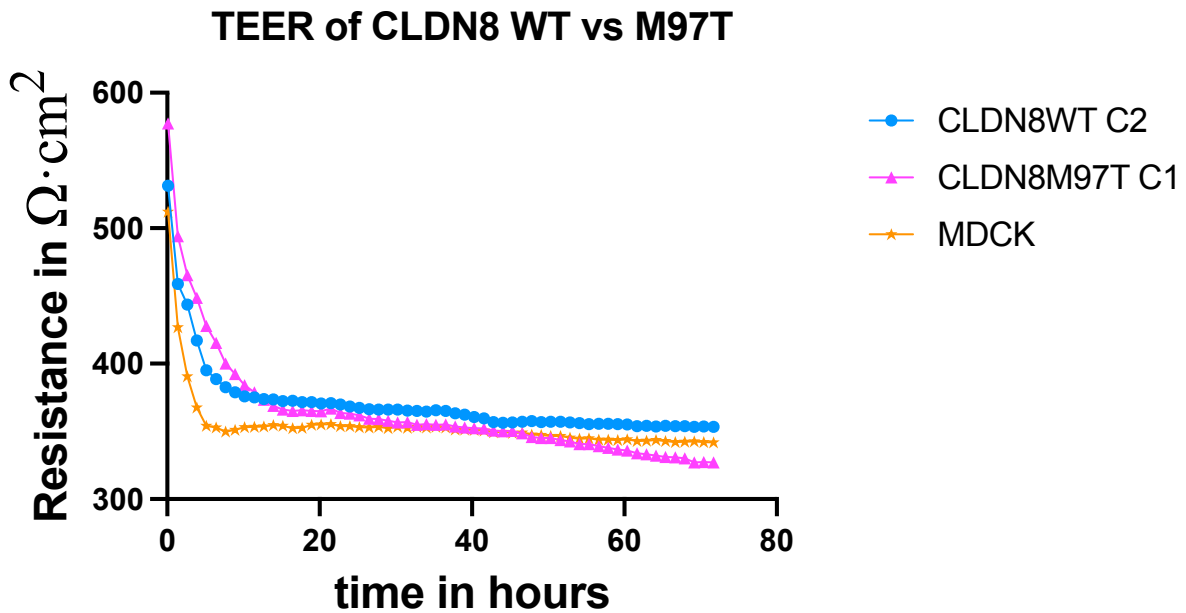


Figure 23: TEER of CLDN8WT vs CLDN8M97T

TEER experiment testing cell monolayers of MDCK II cells transfected with either CLDN8 WT, CLDN8 M97T, or untransfected control MDCK II cells, over the course of 72 hours with time 0 being four days from initial seeding of insert. Each line shown is an average of readings from three wells all containing the same clone. This experiment suggests that there could be a decrease in resistance for this CLDN8 M97T clone although aggregated data suggests any difference is not significant. (See figure 27)

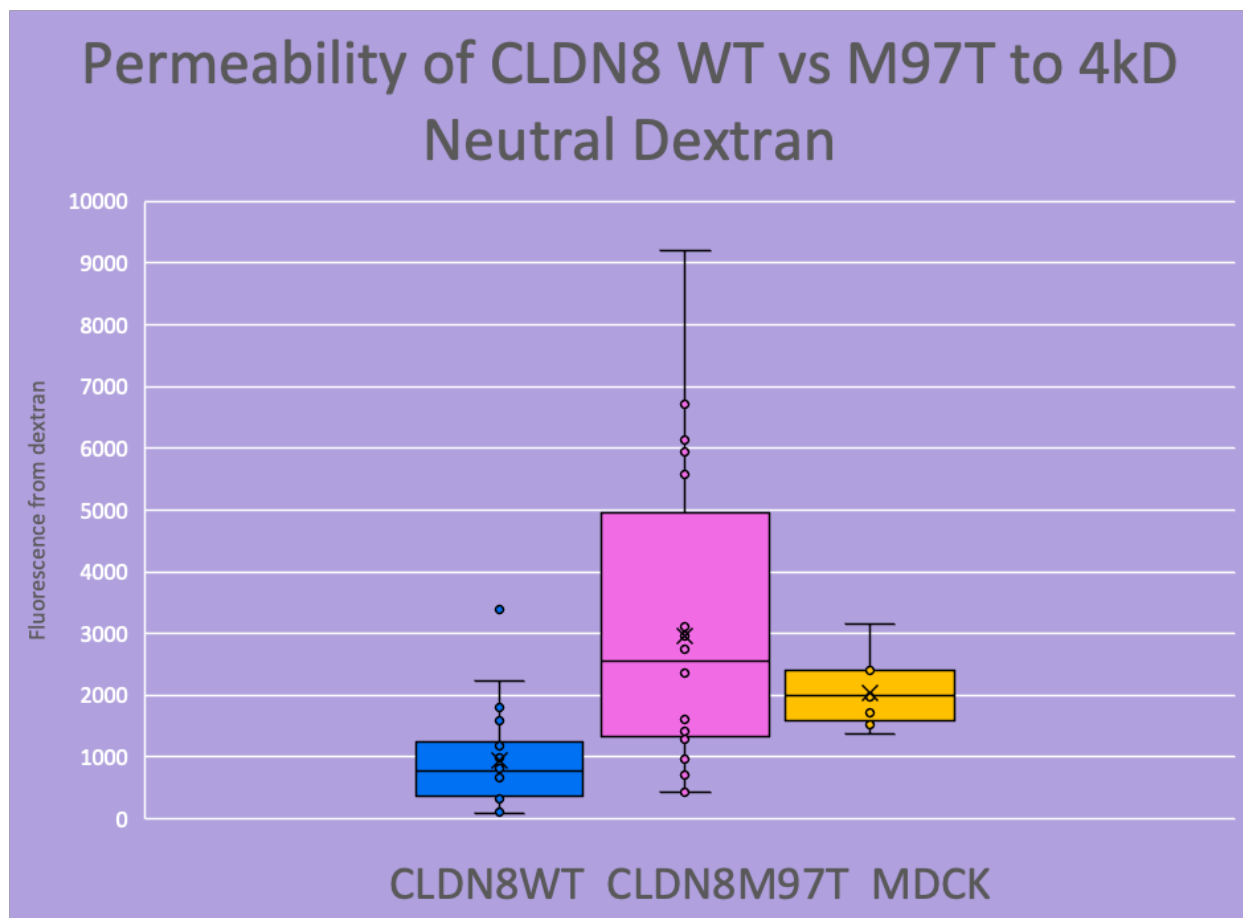


Figure 24: Permeability of CLDN8WT & CLDN8M97T to 4kD Neutral Dextran

Dextran experiment showing the amount of fluorescence due to dextran that made it through a monolayer of MDCK II cells transfected with either CLDN8 WT, CLDN8 M97T, or untransfected control MDCK II cells after 3 hours, (8 days after seeding). This shows a significant increase in permeability in the CLDN8 M97T clones compared to WT. N=2 clones, Student's T-Test p-value<0.001

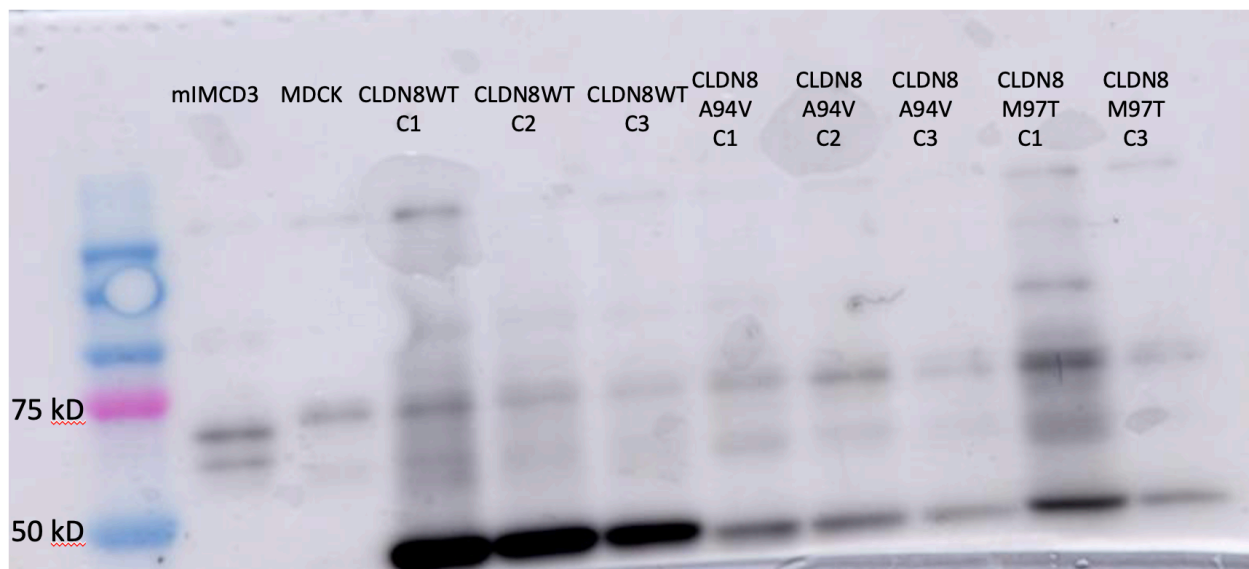


Figure 25: Western Blot of CLDN8WT & Variants

Western blot with primary antibody rabbit CLDN8 (1/500) and HRP-linked secondary antibody (1/5,000) showing control cell lines mIMCD3 (should have endogenous CLDN8 expression but endogenous CLDN8 is smaller than the tagged CLDN8 and would be present below where this blot was cut) and MDCK II (does not have endogenous CLDN8 expression) as well as three separate CLDN8 WT clones and CLDN8 A94V clones and two CLDN8 M97T clones. Endogenous CLDN8 should be around 25 kD and CLDN8 with a GFP tag should be around 50kD.

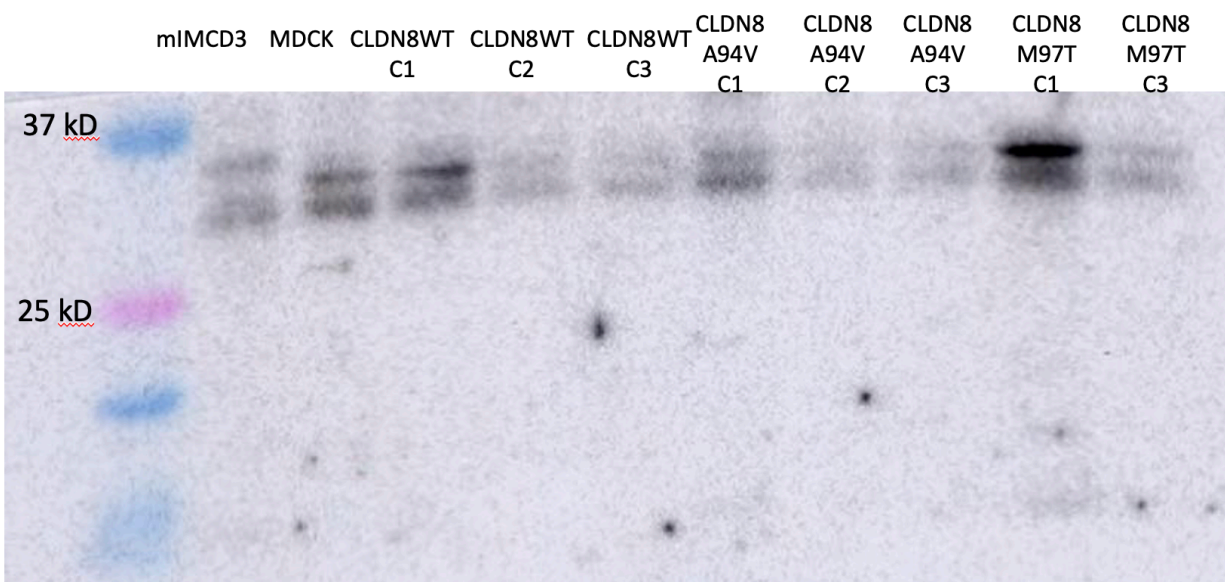


Figure 26: Western Blot Control Showing GAPDH

Western blot control showing mouse GAPDH (1/10,000) with HRP-linked secondary antibody (1/5,000).

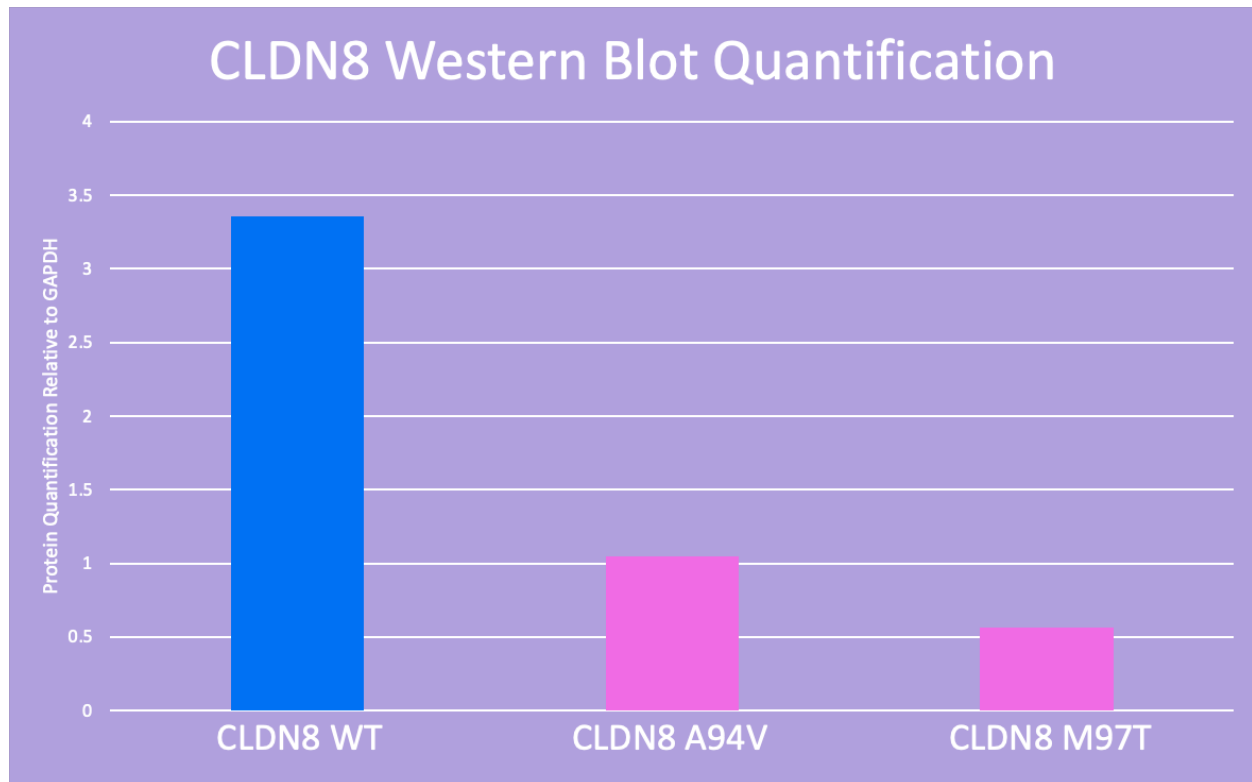


Figure 27: Western Blot Quantification

Western Blot Quantification showing CLDN8 protein relative to GAPDH as an average of N=3 CLDN8 WT clones, N=3 CLDN8 A94V clones and N=2 CLDN8 M97T clones. This shows that cells expressing CLDN8 WT contain far more of the protein than cells expressing either of the CLDN8 variants.

CLDN11 S157F

Confocal imaging failed to show any colocalization to the tight junctions for either CLDN11 WT or CLDN11 S157F (Figure 28). To verify that the plasmid was correct, it was digested with restriction enzymes (SMA1 and HIND3-HF in NEB buffer) to cut out the CLDN sequence and then run on a 1% agarose gel stained with ethidium bromide. This resulted in a band of around 650 base pairs for both WT and variant which suggested that the plasmids for each of them contained the CLDN11 cDNA insert. Next, the plasmid was re-sequenced and

found to be correct and in frame. The primers, shown in Table 3, were specifically designed to establish that the eGFP was in frame with CLDN sequence. IF results using an antibody to CLDN11 also confirmed that the cells were indeed expressing CLDN11 but that it was not localizing to the tight junctions (Figure 29). Due to the lack of localization, further functional analysis could not be performed.

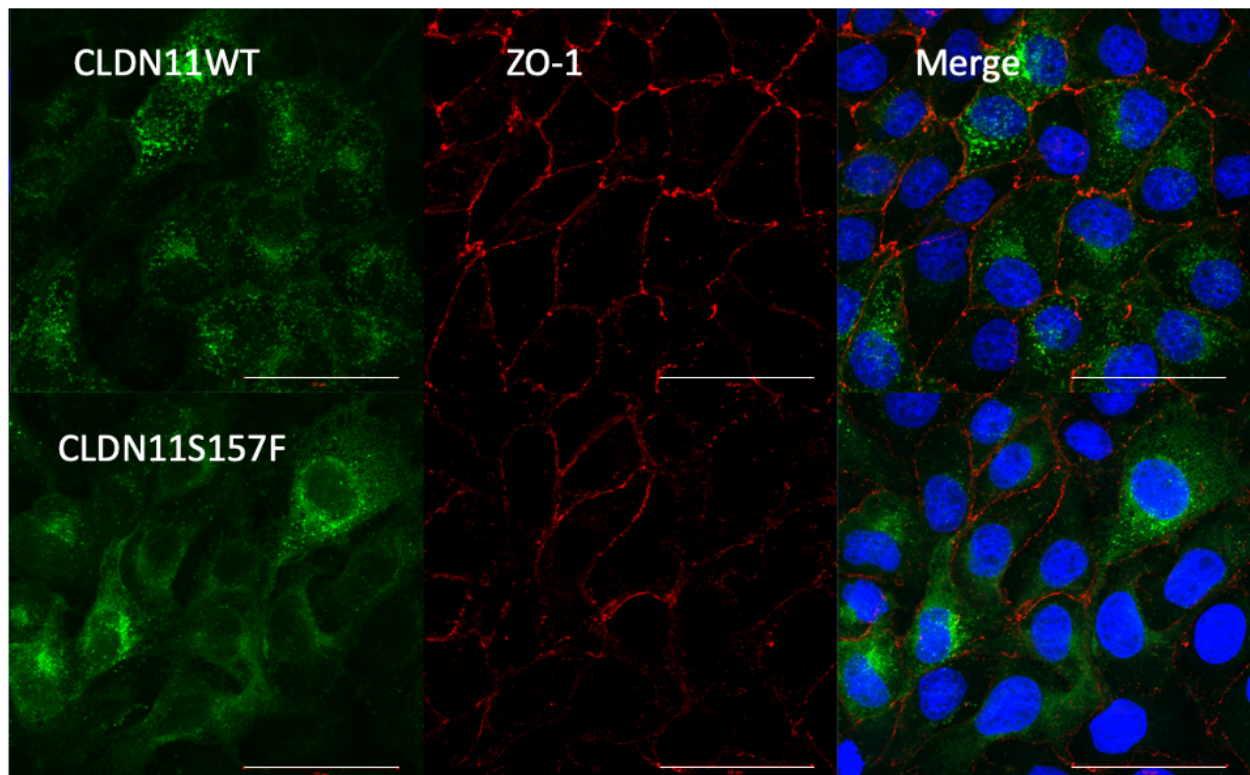


Figure 28: MDCK Cells Stably Transfected with CLDN11WT or CLDN11S157F

Fluorescent images left to right: CLDN11-EGFP fusion protein (green), immunofluorescent detection of tight junction marker zona occludens (ZO-1) (red), and merge with cell nuclei stained blue with DAPI. WT CLDN11 & CLDN11 S157F show no colocalization with ZO-1 in the membrane. Scale bar (shown in white) denotes 50 μ m.

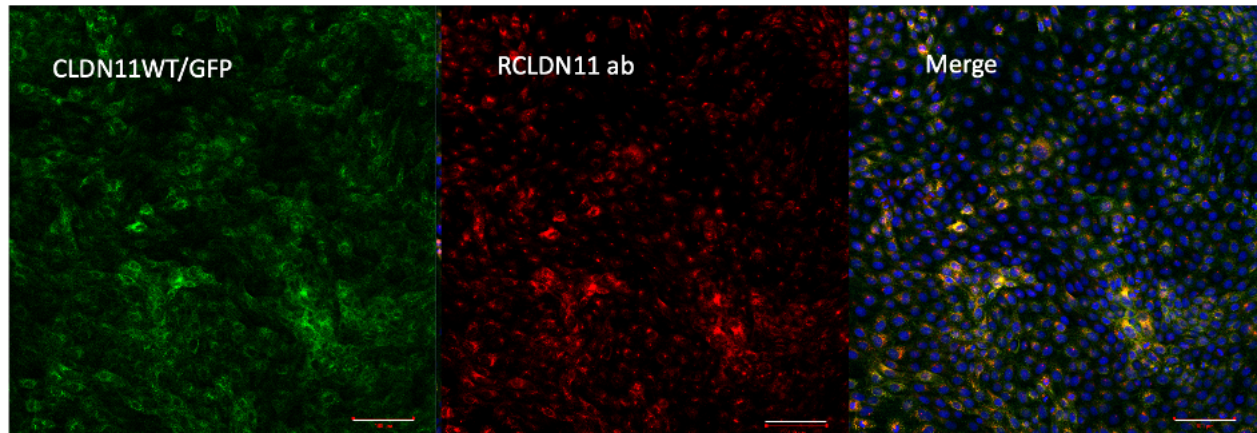


Figure 29: CLDN11WT with CLDN11 Antibody

Fluorescent images left to right: CLDN11-EGFP fusion protein (green), immunofluorescent detection of CLDN11 using RCLDN11 primary antibody with R555 secondary antibody (red), and merge with cell nuclei stained blue with DAPI and yellow signal showing colocalization of CLDN11 with CLDN11 antibody. This suggests that the claudin-11 within the eGFP plasmid is expressed. Scale bar (shown in white) denotes 100 μm .

CLDN17 A94V

Confocal imaging showed that this variant could localize to the tight junctions the same as CLDN17 WT (Figure 30) and this was confirmed by the PCC (Figure 31). Dextran experiments showed that cells expressing CLDN17 A94V had no change in permeability to small molecules compared to cells expressing CLDN17 WT (Figure 32).

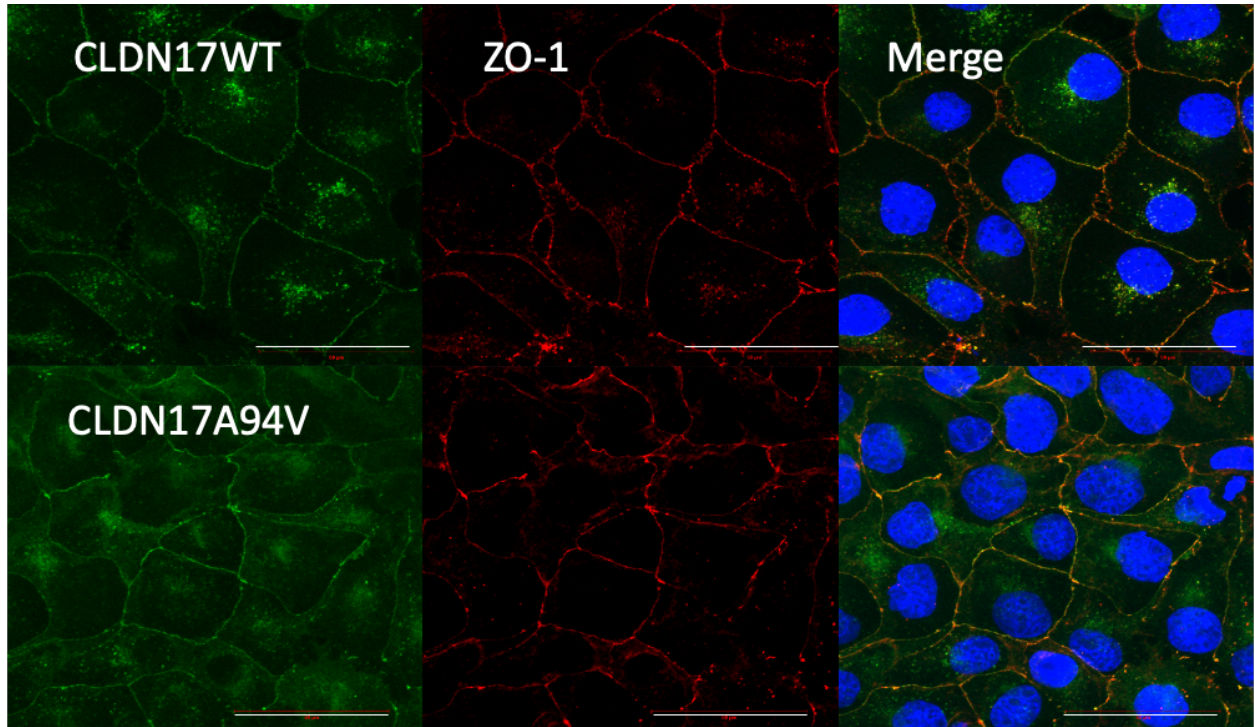


Figure 30: MDCK Cells Stably Transfected with CLDN17WT or CLDN17A94V

Fluorescent images left to right: CLDN17-EGFP fusion protein (green), immunofluorescent detection of tight junction marker zona occludens (ZO-1) (red), and merge with cell nuclei stained blue with DAPI. WT CLDN17 & CLDN17 A94V co-localize with ZO-1 in the membrane (yellow signal). Scale bar (shown in white) denotes 50 μm .

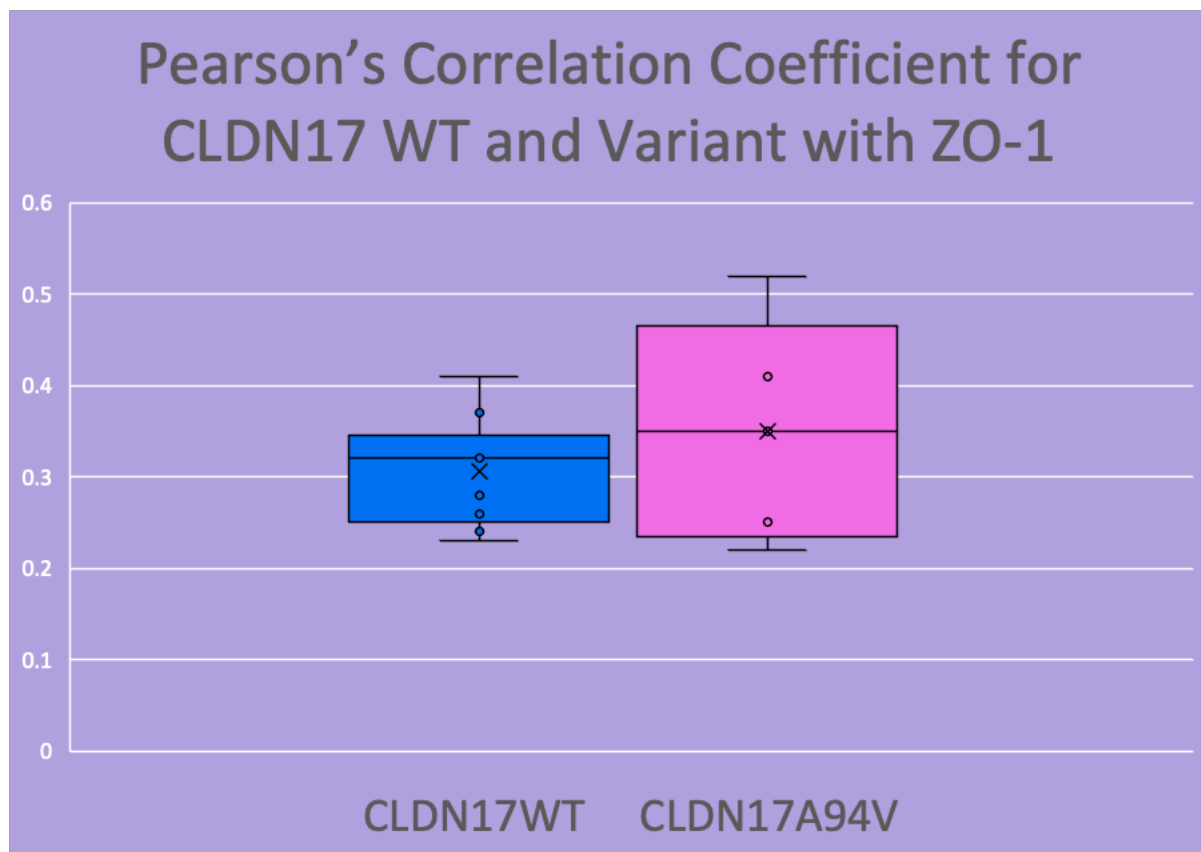


Figure 31: Pearson's Correlation Coefficient for CLDN17WT & CLDN17A94V

PCC shows no significant difference in the colocalization of CLDN17 WT and CLDN17 A94V with ZO-1. N=3 clones of both WT and variant, Student's T-Test p-value=0.37

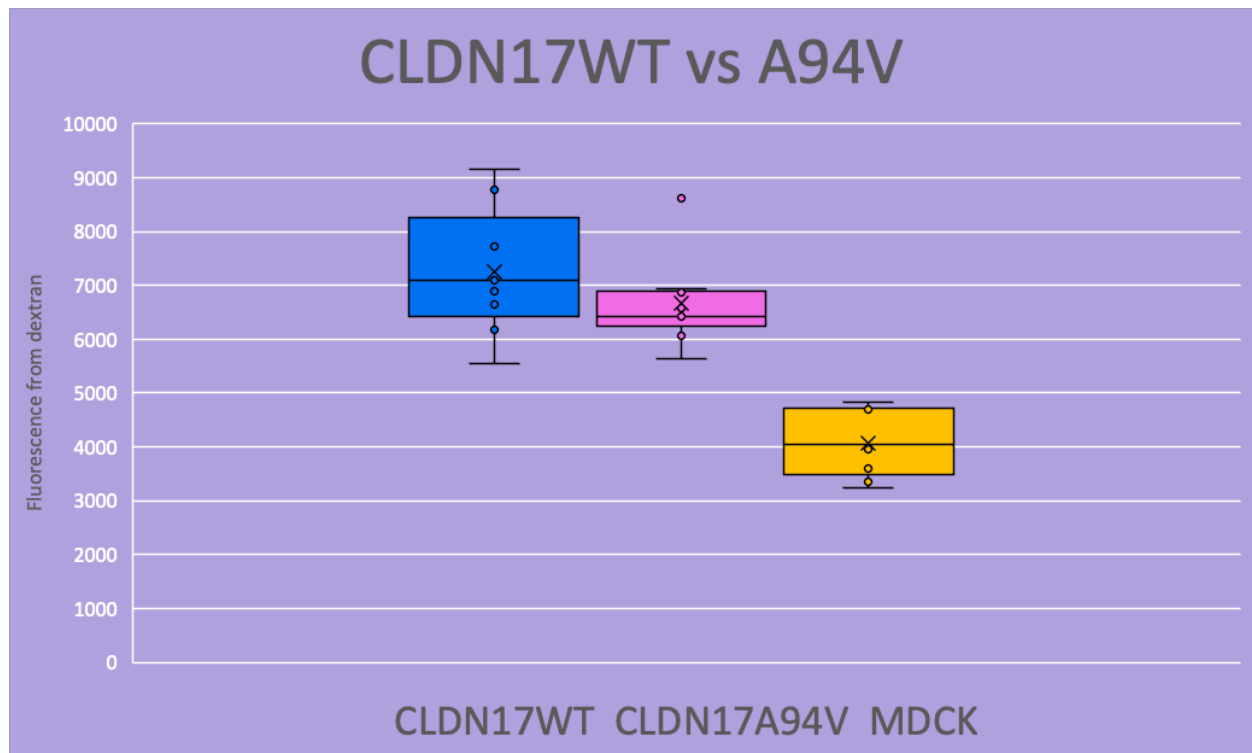


Figure 32: Permeability of CLDN17WT & CLDN17A94V to 4kD Neutral Dextran

Dextran experiment showing the amount of fluorescence due to dextran that made it through a monolayer of MDCK II cells transfected with either CLDN17 WT, CLDN17 A94V, or untransfected control MDCK II cells after 3 hours, (4 days after seeding). This shows there was no significant difference between CLDN17 WT and A94V clones. N=1 clone, Student's T-Test p-value=0.24

Testing of Claudin-8 Antibodies

To prove that the cells transfected with the variant CLDN8 A94V were truly expressing CLDN8, I wanted to do an IF experiment using a CLDN8 antibody on the cells. However, our lab has consistently had issues getting clear and strong signals using CLDN8 antibodies. In an attempt to find a better CLDN8 antibody for current and future experiments, I evaluated four different CLDN8 antibodies (Table 4) from three different companies all of which ostensibly targeted the first extracellular loop of the protein.

I transfected HEK 293 cells (which do not have endogenous CLDN expression) with one of three different WT CLDNs (CLDN4, CLDN8, or CLDN17) so that each flask contained cells that were overexpressing a single WT CLDN. All the antibodies recognized the overexpressed

CLDN8 WT however, two out of the four antibodies exhibited cross-reactivity with at least one other CLDN protein and only the cross-reactive antibodies showed a clearer IF signal than the Invitrogen antibody we were already using.

This demonstrates the importance of antibody validation and confirmed our labs choice to continue using the Invitrogen antibody as it was the best antibody for IF of those that were tested. Of course, this only tested the antibodies against a subset of claudins within a very large protein family. A more rigorous validation process would check each antibody against every member of the family, but this would be both expensive and time consuming. CLDN4 was selected because it is known to dimerize with CLDN8 and therefore may have some similar binding sites for an antibody. CLDN17 was selected because of its sequence similarity to CLDN8.

company	CLDN8 reactivity	CLDN4 reactivity	CLDN17 reactivity
Invitrogen (#40-0700Z)	yes	no	no
Abcam (#183738)	yes	yes	no
Abclonal (#A14470)	yes (dim)	no	no
Abclonal (#A8174)	yes	yes	yes

Table 4: CLDN8 Antibody Reactivity

Table of CLDN8 antibody reactivity using confocal imaging with IF on transfected HEK293 cells with primary antibody concentration of 1/100 and secondary antibody R555 in concentration of 1/500.

Chapter 4: Discussion

Overview of the Variants

We have identified a number of claudin sequence variants that are associated with recurrent calcium phosphate kidney stones. Through functional analysis using MDCK II cells, it appears that some of these could be implicated in the paracellular flux of calcium in the nephron. The majority of the variants in this project, 7/12 caused a change in the second transmembrane domain of the protein which appears to be less evolutionarily conserved than other claudin regions. The transmembrane domains are important for cis interactions between CLDNs so, even if this region tolerates changes more readily than other areas, changes here could still have consequences for protein function. In fact, CLDN variants that affect the second transmembrane domain were associated with neural tube defects in a previous study⁵⁸.

Most of the variants (7/12) in this project are expressed in the distal tubule; CLDN4 A82T, CLDN4 A113T, CLDN7 V55I, CLDN8 A94V, CLDN8 M97T, CLDN17 A94V, and CLDN18 H212D. Five of the variants are expressed in the collecting duct; CLDN4 A82T, CLDN4 A113T, CLDN7 V55I, CLDN8 A94V, and CLDN8 M97T. Three of the variants are expressed in the TAL; CLDN11 S157F, CLDN17 A94V, and CLDN18 H212D. Three of the variants are expressed in the proximal tubule; CLDN11 S157F, CLDN12 M98V and CLDN17 A94V. All four of these sections of the nephron are known to be involved in calcium reabsorption. At least six of the variants are in CLDNs that are thought to function as cation barriers (CLDN4, CLDN6, CLDN8, CLDN11, CLDN18), one is in a CLDN thought to be an anion pore (CLDN17), and one is in a CLDN thought to be a cation pore (CLDN12). The remaining variants are in CLDNs where the literature is either inconsistent (CLDN7) or the function is not known (CLDN23 and CLDN24). This project mainly focused on the *CLDN4* and *CLDN8* variants which have both function (cation barrier) and expression pattern (distal tubule and collecting duct) in common and are known to form heterodimers with each other.

CLDN4

CLDN4 mRNA is expressed in many tissues throughout the body with highest expression in the esophagus and colon according to the GTEx Portal genome browser <https://gtexportal.org/home/>. *CLDN4* is located on the same chromosome as *CLDN3* and bears a strong sequence similarity due their shared evolutionary history where they arose from a gene

duplication event⁶⁰. In the kidney, the CLDN4 protein is expressed in the thin ascending limb, TAL, distal tubule and collecting duct of the nephron where it interacts in cis with CLDN8 to form a heterodimer and functions as a cation barrier or anion pore^{68, 104}. There is even evidence that this CLDN8 interaction is required for CLDN4 to localize to the tight junctions in mouse collecting duct cells (mIMCD-3)¹⁰⁴.

The variant, CLDN4 A82T has a rare substitution of a threonine for an alanine, which is a shift from a hydrophobic to a polar amino acid, in the second transmembrane domain of the protein. A change here could disrupt the localization of the protein to the tight junctions and this variant is listed by ACMG as being of uncertain significance and Varsome predicts this to be a pathogenic change. Functional assays did not show any significant difference between the A82T variant and CLDN4WT. However, this doesn't rule out any potential effects that might still be seen with a calcium specific assay.

The variant CLDN4 A113T has a substitution of a threonine for an alanine, which is a shift from a hydrophobic to a polar amino acid, in the cytosolic loop of the protein. This is a near a region of palmitoylation so an amino acid change here could affect the localization of the protein. Palmitoylation has an important effect on localization by increasing the hydrophobicity of the protein which increases its affinity for the membrane⁶³. This variant is classified by ACMG as benign and Varsome predicts that the change is benign. Functional assays did not show any significant difference between the A113T variant and CLDN4WT.

TEER experiments show no difference between cells expressing CLDN4 A82T, CLDN4 A113T, CLDN4 WT and untransfected MDCK II cells. This is surprising, because CLDN4 is thought to function as a cation barrier and therefore increase the resistance of cell layers, so overexpressing CLDN4 WT would be expected to increase the resistance of the cell monolayer compared to untransfected MDCK II cells. The fact that there is no difference might be due to the fact that the cells already express endogenous CLDN4 so the extra CLDN4 doesn't make a significant difference for cell resistance. The cells are also lacking CLDN8 which forms dimers with CLDN4 when present and in some cell-lines plays a crucial role in helping CLDN4 localize to the tight junctions. This CLDN4/CLDN8 interaction may contribute to the classification of CLDN4 as a cation barrier and when CLDN8 is not present, CLDN4 may not contribute the same resistance property to the cells.

Dextran experiments show that cells transfected with CLDN4 WT, CLDN4 A82T, or CLDN4 A113T causes an increase in permeability to neutral small molecules compared to untransfected MDCK II cells, however there is no difference between CLDN4 WT and the variants. The transfected cells are overexpressing the protein and have a GFP tag attached both of which could contribute to the difference between transfected and untransfected MDCK II cells for this assay. In fact, cells transfected with an empty vector that expresses GFP with no attached CLDN protein also show an increase in permeability to small molecules based on dextran experiments, but not nearly as much of an increase as when there is CLDN protein being overexpressed along with it. This suggests that the CLDN itself is likely contributing to the increase in permeability.

The two CLDN4 variants A82T and A113T were found in the same patient who had East Asian ancestry. This means the patient could either be heterozygous for one doubly mutated *CLDN4* gene or could have compound heterozygosity. Neither of these scenarios were tested during this project because both CLDN4 variants were evaluated separately. There could still be an effect from having both variants at the same time even though no functional differences were seen when looking at each variant on its own.

CLDN6

CLDN6 mRNA has highest expression in the brain, testis, and pancreas according to the GTEx Portal genome browser, but it also has expression in many other tissues throughout the body. It is expressed in the TAL of the nephron in the neonatal kidney where it functions as a cation barrier^{76, 77}. It bears a strong sequence similarity to CLDN9 because the two genes arose from a gene duplication event on chromosome 16.

The variant CLDN6 P211T has a novel substitution of a threonine for a proline which is a change from a hydrophobic to a polar amino acid near the C-terminus of the protein which could influence the PDZ binding domain. ACMG classifies this variant as likely benign and Varsome also predicts this to be a benign change. IF results confirm that the variant localizes to the tight junctions but with an increased affinity compared to CLDN6 WT. An increase in the amount of CLDN6 in the tight junctions might cause the TAL of the nephron to be less permeable to calcium. No further functional analysis was done on this variant. However, because it is

expressed during development, it could still potentially have an impact on kidney function later in life.

CLDN8

CLDN8 mRNA is expressed in many tissues throughout the body with high expression in the kidney and the minor salivary gland according to the GTEx Portal genome browser. In the kidney, the protein is expressed primarily in the distal tubule and collecting duct of the nephron where it is thought to function as a cation barrier⁶⁸. *CLDN8* protein expression appears to be upregulated in the distal tubule and collecting duct of the nephron in response to aldosterone and aldosterone release increases in response to low sodium levels³⁴. The protein is known to interact with *CLDN3*, *CLDN4*, & *CLDN7*⁶⁸. Although it is thought to function as a cation barrier on its own, when it forms a dimer with *CLDN4* it creates an anion pore. It has also been found to compete with *CLDN2* in MDCK II cells resulting in a reduction in the amount of *CLDN2* localized to the tight junctions when *CLDN8* is overexpressed¹⁰⁵. This property of *CLDN8* may contribute to its classification as a cation barrier because *CLDN2* forms a cation pore. *CLDN8* is located on chromosome 21 (the same chromosome as *CLDN17*) and bears some sequence similarity to *CLDN17* since they arose as a gene duplication event⁶⁰.

The variant *CLDN8* A94V has a substitution of a valine for an alanine, both of which are hydrophobic amino acids, in the second transmembrane domain of the protein. This variant was found in a patient with French Canadian ancestry. ACMG and ClinVar both now predict this variant to be benign, but it was classified by ACMG as a variant of uncertain significance when the project started. It was also considered a rare variant at the beginning of the project but no longer meets the threshold to be considered rare which probably contributes to the ACMG classification of benign. Despite the new benign classification by *in silico* analysis, IF results show disrupted localization to the tight junctions. Some of the variant protein does localize to the tight junctions when overexpressed, however the majority of the protein appears to be accumulating in the ER of the cell. Both dextran and TEER experiments show that this variant creates a leakier cell layer compared to wildtype. TEER experiments even show that the cell layers expressing *CLDN8* A94V are more permeable to ions than untransfected MDCK II cells that express no *CLDN8*. Western blot shows a decrease in protein abundance compared to WT

however this could be due to an increase in protein recycling rather than a decrease in protein expression.

This increase in permeability could be caused either through a reduction in the amount of CLDN8 protein that localizes to the tight junctions, by a change in the ion pore function of the variant protein when localized to the tight junctions such as its affinity for other CLDNs, or even by an increase in cellular stress as the protein accumulates in the ER of the cell.

If colocalization is the primary issue, then the next question is whether the colocalization is reduced because it is getting trapped in the ER or whether the CLDN8 A94V variant also has less affinity for the tight junctions compared to CLDN8 WT. In either case, I would hypothesize that the CLDN8 A94V allele has a dominant-negative effect rather than a hypomorphic effect on the cell phenotype compared to untransfected MDCK II cells. This means that even heterozygous carriers of the CLDN8 A94V allele may have increased permeability in the distal nephron where CLDN8 is normally expressed, especially to ions such as calcium. I would further hypothesize that this change could lead to some calcium load that was absorbed by previous sections of the nephron flowing back from the interstitium into the urinary lumen of the distal tubule and collecting duct which have been made more permeable by the mutation.

The variant CLDN8 M97T has a substitution of a threonine for a methionine, which is a change from a hydrophobic to a polar amino acid, in the second transmembrane domain of the protein. When the project started this variant was considered rare but new data has shown that it no longer meets the threshold to be considered rare. This variant was found in one of the few individuals with African ancestry in our cohort and this variant has a higher frequency in African ethnic groups than European ones. ACMG and ClinVar classify this variant as benign and IF results have confirmed that it can localize to the tight junctions. However, it does not localize as well as WT and western blot shows a large decrease in protein abundance compared to WT. This might cause the tight junctions of the distal nephron to be deficient in CLDN8 protein although, having one WT copy of *CLDN8* might be able to somewhat compensate for this.

Dextran experiments show that it increases the permeability of the cell layer to neutral small molecules compared to the wildtype protein. However, TEER experiments show a similar resistance of the cell layers expressing this variant compared to the cell layers expressing the WT protein which might indicate that ionic flux is not significantly different. Still, increasing the permeability in any way could have implications for the overall function of the distal nephron

where CLDN8 is expressed. I would hypothesize that CLDN8 M97T has a hypomorphic effect on the phenotype and may contribute to the heterozygous carrier's risk of developing kidney stones but could have a more severe effect when homozygous.

Another effect I observed for both variants was that the transfected cells seemed to be less adherent in response to trypsinization than CLDN8 WT overexpressing cells. The variant CLDN8 A94V cells always detached from the bottom of the flask within ten minutes of exposure to trypsin while CLDN8 M97T cells and untransfected MDCK II cells were sometimes not fully detached within ten minutes. CLDN8 WT cells on the other hand were almost never fully detached within ten minutes. This may suggest a difference in the strength of the tight junctions or the speed in which the cells reached over-confluence, although all cell lines appeared to grow at a similar rate and were at a similar passage number.

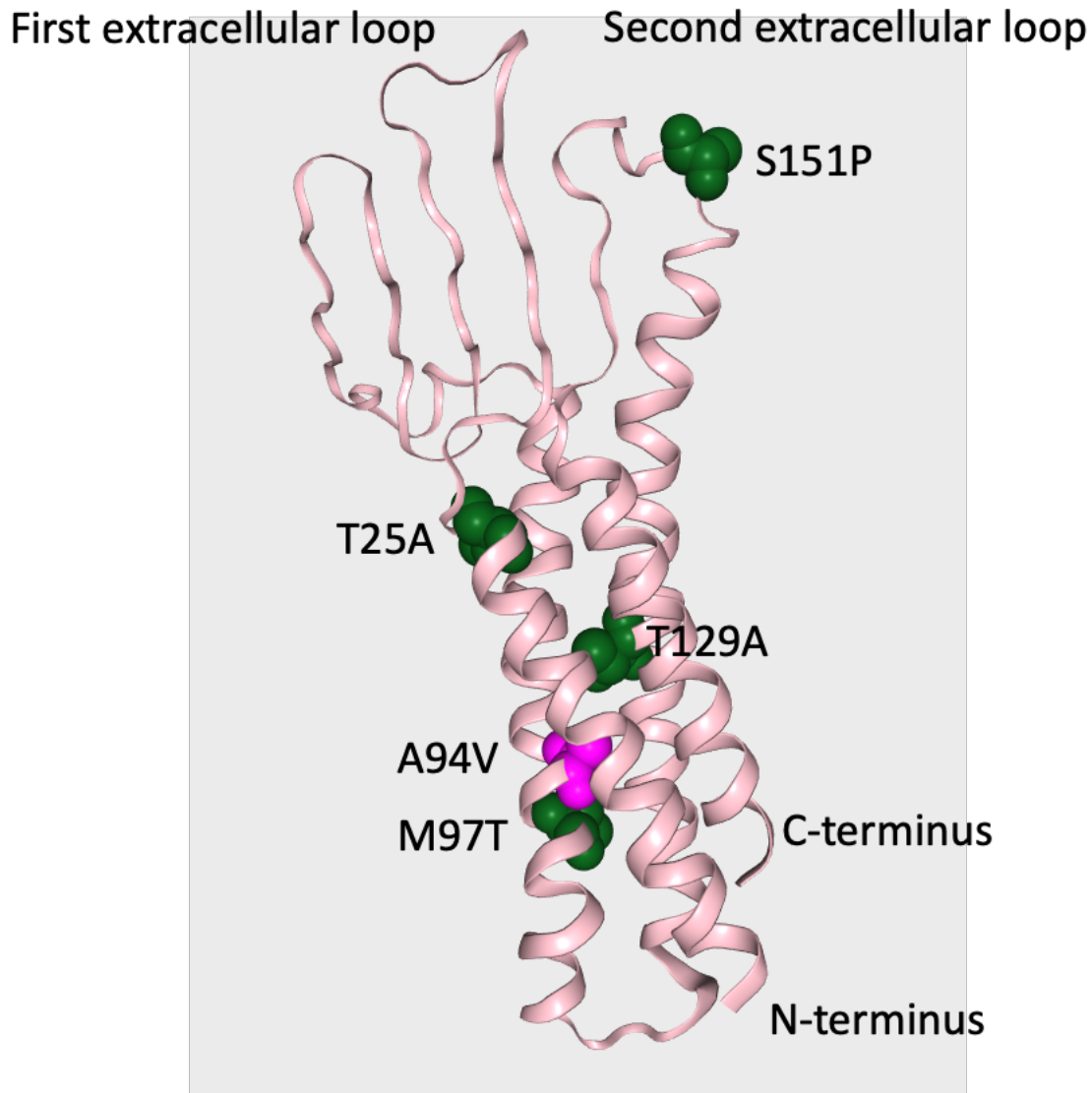


Figure 33: Structure of CLDN8 Protein

Structure of CLDN8 protein adapted from Varsome website < <https://varsome.com/>>, showing location of amino acid change A94V in magenta and location of other known variants in green.

CLDN11

CLDN11 mRNA is expressed in many tissues throughout the body and is highly expressed in the brain and reproductive organs according to the GTEx Portal genome browser. It has an important role in Sertoli cells where it is required for sperm maturation and both expression and proper localization in these cells requires testosterone¹⁰⁶. In the human brain and spinal cord, it co-localizes with CLDN5¹⁰⁷. In mouse studies, knock-out of *CLDN11* results in

low bone-mass, a neurological phenotype, and male sterility¹⁰⁸. *CLDN11* is also expressed in the proximal tubule and thick ascending limb of the nephron where the protein functions as a cation barrier.

The variant *CLDN11* S157F has a novel substitution of a phenylalanine for a serine which is a change from a polar to a hydrophobic amino acid in the second extra-cellular loop of the protein. It is also an increase in the size of the sidechain of the amino acid with the addition of the aromatic ring. This novel variant is classified by ACMG as a variant of uncertain significance, and it is predicted by Varsome to be a pathogenic change. Neither the WT nor variant protein localized to the tight junctions in MDCK II cells making functional analysis difficult. *CLDN11* may require androgens for proper localization in MDCK II cells but this experiment was not attempted due to the time constraints of this project.

CLDN17

CLDN17 mRNA is most highly expressed in the esophagus and reproductive organs according to the GTEx Portal genome browser. In the kidneys it is expressed in the proximal tubule, TAL and the distal tubule of the nephron where it forms an anion selective pore^{72, 74, 109}. The protein is similar in structure to *CLDN8* since they arose as a gene duplication event on chromosome 21.

The variant *CLDN17* A94V has a novel substitution of a valine for an alanine which is a change that maintains the hydrophobicity of the amino acid while increasing the size of the sidechain. This variant is classified by ACMG as a variant of uncertain significance. This variant was found in a patient with ancestry from the Middle East. This is the same amino acid change seen in the previously mentioned *CLDN8* A94V variant. Like the other variant, this amino acid is located in the second transmembrane domain of the protein. However, unlike the *CLDN8* A94V variant, this variant appears to localize normally to the tight junctions and does not cause any change to the permeability of the cell layer. Although *CLDN17* is similar to *CLDN8*, there are still major differences in the sequence, and it has a different expression pattern and function in the nephron which may explain the different effect that this variant has on the protein compared to *CLDN8*.

Limitations of the Eukaryotic Expression Vector and the Transfection Method

The pEGFP plasmid uses a CMV promoter which is known to become silenced via methylation in mammalian cells¹¹⁰. This may be an issue for stably transfected MDCK clones with a high passage number. Indeed, I noted that clones I maintained for greater than 30 days began to show less EGFP signal. In some cases, fusing a GFP tag to the N-terminus rather than C-terminus of a protein affects the localization of the protein within the cell¹¹¹. However, the C-terminus of claudins contains the important PDZ binding domain which a GFP tag may interfere with which is why the N-terminus was chosen instead. However, other labs have had success tagging both the N-terminus and C-terminus of the claudin protein with tags other than GFP such as FLAG^{96, 112}.

All WT transfections apart from CLDN11 WT localized as expected to the tight junctions so, it seems that the N-terminal GFP tag did not affect localization. In the case of CLDN11 the literature suggests that localization of the protein may be dependent on androgens such as testosterone which we did not have access to for these cell culture experiments^{106, 113}.

There are also limitations to the use of MDCK II cells. They express some CLDNs endogenously such as CLDN4 but do not express other CLDNs such as CLDN8. Overexpressing CLDN4 variants may have less of an effect on these cells because they still have endogenous CLDN4 WT. Many CLDNs form heterodimers and these cells may have dimerization partners for some CLDNs but not others which could influence the functional effect of the transfected CLDNs.

Limitations of Bioinformatic Tools

The scope of this project was initially limited to rare or novel variants, but as genomic databases became more diverse some variants that were rare in people of European ancestry, were found to be common in other cohorts. Some of the variants in this project no longer meet the threshold to be considered rare but were still investigated and found to have an effect. This is not surprising because the disease the project is focused on (kidney stones), is a common disease that is most often adult onset so there would be no selective evolutionary pressure against a variant that makes one susceptible to it. Indeed, some GWAS studies have previously identified common variants as associated with kidney stones. However, since the initial project was

limited to only rare and novel variants there could be common, causal variants in our cohort that were overlooked by this study.

We used three different pathogenicity assessments on the Varsome website to classify variants for this project: ACMG, ClinVar, and the Varsome individual pathogenicity scores. The ACMG is an *in silico* classification tool that is most useful for identifying and classifying dominant variants with high penetrance¹¹⁴. Recessive disease genes and variants in genes where less is known about the gene's function are frequently miscategorized as benign. It also is not set up in a way that considers GWAS associations or genes that contribute to a polygenic risk score. Frequency of the genetic variant is taken into account when assessing pathogenicity using this tool, which means common variants will almost always be classified as benign. Indeed, the two potentially pathogenic variants discovered in this project are classified as benign by the ACMG score probably due to their frequency in the general population.

ClinVar is a database that categorizes variants based on reported functional effects submitted by labs and testing facilities. Only a few of the variants in this project had a ClinVar classification which greatly limited its utility as a classification tool and both of the variants that it classified as benign (CLDN8 A94V & CLDN8 M97T) were found to have a potentially pathogenic effect in this study.

Varsome's individual pathogenicity score uses a combination of *in silico* predictive tools to assess the pathogenicity of variants including MutationTaster and SIFT. In this study, the pathogenicity score was used to prioritize some of the variants over others but was not used to rule out any of the variants. This prediction fluctuated throughout the project as the site was updated which caused discrepancies in the classification of variants at the end of the project compared to the classification at the beginning. In short, although bioinformatic tools are still useful for initially evaluating genetic variants, they don't replace functional validation, as was demonstrated by this project.

Other Limitations of This Project

The patients sequenced for this study were all recruited from urology clinics in Montreal, Quebec and the majority had European ancestry. There were patients of Asian, African, and Hispanic descent as well, but the vast majority identified as either broadly European Canadian or specifically French Canadian. Therefore, the patients sequenced for this project do not represent

the average kidney stone patient or even the average Canadian kidney stone patient. Only the CLDN genes of the patients were sequenced which neglects other genetic variants that could be implicated in the etiology of their disease. This study did not investigate synonymous variants or noncoding variants even within CLDN genes which could still influence splicing or RNA stability.

Chapter 5: Conclusion & Future Directions

Remaining *CLDN* Variants

CLDN7 V55I, CLDN18 H212D, and CLDN12 M98V are the most interesting of the remaining variants as they have verified expression in the nephron of the kidney. CLDN7 is expressed in the thin descending limb, the distal tubule and collecting duct of the nephron and knock-out mouse models exhibit chronic dehydration and wasting of Na⁺, K⁺, and Cl⁻ ^{115, 116}. CLDN18 is expressed in the TAL and the distal tubule of the nephron where it forms a cation barrier and CLDN12 is expressed in the proximal tubule where it forms a cation pore^{72, 76}.

The other remaining variants CLDN23 A90T, and CLDN24 V97I are predicted by both ACMG and Varsome to be benign and there is little evidence that the WT CLDN has significant expression in the human nephron. However, this does not rule out an effect on kidney stone development through intestinal expression or another pathway. These variants should still be evaluated when time permits.

Identifying Additional *CLDN* Variants Using the UK Biobank

This project has provided a proof of concept for a workflow from patient sequencing to functional analysis of *CLDN* variants. Future projects could use the same methodology to test *CLDN* variants identified by GWAS or other bioinformatic investigations. Our lab is currently using the UK Biobank to identify *CLDN* variants that are significantly associated with kidney stones for further analysis. Future undertakings could expand to test *CLDN* variants that are associated with other diseases and other organs such as the gastrointestinal tract.

Further Sequencing of Patients

All the patients in our cohort were heterozygous carriers of *CLDN* variants so it would be prudent to do further sequencing of other genes known to affect ion homeostasis to see if they have other variants in the same pathway that could contribute to the phenotype. It would also be interesting to look at some of the synonymous variants in *CLDN* genes such as the *CLDN14* variant rs219780[C] which has been associated with kidney stones⁸⁶. This could help us to determine a polygenic risk score for each patient and potentially elucidate which treatments would be most effective for the root cause of their condition.

Other Methods to Determine Calcium Permeability

Although TEER assays can give a reasonable approximation of ion permeability, they do not differentiate between different kinds of cations meanwhile, neutral dextrans only assess permeability based on size. It would therefore be prudent to do further studies using either positively charged dextrans to measure permeability to monovalent versus divalent cations and fluorescently labeled calcium to directly assess the permeability of the cell layer to calcium specifically.

The Role of Hormones in CLDN Expression and Localization

The relationship between hormones and CLDN expression is vastly understudied. In the case of CLDN11 the literature suggests that both expression and localization of the protein may be dependent on androgens such as testosterone which we did not have access to for these cell culture experiments and may explain the lack of localization^{106, 113}. There is evidence that CLDN8 expression and localization in the distal nephron is influenced by aldosterone³⁴.

Estrogen directly promotes expression of CLDN5 through estrogen response elements within the *CLDN5* promoter¹¹⁷. This increase in CLDN5 protein in response to estrogen has been confirmed by in vivo experiments in both rats and mice¹¹⁷. There is also some evidence that estrogen may have a protective effect against calcium-oxalate based kidney stones³⁷. Therefore, testing the effects of various hormones, particularly testosterone, estrogen, and aldosterone on both WT and variant CLDNs could be a fruitful undertaking. This could shed further light on the male sex bias in kidney stone cohorts and elucidate some of the common mechanisms behind kidney stones and other complex diseases.

Conclusion

This project has demonstrated functional differences in CLDN8 variants found in kidney stone patients and mapped a path from patient sequencing to functional validation of rare genes. CLDN8 normally functions as a barrier to cations in the distal tubule and collecting duct of the nephron. The cells in these nephron segments are known to have very impermeable tight junctions that should not allow ions like calcium to cross except via active transport. Variants in *CLDN8* could be a risk factor for the development of calcium-based kidney stones by increasing the permeability of tight junctions in the distal tubule and collecting duct of the nephron. This

could cause calcium ions to inappropriately diffuse through this layer, potentially allowing calcium reabsorbed by prior nephron segments to re-enter the nephron. This could in turn contribute to hypercalciuria and could increase the chance of a stone nucleating event in these distal segments.

Combinations of non-synonymous CLDN variants with other genetic variants such as synonymous CLDN14 variants could potentially have an additive effect for kidney stone risk. Expanding the list of causal variants will help clinicians more accurately predict the risk of kidney stone recurrence for patients, especially younger patients who lack the typical environmental risk factors. Functional validation of kidney stone risk genes also provides an opportunity for targeting novel disease pathways in the development of future therapeutics to treat and prevent the development of disease.

References

1. Gamero-Estevez, E.; Andonian, S.; Jean-Claude, B.; Gupta, I.; Ryan, A. K., Temporal Effects of Quercetin on Tight Junction Barrier Properties and Claudin Expression and Localization in MDCK II Cells. *Int J Mol Sci* **2019**, *20* (19).
2. Charat, T.; Krambeck, A. E.; Rule, A. D., Determining the true burden of kidney stone disease. *Nature Reviews. Nephrology* **2020**, *16* (12), 736-746.
3. Phillips, R.; Hanchanale, V. S.; Myatt, A.; Somani, B.; Nabi, G.; Biyani, C. S., Citrate salts for preventing and treating calcium containing kidney stones in adults. *Cochrane Database Syst Rev* **2015**, *2015* (10), Cd010057.
4. Curry, J. N.; Saurette, M.; Askari, M.; Pei, L.; Filla, M. B.; Beggs, M. R.; Rowe, P. S.; Fields, T.; Sommer, A. J.; Tanikawa, C.; Kamatani, Y.; Evan, A. P.; Totonchi, M.; Alexander, R. T.; Matsuda, K.; Yu, A. S., Claudin-2 deficiency associates with hypercalciuria in mice and human kidney stone disease. *J Clin Invest* **2020**, *130* (4), 1948-1960.
5. Rule, A. D.; Bergstralh, E. J.; Melton, L. J., 3rd; Li, X.; Weaver, A. L.; Lieske, J. C., Kidney stones and the risk for chronic kidney disease. *Clin J Am Soc Nephrol* **2009**, *4* (4), 804-11.
6. Gambaro, G.; Croppi, E.; Bushinsky, D.; Jaeger, P.; Cupisti, A.; Ticinesi, A.; Mazzaferro, S.; D'Addessi, A.; Ferraro, P. M., The Risk of Chronic Kidney Disease Associated with Urolithiasis and its Urological Treatments: A Review. *J Urol* **2017**, *198* (2), 268-273.
7. Tan, R. Y. P.; Rao, N. N.; Horwood, C. M.; Passaris, G.; Juneja, R., Recurrent nephrolithiasis and loss of kidney function: a cohort study. *Int Urol Nephrol* **2023**.
8. Khan, S. R.; Pearle, M. S.; Robertson, W. G.; Gambaro, G.; Canales, B. K.; Doizi, S.; Traxer, O.; Tiselius, H.-G., Kidney stones. *Nature Reviews Disease Primers* **2016**, *2* (1), 16008.
9. Cicerello, E., Uric acid nephrolithiasis: An update. *Urologia* **2018**, *85* (3), 93-98.
10. Bapir, R.; Bhatti, K. H.; Eliwa, A.; García-Perdomo, H. A.; Gherabi, N.; Hennessey, D.; Magri, V.; Mourmouris, P.; Ouattara, A.; Perletti, G.; Philipraj, J.; Stamatiou, K.; Adetola Tolani, M.; Tzelves, L.; Trinchieri, A.; Buchholz, N., Risk of urinary stone formation associated to proton pump inhibitors: A systematic review and metanalysis. *Arch Ital Urol Androl* **2022**, *94* (4), 507-514.
11. Letavernier, E.; Daudon, M., Vitamin D, Hypercalciuria and Kidney Stones. *Nutrients* **2018**, *10* (3).
12. Fontenelle, L. F.; Sarti, T. D., Kidney Stones: Treatment and Prevention. *Am Fam Physician* **2019**, *99* (8), 490-496.
13. Velázquez, H., Thiazide diuretics. *Ren Physiol* **1987**, *10* (3-4), 184-97.
14. Goldfarb, D. S.; Fischer, M. E.; Keich, Y.; Goldberg, J., A twin study of genetic and dietary influences on nephrolithiasis: a report from the Vietnam Era Twin (VET) Registry. *Kidney Int* **2005**, *67* (3), 1053-61.
15. Hunter, D. J.; Lange, M.; Snieder, H.; MacGregor, A. J.; Swaminathan, R.; Thakker, R. V.; Spector, T. D., Genetic contribution to renal function and electrolyte balance: a twin study. *Clin Sci (Lond)* **2002**, *103* (3), 259-65.
16. Howles, S. A.; Thakker, R. V., Genetics of kidney stone disease. *Nat Rev Urol* **2020**, *17* (7), 407-421.

17. Singh, P.; Harris, P. C.; Sas, D. J.; Lieske, J. C., The genetics of kidney stone disease and nephrocalcinosis. *Nature Reviews Nephrology* **2022**, *18* (4), 224-240.
18. Zhuo, J. L.; Li, X. C., Proximal nephron. *Compr Physiol* **2013**, *3* (3), 1079-123.
19. Alexander, R. T.; Dimke, H., Molecular mechanisms underlying paracellular calcium and magnesium reabsorption in the proximal tubule and thick ascending limb. *Annals of the New York Academy of Sciences* **2022**, *1518* (1), 69-83.
20. King, S. M.; Higgins, J. W.; Nino, C. R.; Smith, T. R.; Paffenroth, E. H.; Fairbairn, C. E.; Docuyan, A.; Shah, V. D.; Chen, A. E.; Presnell, S. C.; Nguyen, D. G., 3D Proximal Tubule Tissues Recapitulate Key Aspects of Renal Physiology to Enable Nephrotoxicity Testing. *Front Physiol* **2017**, *8*, 123.
21. Zacchia, M.; Capolongo, G.; Rinaldi, L.; Capasso, G., The importance of the thick ascending limb of Henle's loop in renal physiology and pathophysiology. *Int J Nephrol Renovasc Dis* **2018**, *11*, 81-92.
22. Blaine, J.; Chonchol, M.; Levi, M., Renal control of calcium, phosphate, and magnesium homeostasis. *Clin J Am Soc Nephrol* **2015**, *10* (7), 1257-72.
23. Davies, J. H.; Moon, R. J., Hypercalcemia. In *Encyclopedia of Endocrine Diseases (Second Edition)*, Huhtaniemi, I.; Martini, L., Eds. Academic Press: Oxford, 2019; pp 366-377.
24. Jeon, U. S., Kidney and calcium homeostasis. *Electrolyte Blood Press* **2008**, *6* (2), 68-76.
25. Capasso, G.; Geibel, P. J.; Damiano, S.; Jaeger, P.; Richards, W. G.; Geibel, J. P., The calcium sensing receptor modulates fluid reabsorption and acid secretion in the proximal tubule. *Kidney Int* **2013**, *84* (2), 277-84.
26. Curry, J. N.; Yu, A. S. L., Paracellular calcium transport in the proximal tubule and the formation of kidney stones. *Am J Physiol Renal Physiol* **2019**, *316* (5), F966-f969.
27. McCormick, J. A.; Ellison, D. H., Distal convoluted tubule. *Compr Physiol* **2015**, *5* (1), 45-98.
28. Kok, D. J.; Schell-Feith, E. A., Risk factors for crystallization in the nephron: the role of renal development. *J Am Soc Nephrol* **1999**, *10 Suppl 14*, S364-70.
29. Kok, D. J., Crystallization and stone formation inside the nephron. *Scanning Microsc* **1996**, *10* (2), 471-84; discussion 484-6.
30. Weaver, C. M.; Peacock, M., Calcium. *Adv Nutr* **2019**, *10* (3), 546-548.
31. Houillier, P.; Lievre, L.; Hureau, M.; Prot-Bertoye, C., Mechanisms of paracellular transport of magnesium in intestinal and renal epithelia. *Annals of the New York Academy of Sciences* **2023**, *n/a* (n/a).
32. de Baaij, J. H. F., Magnesium reabsorption in the kidney. *Am J Physiol Renal Physiol* **2023**, *324* (3), F227-f244.
33. Mirabito Colafella, K. M.; Bovée, D. M.; Danser, A. H. J., The renin-angiotensin-aldosterone system and its therapeutic targets. *Exp Eye Res* **2019**, *186*, 107680.
34. Sassi, A.; Wang, Y.; Chassot, A.; Roth, I.; Ramakrishnan, S.; Olivier, V.; Staub, O.; Udwan, K.; Féraillé, E., Expression of claudin-8 is induced by aldosterone in renal collecting duct principal cells. *American Journal of Physiology-Renal Physiology* **2021**, *321*.
35. Kittanamongkolchai, W.; Mara, K. C.; Mehta, R. A.; Vaughan, L. E.; Denic, A.; Knoedler, J. J.; Enders, F. T.; Lieske, J. C.; Rule, A. D., Risk of Hypertension among First-Time Symptomatic Kidney Stone Formers. *Clin J Am Soc Nephrol* **2017**, *12* (3), 476-482.

36. More, A. S.; Mishra, J. S.; Hankins, G. D.; Kumar, S., Prenatal Testosterone Exposure Decreases Aldosterone Production but Maintains Normal Plasma Volume and Increases Blood Pressure in Adult Female Rats1. *Biology of Reproduction* **2016**, *95* (2).
37. Zhao, Z.; Mai, Z.; Ou, L.; Duan, X.; Zeng, G., Serum estradiol and testosterone levels in kidney stones disease with and without calcium oxalate components in naturally postmenopausal women. *PLoS One* **2013**, *8* (9), e75513.
38. Hsu, Y. J.; Dimke, H.; Schoeber, J. P.; Hsu, S. C.; Lin, S. H.; Chu, P.; Hoenderop, J. G.; Bindels, R. J., Testosterone increases urinary calcium excretion and inhibits expression of renal calcium transport proteins. *Kidney Int* **2010**, *77* (7), 601-8.
39. Tang, T. Y.; Lee, J. I.; Shen, J. T.; Lee, Y. C.; Wang, H. S.; Tsao, Y. H.; Wu, Y. H.; Huang, S. P.; Chen, S. C.; Jhan, J. H.; Geng, J. H., The association between menopause, postmenopausal hormone therapy, and kidney stone disease in Taiwanese women. *Ann Epidemiol* **2023**, *78*, 13-18.
40. Fuster, D. G.; Morard, G. A.; Schneider, L.; Mattmann, C.; Lüthi, D.; Vogt, B.; Dhayat, N. A., Association of urinary sex steroid hormones with urinary calcium, oxalate and citrate excretion in kidney stone formers. *Nephrology Dialysis Transplantation* **2020**, *37* (2), 335-348.
41. Halbritter, J.; Seidel, A.; Müller, L.; Schönauer, R.; Hoppe, B., Update on Hereditary Kidney Stone Disease and Introduction of a New Clinical Patient Registry in Germany. *Front Pediatr* **2018**, *6*, 47-47.
42. Halbritter, J., Genetics of kidney stone disease-Polygenic meets monogenic. *Nephrol Ther* **2021**, *17s*, S88-s94.
43. Palsson, R.; Indridason, O. S.; Edvardsson, V. O.; Oddsson, A., Genetics of common complex kidney stone disease: insights from genome-wide association studies. *Urolithiasis* **2019**, *47* (1), 11-21.
44. Urabe, Y.; Tanikawa, C.; Takahashi, A.; Okada, Y.; Morizono, T.; Tsunoda, T.; Kamatani, N.; Kohri, K.; Chayama, K.; Kubo, M.; Nakamura, Y.; Matsuda, K., A genome-wide association study of nephrolithiasis in the Japanese population identifies novel susceptible Loci at 5q35.3, 7p14.3, and 13q14.1. *PLoS Genet* **2012**, *8* (3), e1002541.
45. Hopp, K.; Cogal, A. G.; Bergstralh, E. J.; Seide, B. M.; Olson, J. B.; Meek, A. M.; Lieske, J. C.; Milliner, D. S.; Harris, P. C., Phenotype-Genotype Correlations and Estimated Carrier Frequencies of Primary Hyperoxaluria. *J Am Soc Nephrol* **2015**, *26* (10), 2559-70.
46. Hebert, S. C., Bartter syndrome. *Curr Opin Nephrol Hypertens* **2003**, *12* (5), 527-32.
47. Gao, B.; Yasui, T.; Itoh, Y.; Tozawa, K.; Hayashi, Y.; Kohri, K., A polymorphism of matrix Gla protein gene is associated with kidney stones. *J Urol* **2007**, *177* (6), 2361-5.
48. Vezzoli, G.; Terranegra, A.; Arcidiacono, T.; Gambaro, G.; Milanesi, L.; Mosca, E.; Soldati, L., Calcium kidney stones are associated with a haplotype of the calcium-sensing receptor gene regulatory region. *Nephrol Dial Transplant* **2010**, *25* (7), 2245-52.
49. Vezzoli, G.; Terranegra, A.; Aloia, A.; Arcidiacono, T.; Milanesi, L.; Mosca, E.; Mingione, A.; Spotti, D.; Cusi, D.; Hou, J.; Hendy, G. N.; Soldati, L.; Paloschi, V.; Dogliotti, E.; Brasacchio, C.; Dell'Antonio, G.; Montorsi, F.; Bertini, R.; Bellinzoni, P.; Guazzoni, G.; Borghi, L.; Guerra, A.; Allegri, F.; Ticinesi, A.; Meschi, T.; Nouvenne, A.; Lupo, A.; Fabris, A.; Gambaro, G.; Strazzullo, P.; Rendina, D.; De Filippo, G.; Brandi, M. L.; Croppi, E.; Cianferotti, L.; Trinchieri, A.; Caudarella, R.; Cupisti, A.; Anglani, F.; Del Prete, D., Decreased

transcriptional activity of calcium-sensing receptor gene promoter 1 is associated with calcium nephrolithiasis. *J Clin Endocrinol Metab* **2013**, *98* (9), 3839-47.

50. Patel, Y. P.; Pandey, S. N.; Patel, S. B.; Parikh, A.; Soni, S.; Shete, N.; Srivastava, R.; Raval, M. A.; Ganpule, A. P.; Patel, S. G.; Desai, M. R., Haplotype of CaSR gene is associated with risk of renal stone disease in West Indian population. *Urolithiasis* **2022**, *51* (1), 25.
51. Mossetti, G.; Rendina, D.; Viceconti, R.; Manno, G.; Guadagno, V.; Strazzullo, P.; Nunziata, V., The relationship of 3' vitamin D receptor haplotypes to urinary supersaturation of calcium oxalate salts and to age at onset and familial prevalence of nephrolithiasis. *Nephrology Dialysis Transplantation* **2004**, *19* (9), 2259-2265.
52. Bid, H. K.; Kumar, A.; Kapoor, R.; Mittal, R. D., Association of vitamin D receptor-gene (FokI) polymorphism with calcium oxalate nephrolithiasis. *J Endourol* **2005**, *19* (1), 111-5.
53. Morrison, N. A.; Qi, J. C.; Tokita, A.; Kelly, P. J.; Crofts, L.; Nguyen, T. V.; Sambrook, P. N.; Eisman, J. A., Prediction of bone density from vitamin D receptor alleles. *Nature* **1994**, *367* (6460), 284-7.
54. Xi, Q. L.; Wang, S. G.; Ye, Z. Q.; Zhu, Z. W.; Li, C.; Bai, J.; Yu, X.; Liu, J. H., Effect of silencing VDR gene in kidney on renal epithelial calcium transporter proteins and urinary calcium excretion in genetic hypercalciuric stone-forming rats. *Urology* **2011**, *78* (6), 1442.e1-7.
55. Frick, K. K.; Krieger, N. S.; Bushinsky, D. A., Modeling hypercalciuria in the genetic hypercalciuric stone-forming rat. *Curr Opin Nephrol Hypertens* **2015**, *24* (4), 336-44.
56. Anderson, J. M.; Van Itallie, C. M., Physiology and function of the tight junction. *Cold Spring Harb Perspect Biol* **2009**, *1* (2), a002584.
57. Wang, D. W.; Zhang, W. H.; Danil, G.; Yang, K.; Hu, J. K., The role and mechanism of claudins in cancer. *Front Oncol* **2022**, *12*, 1051497.
58. Baumholtz, A. I.; De Marco, P.; Capra, V.; Ryan, A. K., Functional Validation of CLDN Variants Identified in a Neural Tube Defect Cohort Demonstrates Their Contribution to Neural Tube Defects. *Front Neurosci* **2020**, *14*, 664.
59. Muto, S., Physiological roles of claudins in kidney tubule paracellular transport. *Am J Physiol Renal Physiol* **2017**, *312* (1), F9-f24.
60. Lal-Nag, M.; Morin, P. J., The claudins. *Genome Biol* **2009**, *10* (8), 235.
61. Heinemann, U.; Schuetz, A., Structural Features of Tight-Junction Proteins. *Int J Mol Sci* **2019**, *20* (23).
62. Colpitts, C. C.; Baumert, T. F., Claudins in viral infection: from entry to spread. *Pflugers Arch* **2017**, *469* (1), 27-34.
63. Van Itallie, C. M.; Gambling, T. M.; Carson, J. L.; Anderson, J. M., Palmitoylation of claudins is required for efficient tight-junction localization. *J Cell Sci* **2005**, *118* (Pt 7), 1427-36.
64. Aono, S.; Hirai, Y., Phosphorylation of claudin-4 is required for tight junction formation in a human keratinocyte cell line. *Exp Cell Res* **2008**, *314* (18), 3326-39.
65. Fujibe, M.; Chiba, H.; Kojima, T.; Soma, T.; Wada, T.; Yamashita, T.; Sawada, N., Thr203 of claudin-1, a putative phosphorylation site for MAP kinase, is required to promote the barrier function of tight junctions. *Exp Cell Res* **2004**, *295* (1), 36-47.
66. Itoh, M.; Furuse, M.; Morita, K.; Kubota, K.; Saitou, M.; Tsukita, S., Direct binding of three tight junction-associated MAGUKs, ZO-1, ZO-2, and ZO-3, with the COOH termini of claudins. *J Cell Biol* **1999**, *147* (6), 1351-63.

67. Simard, A.; Di Pietro, E.; Young, C. R.; Plaza, S.; Ryan, A. K., Alterations in heart looping induced by overexpression of the tight junction protein Claudin-1 are dependent on its C-terminal cytoplasmic tail. *Mech Dev* **2006**, *123* (3), 210-27.
68. Günzel, D.; Yu, A. S., Claudins and the modulation of tight junction permeability. *Physiol Rev* **2013**, *93* (2), 525-69.
69. Frische, S.; Alexander, R. T.; Ferreira, P.; Tan, R. S. G.; Wang, W.; Svenningsen, P.; Skjød, K.; Dimke, H., Localization and regulation of claudin-14 in experimental models of hypercalcemia. *Am J Physiol Renal Physiol* **2021**, *320* (1), F74-f86.
70. Furuse, M.; Fujita, K.; Hiiragi, T.; Fujimoto, K.; Tsukita, S., Claudin-1 and -2: novel integral membrane proteins localizing at tight junctions with no sequence similarity to occludin. *J Cell Biol* **1998**, *141* (7), 1539-50.
71. Wu, V. M.; Schulte, J.; Hirschi, A.; Tepass, U.; Beitel, G. J., Sinuous is a Drosophila claudin required for septate junction organization and epithelial tube size control. *J Cell Biol* **2004**, *164* (2), 313-23.
72. Plain, A.; Alexander, R. T., Claudins and nephrolithiasis. *Curr Opin Nephrol Hypertens* **2018**, *27* (4), 268-276.
73. Kirk, A.; Campbell, S.; Bass, P.; Mason, J.; Collins, J., Differential expression of claudin tight junction proteins in the human cortical nephron. *Nephrol Dial Transplant* **2010**, *25* (7), 2107-19.
74. Prot-Bertoye, C.; Houillier, P., Claudins in Renal Physiology and Pathology. *Genes (Basel)* **2020**, *11* (3).
75. Fujita, H.; Sugimoto, K.; Inatomi, S.; Maeda, T.; Osanai, M.; Uchiyama, Y.; Yamamoto, Y.; Wada, T.; Kojima, T.; Yokozaki, H.; Yamashita, T.; Kato, S.; Sawada, N.; Chiba, H., Tight junction proteins claudin-2 and -12 are critical for vitamin D-dependent Ca²⁺ absorption between enterocytes. *Mol Biol Cell* **2008**, *19* (5), 1912-21.
76. Hou, J., A connected tale of claudins from the renal duct to the sensory system. *Tissue Barriers* **2013**, *1* (3), e24968.
77. Angelow, S.; Ahlstrom, R.; Yu, A. S., Biology of claudins. *Am J Physiol Renal Physiol* **2008**, *295* (4), F867-76.
78. Leiz, J.; Schmidt-Ott, K. M., Claudins in the Renal Collecting Duct. *Int J Mol Sci* **2019**, *21* (1).
79. Van Itallie, C. M.; Mitic, L. L.; Anderson, J. M., Claudin-2 forms homodimers and is a component of a high molecular weight protein complex. *J Biol Chem* **2011**, *286* (5), 3442-50.
80. Beggs, M. R.; Young, K.; Pan, W.; O'Neill, D. D.; Saurette, M.; Plain, A.; Rievaj, J.; Doschak, M. R.; Cordat, E.; Dimke, H.; Alexander, R. T., Claudin-2 and claudin-12 form independent, complementary pores required to maintain calcium homeostasis. *Proc Natl Acad Sci U S A* **2021**, *118* (48).
81. Plain, A.; Pan, W.; O'Neill, D.; Ure, M.; Beggs, M. R.; Farhan, M.; Dimke, H.; Cordat, E.; Alexander, R. T., Claudin-12 Knockout Mice Demonstrate Reduced Proximal Tubule Calcium Permeability. *Int J Mol Sci* **2020**, *21* (6).
82. Breiderhoff, T.; Himmerkus, N.; Stuiiver, M.; Mutig, K.; Will, C.; Meij, I. C.; Bachmann, S.; Bleich, M.; Willnow, T. E.; Müller, D., Deletion of claudin-10 (Cldn10) in the thick ascending limb impairs paracellular sodium permeability and leads to hypermagnesemia and nephrocalcinosis. *Proc Natl Acad Sci U S A* **2012**, *109* (35), 14241-6.

83. Askari, M.; Karamzadeh, R.; Ansari-Pour, N.; Karimi-Jafari, M. H.; Almadani, N.; Sadighi Gilani, M. A.; Gourabi, H.; Vosough Taghi Dizaj, A.; Mohseni Meybodi, A.; Sadeghi, M.; Bashamboo, A.; McElreavey, K.; Totonchi, M., Identification of a missense variant in CLDN2 in obstructive azoospermia. *J Hum Genet* **2019**, *64* (10), 1023-1032.
84. Arcidiacono, T.; Simonini, M.; Lanzani, C.; Citterio, L.; Salvi, E.; Barlassina, C.; Spotti, D.; Cusi, D.; Manunta, P.; Vezzoli, G., Claudin-14 Gene Polymorphisms and Urine Calcium Excretion. *Clin J Am Soc Nephrol* **2018**, *13* (10), 1542-1549.
85. Ullah, I.; Murtaza, K.; Ammara, H.; Misbah; Bhinder, M. A.; Riaz, A.; Shehzad, W.; Zahoor, M. Y., Association study of CLDN14 variations in patients with kidney stones. *Open Life Sci* **2022**, *17* (1), 81-92.
86. Thorleifsson, G.; Holm, H.; Edvardsson, V.; Walters, G. B.; Styrkarsdottir, U.; Gudbjartsson, D. F.; Sulem, P.; Halldorsson, B. V.; de Vegt, F.; d'Ancona, F. C.; den Heijer, M.; Franzson, L.; Christiansen, C.; Alexandersen, P.; Rafnar, T.; Kristjansson, K.; Sigurdsson, G.; Kiemenev, L. A.; Bodvarsson, M.; Indridason, O. S.; Palsson, R.; Kong, A.; Thorsteinsdottir, U.; Stefansson, K., Sequence variants in the CLDN14 gene associate with kidney stones and bone mineral density. *Nat Genet* **2009**, *41* (8), 926-30.
87. Elshamaa, M. F.; Fadel, F. I.; Kamel, S.; Farouk, H.; Alahmady, M.; Ramadan, Y., Genetic polymorphisms in CLDN14 (rs219780) and ALP (rs1256328) genes are associated with risk of nephrolithiasis in Egyptian children. *Turk J Urol* **2021**, *47* (1), 73-80.
88. Guha, M.; Bankura, B.; Ghosh, S.; Pattanayak, A. K.; Ghosh, S.; Pal, D. K.; Puri, A.; Kundu, A. K.; Das, M., Polymorphisms in CaSR and CLDN14 Genes Associated with Increased Risk of Kidney Stone Disease in Patients from the Eastern Part of India. *PLoS One* **2015**, *10* (6), e0130790.
89. Ure, M. E.; Heydari, E.; Pan, W.; Ramesh, A.; Rehman, S.; Morgan, C.; Pinsk, M.; Erickson, R.; Herrmann, J. M.; Dimke, H.; Cordat, E.; Lemaire, M.; Walter, M.; Alexander, R. T., A variant in a cis-regulatory element enhances claudin-14 expression and is associated with pediatric-onset hypercalciuria and kidney stones. *Hum Mutat* **2017**, *38* (6), 649-657.
90. Wilcox, E. R.; Burton, Q. L.; Naz, S.; Riazuddin, S.; Smith, T. N.; Ploplis, B.; Belyantseva, I.; Ben-Yosef, T.; Liburd, N. A.; Morell, R. J.; Kachar, B.; Wu, D. K.; Griffith, A. J.; Riazuddin, S.; Friedman, T. B., Mutations in the gene encoding tight junction claudin-14 cause autosomal recessive deafness DFNB29. *Cell* **2001**, *104* (1), 165-72.
91. Dimke, H.; Desai, P.; Borovac, J.; Lau, A.; Pan, W.; Alexander, R. T., Activation of the Ca(2+)-sensing receptor increases renal claudin-14 expression and urinary Ca(2+) excretion. *Am J Physiol Renal Physiol* **2013**, *304* (6), F761-9.
92. Gong, Y.; Renigunta, V.; Himmerkus, N.; Zhang, J.; Renigunta, A.; Bleich, M.; Hou, J., Claudin-14 regulates renal Ca⁺⁺ transport in response to CaSR signalling via a novel microRNA pathway. *Embo j* **2012**, *31* (8), 1999-2012.
93. Vall-Palomar, M.; Madariaga, L.; Ariceta, G., Familial hypomagnesemia with hypercalciuria and nephrocalcinosis. *Pediatr Nephrol* **2021**, *36* (10), 3045-3055.
94. Hou, J.; Goodenough, D. A., Claudin-16 and claudin-19 function in the thick ascending limb. *Curr Opin Nephrol Hypertens* **2010**, *19* (5), 483-8.
95. Müller, D.; Kausalya, P. J.; Meij, I. C.; Hunziker, W., Familial hypomagnesemia with hypercalciuria and nephrocalcinosis: blocking endocytosis restores surface expression of a novel

- Claudin-16 mutant that lacks the entire C-terminal cytosolic tail. *Hum Mol Genet* **2006**, *15* (7), 1049-58.
96. Konrad, M.; Schaller, A.; Seelow, D.; Pandey, A. V.; Waldegger, S.; Lesslauer, A.; Vitzthum, H.; Suzuki, Y.; Luk, J. M.; Becker, C.; Schlingmann, K. P.; Schmid, M.; Rodriguez-Soriano, J.; Ariceta, G.; Cano, F.; Enriquez, R.; Juppner, H.; Bakkaloglu, S. A.; Hediger, M. A.; Gallati, S.; Neuhauss, S. C.; Nurnberg, P.; Weber, S., Mutations in the tight-junction gene claudin 19 (CLDN19) are associated with renal magnesium wasting, renal failure, and severe ocular involvement. *Am J Hum Genet* **2006**, *79* (5), 949-57.
97. Müller, D.; Kausalya, P. J.; Claverie-Martin, F.; Meij, I. C.; Eggert, P.; Garcia-Nieto, V.; Hunziker, W., A novel claudin 16 mutation associated with childhood hypercalciuria abolishes binding to ZO-1 and results in lysosomal mistargeting. *Am J Hum Genet* **2003**, *73* (6), 1293-301.
98. Kriuchkova, N.; Breiderhoff, T.; Müller, D.; Yilmaz, D. E.; Demirci, H.; Drewell, H.; Günzel, D.; Himmerkus, N.; Bleich, M.; Persson, P. B.; Mutig, K., Furosemide rescues hypercalciuria in Familial Hypomagnesaemia with Hypercalciuria and Nephrocalcinosis model. *Acta Physiologica* **2023**, *n/a* (n/a), e13927.
99. Dukes, J. D.; Whitley, P.; Chalmers, A. D., The MDCK variety pack: choosing the right strain. *BMC Cell Biol* **2011**, *12*, 43-43.
100. Barker, G.; Simmons, N. L., Identification of two strains of cultured canine renal epithelial cells (MDCK cells) which display entirely different physiological properties. *Q J Exp Physiol* **1981**, *66* (1), 61-72.
101. Dunn, K. W.; Kamocka, M. M.; McDonald, J. H., A practical guide to evaluating colocalization in biological microscopy. *Am J Physiol Cell Physiol* **2011**, *300* (4), C723-42.
102. Adler, J.; Parmryd, I., Quantifying colocalization: The case for discarding the Manders overlap coefficient. *Cytometry A* **2021**, *99* (9), 910-920.
103. Aguinis, H.; Vassar, M.; Wayant, C., On reporting and interpreting statistical significance and p values in medical research. *BMJ Evid Based Med* **2021**, *26* (2), 39-42.
104. Hou, J.; Renigunta, A.; Yang, J.; Waldegger, S., Claudin-4 forms paracellular chloride channel in the kidney and requires claudin-8 for tight junction localization. *Proceedings of the National Academy of Sciences* **2010**, *107* (42), 18010-18015.
105. Angelow, S.; Schneeberger, E. E.; Yu, A. S., Claudin-8 expression in renal epithelial cells augments the paracellular barrier by replacing endogenous claudin-2. *J Membr Biol* **2007**, *215* (2-3), 147-59.
106. Kaitu'u-Lino, T. J.; Sluka, P.; Foo, C. F.; Stanton, P. G., Claudin-11 expression and localisation is regulated by androgens in rat Sertoli cells in vitro. *Reproduction* **2007**, *133* (6), 1169-79.
107. Uchida, Y.; Sumiya, T.; Tachikawa, M.; Yamakawa, T.; Murata, S.; Yagi, Y.; Sato, K.; Stephan, A.; Ito, K.; Ohtsuki, S.; Couraud, P. O.; Suzuki, T.; Terasaki, T., Involvement of Claudin-11 in Disruption of Blood-Brain, -Spinal Cord, and -Arachnoid Barriers in Multiple Sclerosis. *Mol Neurobiol* **2019**, *56* (3), 2039-2056.
108. Lindsey, R. C.; Xing, W.; Pourteymoor, S.; Godwin, C.; Gow, A.; Mohan, S., Novel Role for Claudin-11 in the Regulation of Osteoblasts via Modulation of ADAM10-Mediated Notch Signaling. *J Bone Miner Res* **2019**, *34* (10), 1910-1922.

109. Krug, S. M.; Günzel, D.; Conrad, M. P.; Rosenthal, R.; Fromm, A.; Amasheh, S.; Schulzke, J. D.; Fromm, M., Claudin-17 forms tight junction channels with distinct anion selectivity. *Cell Mol Life Sci* **2012**, *69* (16), 2765-78.
110. Wang, X. Y.; Yi, D. D.; Wang, T. Y.; Wu, Y. F.; Chai, Y. R.; Xu, D. H.; Zhao, C. P.; Song, C., Enhancing expression level and stability of transgene mediated by episomal vector via buffering DNA methyltransferase in transfected CHO cells. *J Cell Biochem* **2019**, *120* (9), 15661-15670.
111. Palmer, E.; Freeman, T., Investigation into the use of C- and N-terminal GFP fusion proteins for subcellular localization studies using reverse transfection microarrays. *Comp Funct Genomics* **2004**, *5* (4), 342-53.
112. Ikari, A.; Atomi, K.; Takiguchi, A.; Yamazaki, Y.; Hayashi, H.; Hirakawa, J.; Sugatani, J., Enhancement of cell–cell contact by claudin-4 in renal epithelial madin-darby canine kidney cells. *Journal of Cellular Biochemistry* **2012**, *113* (2), 499-507.
113. McCabe, M. J.; Tarulli, G. A.; Meachem, S. J.; Robertson, D. M.; Smooker, P. M.; Stanton, P. G., Gonadotropins regulate rat testicular tight junctions in vivo. *Endocrinology* **2010**, *151* (6), 2911-22.
114. Houge, G.; Laner, A.; Cirak, S.; de Leeuw, N.; Scheffer, H.; den Dunnen, J. T., Stepwise ABC system for classification of any type of genetic variant. *European Journal of Human Genetics* **2022**, *30* (2), 150-159.
115. Hou, J., Regulation of paracellular transport in the distal nephron. *Curr Opin Nephrol Hypertens* **2012**, *21* (5), 547-51.
116. Tatum, R.; Zhang, Y.; Salleng, K.; Lu, Z.; Lin, J. J.; Lu, Q.; Jeansonne, B. G.; Ding, L.; Chen, Y. H., Renal salt wasting and chronic dehydration in claudin-7-deficient mice. *Am J Physiol Renal Physiol* **2010**, *298* (1), F24-34.
117. Greene, C.; Hanley, N.; Campbell, M., Claudin-5: gatekeeper of neurological function. *Fluids and Barriers of the CNS* **2019**, *16* (1), 3.

Appendix



September 18, 2015

Dr. Tomoko Takano

MUHC

1001 boul. Decarie,

Glen site, room EM1.3244

Montreal, Quebec CA H4A 3J1

Re: MUHC Authorization to Conduct Human Subjects Research 14-466-BMB

Dear Dr. Takano:

We are writing to confirm that the study titled “ **McGill University Kidney Disease Biobank - from Birth to Adulthood**” was submitted for all institutional reviews required by the Ministry of Health and Social Services and the McGill University Health Centre policy.

The MUHC Research Ethics Board (REB) has notified us that ethical approval to conduct your study has been provided.

Please refer to the MUHC Study Code **14-466-BMB** in all future correspondence relating to this study.

Important Note:

You are required to advise the MUHC once the study has been initiated. Please complete the Study Status Report through the eReviews system to indicate the date the study became active.

In accordance with RI MUHC Policies (SOP-CR022), it is the investigator’s responsibility to ensure that staff involved in the study has been certified to conduct clinical research. Research staff can register on the RI MUHC portal under the Clinical Research section. Should you have any questions, please do not hesitate to contact us at qaclinicalresearch@muhc.mcgill.ca.

On behalf of the MUHC, we wish you every success with the conduct of the research.

Sincerely,

A handwritten signature in blue ink, appearing to read "Eugene Bereza".

Eugene Bereza MD, CM, CCFP
Director, Centre for Applied Ethics



Centre universitaire de santé McGill
McGill University Health Centre

McGill University Health Centre

Enclosures

Annual renewal submission form - Harmonized

Protocol title: **McGill University Kidney Disease Biobank - From Birth to Adulthood**

Project number(s): **MP-37-2016-1661, 14-466-MUHC, eReviews_4468**

Form: **F9H-96612**

Nagano identifier: **14-466-MUHC**

First submit date: **2022-06-22**

Principal investigator: **Tomoko Takano**

Last submit date: **2022-06-22**

Project's REB approbation date: **2015-09-09**

Form status: **Form approved**

Administration - REB

1. **MUHC REB Panel & Co-chair(s):**

Cells, tissues, genetics & qualitative research (CTGQ)

Co-chair: Marie Hirtle

reb.ctgq@muhc.mcgill.ca

2. **REB Decision:**

Approved - REB delegated review

3. **Renewal Period Granted:**

From 2022-07-29 to 2023-07-28.

4. **Date of the REB final decision & signature**

2022-08-02

Signature



Sheldon Levy

MUHC REB Coordinator

for MUHC REB Co-chair mentioned above

2022-08-02 16:02

General information

1. **Indicate the name of the Principal Investigator in our institution (MUHC)**

Takano, Tomoko

Required information for renewal

1. **Date when the research project is expected to end at your institution:**

Date unknown

Please indicate (approximately) in what year you expect the project to end.

Recruitment continues

2. **Indicate the current status of the research project at your institution:**

Project is in progress and recruitment is ongoing

3. Please indicate the type of "participants" implicated in your research project

Individuals

Number of participants to recruit initially for your institution according to the protocol and / or the contract:

999

Number of participants that have been recruited to the study (have signed a consent form):

942

Number of minors:

56

Number of incompetent adults:

0

Were any of these participants excluded based on the inclusion or exclusion criteria (screen fails)?

No

Have any of these participants been withdrawn during the project?

Yes

Indicate the number

4

Indicate the reason (if known)

4 since last renewal: Unknown

Did any of the participants stop participating in the project?

Yes

Indicate the number

1

Indicate the reason, if known

1 since last renewal: Lost to followup

Did any participants die while participating in the project?

Yes

Indicate the number

14

Number of participants whose participation has not yet ended (in follow-up and on treatment):

923

Number of participants who have completed all study procedures (follow-up completed):

0

4. **In terms of what you are responsible to report, over the past year, relative to the situation at the time of the last REB renewal (or initial approval):**

Have there been any unreported changes to the REB affecting the study documents?

No

Were there unanticipated problems, serious adverse reactions, major deviations or other events or information altering the ethical acceptability or balance between risks and benefits of the project that were not reported to the REB?

No

Were there any temporary interruptions to the project?

No

Have the results of the project been submitted for publication, presented or published?

No

Should the REB be notified of a conflict of interest situation (of any kind) affecting one or more members of the research team, that was not reported at the time of the last approval of the project?

No

Has there been an allegation related to a breach in ethical compliance (eg: complaint from a participant, non-compliance with rules relating to ethics or integrity) concerning one or more researchers?

No

Does the sponsor require the submission of minor deviations from the protocol or other report that does not identify any impact on participant safety?

No

Signature

Answer of: Pascale, Giuseppe

1. **I certify that the information provided on this form is correct.**

Giuseppe Pascale
2022-06-22 14:16